

Reprinted from Proc. Summer School of Theoretical Physics,  
Les Houches, France, July 1973, pp.149-234  
Published 1977, Gordon and Breach.

27

# Six Lectures on General Fluid Dynamics and Two on Hydromagnetic Dynamo Theory

H. Keith Moffatt

*Department of Applied Mathematics and Theoretical Physics,  
Silver Street, Cambridge, England*

## Contents

Lecture 1	Introductory Ideas and Equations . . . . .	153
	1.1 Preamble . . . . .	153
	1.2 What is a Fluid? . . . . .	154
	1.3 Conservation of Mass . . . . .	157
	1.4 The Momentum Equation . . . . .	158
	1.5 The Energy Equation . . . . .	159
	1.6 Entropy Equation and Equation of Heat Transfer . . . . .	160
	1.7 Constitutive Relations for a Newtonian Fluid . . . . .	161
	1.8 The Navier–Stokes Equation . . . . .	162
Lecture 2	Some Exact Solutions of the Navier–Stokes Equations . . . . .	163
	2.1 Incompressibility . . . . .	163
	2.2 Rectilinear Flows . . . . .	164
	2.3 Flow Between Rotating Cylinders . . . . .	166
	2.4 The Round Jet . . . . .	168
Lecture 3	Flows in which Inertia Forces are Negligible . . . . .	170
	3.1 The Reynolds Number . . . . .	170
	3.2 Uniqueness, Minimum Dissipation, Reversibility and Reciprocity . . . . .	172
	3.3 Motion of a Particle of Arbitrary Shape . . . . .	174
	3.4 The Translating Sphere . . . . .	176
	3.5 Flow Near a Sharp Corner . . . . .	178
	3.6 Flow in a Thin Film . . . . .	181
Lecture 4	High Reynolds Number Flow: the Euler Limit . . . . .	186
	4.1 The General Character of Laminar Flow at High Reynolds Number . . . . .	186
	4.2 Kelvin’s Theorem and Related Results . . . . .	187
	4.3 Irrotational Flow . . . . .	189
	4.4 The Pressure Distribution in Irrotational Flow . . . . .	191
Lecture 5	Boundary-Layer Theory . . . . .	193
	5.1 The Euler Limit and the Prandtl Limit . . . . .	193
	5.2 Reduction of the Boundary-Layer Equation by Dimensional Arguments . . . . .	195
	5.3 Flow in a Diverging Channel; an Example of the Non-Existence of a Boundary Layer . . . . .	198
	5.4 Flow in a Converging Channel . . . . .	199
	5.5 Impulsive Motion of a Cylinder . . . . .	201
	5.6 Boundary Layer Separation . . . . .	203

	5.7	Flow Past Streamlined Cylinders (Airfoils) . . . . .	204
	5.8	A Mechanism for Lift Production for Hovering Insects . . . . .	205
Lecture 6		Instability of Steady Flow . . . . .	206
	6.1	General Remarks . . . . .	206
	6.2	Centrifugal Instability. . . . .	208
Lecture 7		The Dynamo Problem . . . . .	212
	7.1	The Self-Excited Disc Dynamo . . . . .	212
	7.2	The Induction Equation . . . . .	215
	7.3	Field Exclusion by Differential Rotation . . . . .	216
	7.4	Generation of Toroidal Field by Differential Rotation . . . . .	218
	7.5	The 3-Sphere Dynamo . . . . .	219
Lecture 8		Turbulence and Mean-Field Electrodynamics . . . . .	221
	8.1	Motivation . . . . .	221
	8.2	The Mean Electromotive Force Generated in Homogeneous Turbulence (Steenbeck, Krause, Rädler, 1966) . . . . .	223
	8.3	The Diffusion Dominated Limit . . . . .	225
	8.4	The Weak Diffusion Limit . . . . .	226
	8.5	Exponential Growth of the Mean Field . . . . .	227
	8.6	Non-uniform $\alpha$ , Differential Rotation and Meridional Circulation . . . . .	229
	8.7	Self-Regulating Mechanisms . . . . .	230
	8.8	Conclusion . . . . .	231
		References and Bibliography . . . . .	231

## Lecture 1 Introductory Ideas and Equations

### 1.1 Preamble

The wheel-shaped picture in figure 1.1 gives an indication of the way in which a rather self-centred fluid dynamicist views the world. He naturally places himself at the centre of things and looks out in various directions at adjacent scientific disciplines where his skills may either receive nourishment or find application. They receive nourishment from certain branches of pure mathematics, and in particular from the theory of partial differential equations; and they find a wealth of applications in aerodynamics, geophysics, astrophysics, and in chemical, biological, nuclear, civil and nautical engineering. The spokes of the wheel radiate out to a vast range of fascinating problems that arise within these major disciplines; the picture gives an indication of the vastness, although it is certainly far from complete; most fluid dynamicists would however claim an interest in at least one of the fields of research included in this picture.

Part of the fascination of the subject is that a thorough grasp of the basic principles provides the key to an understanding of such a diverse range of problems as that depicted. There can be few other compact fields of knowledge that can embrace in such a comprehensive manner such apparently disparate topics as the general circulation of the ocean on the one hand and the swimming of microscopic organisms on the other; or as the thermal convection in a stellar atmosphere on the one hand and the formation of sand ripples on a beach on the other. Yet it frequently happens that a discovery in one such area of research leads directly or indirectly to a discovery, or a deepening of understanding (which amounts to the same thing), in another area of research far removed from the first in terms of physical context, yet related through the fundamental principles of fluid dynamics.

In these lectures, I shall endeavour to develop and illustrate these fundamental principles, avoiding mathematical complexity where to avoid is not to evade, and putting the emphasis on physical discussion and clarification. I shall draw examples from all of the sectors of the wheel-picture and in so doing will endeavour to amplify and reinforce these introductory comments. Limitations of time will force me to be selective in my treatment and to invite accusations of superficiality; but I must claim immunity from such accusations at the outset; these lectures are intended to convey knowledge by the spoken rather than the written word; and excellent textbooks are available which provide the detailed treatment that time will not permit me. These books are listed in the bibliography on p. 231, but I should like to make specific reference here to G. K. Batchelor's "Introduction to Fluid

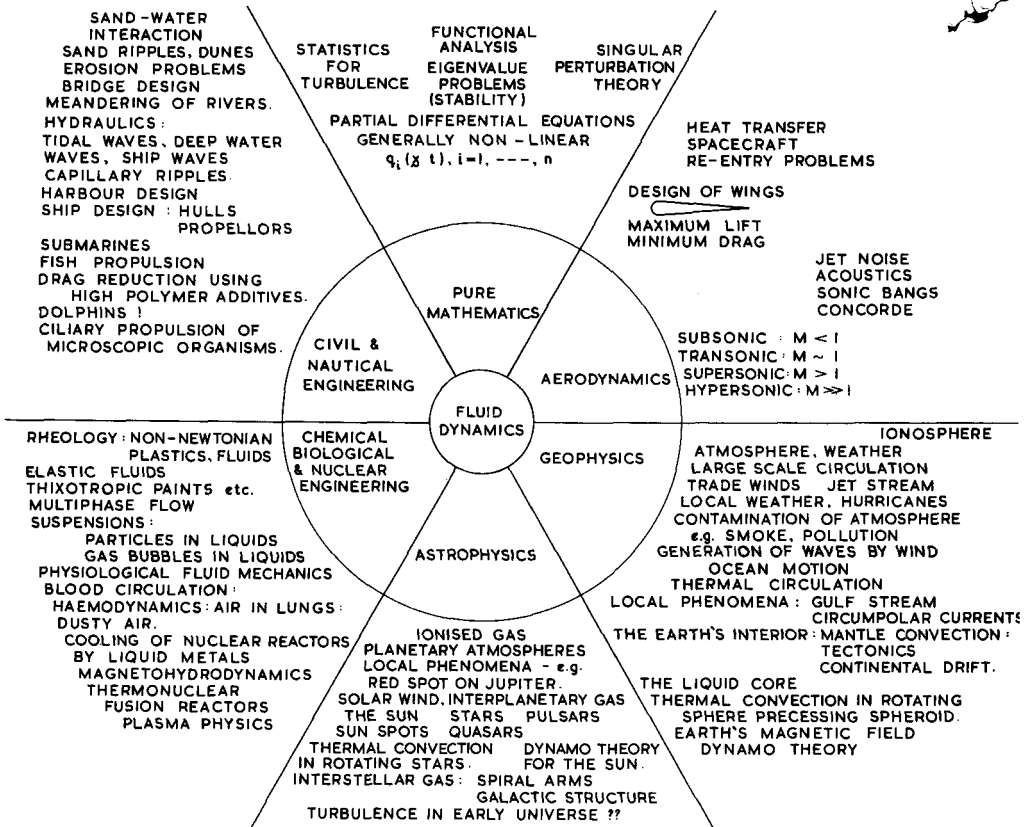


Figure 1.1 The fluid dynamicist's view of the world

Dynamics" by which I have been much influenced both in my general approach to the subject, and in my selection and ordering of material for these lectures.

Most of the problems and methods discussed in Lectures 1-6 may be classed as part of the "standard knowledge" of modern fluid mechanics, and I have made no attempt to seek out original references from the remote past. I have felt it useful to include references to original papers only where these contain results that have not yet found their way into standard textbooks.

## 1.2 What is a Fluid?

The practical man will answer the question by citing examples from everyday experience—air, water, honey, blood, mercury, etc. The physicist would

undoubtedly wish to include liquid helium in the catalogue because of its interesting quantum behaviour; the astrophysicist would wish to include ionised hydrogen if only because that is what most of the universe consists of. The unifying feature of course is that a fluid in general *flows* in response to applied forces, unlike an elastic solid which is merely distorted in response to applied forces to a new equilibrium strained configuration. The distinction between solids and fluids is not precise, since there are many substances (e.g. thixotropic paints, silly putty, etc.) that exhibit fluid properties under some circumstances and solid properties under others; for this reason, many exponents of modern continuum mechanics avoid the terms “fluid” and “solid” altogether, and prefer to talk solely in terms of “continuous media”. The fundamental principles of conservation of mass, momentum and energy in §1.3–1.6 below are universally valid for any continuous medium; it is the constitutive relation introduced in §1.7 that restricts the subsequent discussion to fluids as commonly understood.

The fluids listed above exhibit a range of properties displayed in table 1,

TABLE 1

	air	water	honey	blood	mercury	ionised hydrogen
Newtonian	yes	yes	yes	usually	yes	yes
compressible	yes	no	no	no	no	yes
viscous	no	no	yes	yes	no	no
electrically conducting	no	no	no	no	yes	yes

which requires an immediate word of caution and qualification. To say that air is compressible and that water is not is obviously an oversimplification: the compressibility of water manifests itself in the finite speed of sound in water (1.5 km/sec.); conversely, there are many circumstances when air flows as if incompressible (see §2.1 below). However compressibility effects are undoubtedly less important in water than in air, and it is a common use of words to say that water is an *incompressible fluid*, with the mental reservation that there are always circumstances where its very small compressibility may conceivably be important. Similar comments apply to the Newtonian property (see §1.4 below) and the property of electrical conductivity.

The property of viscosity (or internal friction) demands more careful consideration. In everyday language, honey is certainly viscous, and water is certainly “not viscous”. It is not however perfectly inviscid, and it is well-known that its small viscosity can have a dramatic effect out of all proportion to its apparent magnitude. For example, “inviscid” theory tells us that a solid cylinder jerked into motion perpendicular to its generators will generate

a potential flow with streamlines (relative to the cylinder) as sketched in figure 1.2a; the observed streamlines (by contrast) for a cylinder radius of say 5 cm. and a speed  $U = 20$  cm/sec. in water settle down to the form indicated in figure 1.2b, with turbulence (vigorous random unsteadiness) in the wake downstream of the cylinder. The two flow patterns are quite similar near the "front stagnation point" A, but downstream of the cylinder they could hardly be more different; and the difference is entirely attributable to the effects of viscosity, which, though small far from the cylinder, are of crucial importance in a thin layer on the cylinder surface (the "boundary layer") which is where the departures from the potential flow of figure 1.2a in fact originate.

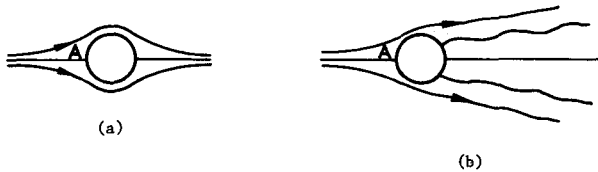


**Figure 1.2** Flow past a circular cylinder: (a) potential flow; (b) observed flow

The fact that viscosity, no matter how small, can have a dramatic effect on a flow field was the chief stumbling-block in the development of fluid mechanics through the nineteenth century. The gulf between theory and observation began to close only with the development of boundary-layer theory, dating from Prandtl (1905). If all goes according to plan, we should get to this theory in lecture 5 of this course; and the reasons for including viscosity from the outset as the fundamental non-negligible fluid property may at that stage become clear.

Now, a word concerning the continuum approximation. I am speaking here mainly to physicists who are all too aware of the ever-increasing complexity in the structure of matter when viewed on an ever-decreasing length-scale. In continuum mechanics, we firmly and unashamedly take the macroscopic point of view and look only at behaviour on a length-scale and time-scale large compared with scales characteristic of atomic and molecular process. From this point of view, a material "particle" may be regarded as a volume element of the medium of vanishing dimensions; from the microscopic point of view, of course, its dimensions must not vanish but must remain large enough to contain a very large number of molecules of the medium.

### 1.3 Conservation of Mass

The flow of a fluid (or, more generally, the motion of any continuum) is completely specified by the paths

$$\mathbf{x} = \mathbf{x}(\mathbf{a}, t) \quad (1.1)$$

of its constituent particles, where  $\mathbf{a}$  labels a particular particle and may be taken to be its position at time  $t = 0$ , i.e.

$$\mathbf{a} = \mathbf{x}(\mathbf{a}, 0). \quad (1.2)$$

Equation (1.1) may be regarded as a mapping from the  $\mathbf{a}$ -space to the  $\mathbf{x}$ -space; clearly

$$dx_i = \frac{\partial x_i}{\partial a_j} da_j, \quad (1.3)$$

and the volume element  $d^3\mathbf{a}$  around  $\mathbf{a}$  transforms under the mapping into

$$d^3\mathbf{x} = |J| d^3\mathbf{a}, \quad (1.4)$$

where

$$J = \det(\partial x_i / \partial a_j), \quad (1.5)$$

i.e.  $J$  is the determinant of the transformation matrix  $\partial x_i / \partial a_j$ .

Conservation of the mass of the fluid particle identified with the volume element  $d^3\mathbf{x}$  implies that

$$\frac{D}{Dt}(\rho(\mathbf{x}, t) d^3\mathbf{x}) = \frac{D}{Dt}(\rho(\mathbf{x}, t) |J|) d^3\mathbf{a} = 0, \quad (1.6)$$

where  $D/Dt$  indicates time differentiation keeping  $\mathbf{a}$  fixed and  $\rho(\mathbf{x}, t)$  is the fluid density (mass per unit volume) at position  $\mathbf{x}$  and time  $t$ . (It is of course the continuum approximation that enables us to introduce such a quantity.) Equation (1.6) is the *Lagrangian form* of the equation of mass-conservation.

The velocity of the particle at  $\mathbf{x}$  is given by

$$\mathbf{v}(\mathbf{a}, t) = \frac{\partial}{\partial t} \mathbf{x}(\mathbf{a}, t) = \mathbf{u}(\mathbf{x}, t), \text{ say.} \quad (1.7)$$

A more familiar form of the equation of mass-conservation (the Eulerian form) involves both  $\rho$  and  $\mathbf{u}$ . Let  $S$  be a fixed closed surface in  $\mathbf{x}$ -space enclosing a volume  $V$ ; then the rate of change of mass within  $S$  resulting from mass flux  $\rho\mathbf{u}$  across  $S$  is given by

$$\frac{d}{dt} \int_V \rho(\mathbf{x}, t) d^3\mathbf{x} = - \int_S \rho\mathbf{u} \cdot \mathbf{n} dS = - \int_V \nabla \cdot (\rho\mathbf{u}) d^3\mathbf{x}, \quad (1.8)$$

using the divergence theorem. It follows that

$$\int_V \left( \frac{\partial \rho}{\partial t} + \nabla \cdot (\rho \mathbf{u}) \right) d^3\mathbf{x} = 0$$

and, since the volume  $V$  is arbitrary,

$$\frac{\partial \rho}{\partial t} + \nabla \cdot (\rho \mathbf{u}) = 0. \quad (1.9)$$

Alternatively, expanding the divergence,

$$\frac{D\rho}{Dt} \equiv \frac{\partial \rho}{\partial t} + \mathbf{u} \cdot \nabla \rho = -\rho \nabla \cdot \mathbf{u}. \quad (1.10)$$

Comparison with (1.6) shows that

$$\frac{D}{Dt} |J| = -|J| \nabla \cdot \mathbf{u}. \quad (1.11)$$

If a flow is such that the density of any material volume element remains constant, then  $D\rho/Dt = 0$ , and so from (1.10),

$$\nabla \cdot \mathbf{u} = 0. \quad (1.12)$$

This is the well-known “incompressibility condition”. A flow field satisfying (1.12) is an *incompressible flow*; (some people prefer the term “isochoric” with good reason).

#### 1.4 The Momentum Equation

Now let  $S_a$  be a closed surface consisting of material particles moving with the fluid and let  $V_a$  be the volume inside  $S_a$ ; we use the suffix  $a$  to emphasise that the surface  $S_a$  is permanently identified with the fluid particles that initially lie on it. Note that for any field  $\psi(\mathbf{x}, t)$ ,

$$\frac{d}{dt} \int_{V_a} \rho \psi dV = \int_{V_a} \rho \frac{D\psi}{Dt} dV, \quad (1.13)$$

by virtue of (1.6), (where we use  $dV$  as an abbreviation for  $d^3\mathbf{x}$ ).

We assume that the forces on the fluid in  $V_a$  consist of (i) a volume force distribution  $\rho \mathbf{f}(\mathbf{x}, t)$  per unit volume, and an area force distribution (surface traction)  $\boldsymbol{\tau}(\mathbf{n}; \mathbf{x}, t)$  per unit area over the surface  $S_a$ , where  $\mathbf{n}$  is the unit outward normal on  $S_a$ ;  $\boldsymbol{\tau}$  represents the action of the fluid outside  $S_a$  on the fluid inside  $S_a$  and it includes both pressure and viscous effects. The surface traction is linearly related to  $\mathbf{n}$  *via* the stress tensor  $\sigma_{ij}(\mathbf{x}, t)$ :

$$\tau_i = \sigma_{ij} n_j. \quad (1.14)$$

Local angular momentum balance implies that  $\sigma_{ij}$  is symmetric. (This requires the assumption that there is no volume torque distribution, and therefore excludes such exotic possibilities as suspensions of ferromagnetic particles each subjected to the torque of an applied magnetic field.) The total force balance of the fluid inside  $S_a$  is given by

$$\frac{d}{dt} \int_{V_a} \rho u_i dV = \int_{S_a} \tau_i dS + \int_{V_a} \rho f_i dV. \quad (1.15)$$

Use of (1.13), (1.14), the divergence theorem, and the fact that  $V_a$  is arbitrary, leads to the momentum equation (in Lagrangian form)

$$\rho \frac{Du_i}{Dt} = \frac{\partial}{\partial x_j} \sigma_{ij} + \rho f_i. \quad (1.16)$$

The alternative Eulerian form, from (1.10) and (1.16), is

$$\frac{\partial}{\partial t} (\rho u_i) + \frac{\partial}{\partial x_j} (\rho u_i u_j - \sigma_{ij}) = \rho f_i. \quad (1.17)$$

When  $\mathbf{f} = 0$ , this has the structure of a conservation equation as it should; the conserved quantity is the momentum, with density  $\rho u_i$ ; the momentum flux tensor is

$$\Pi_{ij} = \rho u_i u_j - \sigma_{ij}. \quad (1.18)$$

For *steady* flow, under no volume forces, we have the important momentum integral theorem:

$$\int_S (\rho u_i u_j - \sigma_{ij}) n_j dS = 0, \quad (1.19)$$

where  $S$  again is a fixed (Eulerian) surface in  $\mathbf{x}$ -space.

## 1.5 The Energy Equation

Since, under the continuum hypothesis, we restrict attention to flow phenomena whose time-scale is large compared with times characteristic of molecular processes, we may reasonably assume that these molecular processes are at each instant in statistical equilibrium, and that the laws of equilibrium thermodynamics apply to each element of fluid even while it is being distorted in its motion. Let  $e(\mathbf{x}, t)$  be the internal energy per unit mass of the fluid element at position  $\mathbf{x}$  and time  $t$ . The energy balance of the fluid inside the Lagrangian surface  $S_a$  is then given by

$$\frac{d}{dt} \int_{V_a} (\frac{1}{2} \mathbf{u}^2 + e) \rho dV = \int_{S_a} \tau_i u_i dS + \int_{V_a} \rho f_i u_i dV + \int_{S_a} (-\mathbf{q} \cdot \mathbf{n}) dS. \quad (1.20)$$

This equation says that the rate of change of the total energy (kinetic plus internal) in  $V_a$  is equal to the rate of working of the surface tractions  $\tau$  and the volume forces  $\mathbf{f}$ , plus the rate of transfer of heat (represented by the heat flux  $\mathbf{q}$ ) across  $S_a$  by molecular processes. Use of (1.13), (1.14), the divergence theorem, and the fact that  $V_a$  is arbitrary leads to

$$\rho \frac{D}{Dt} \left( \frac{1}{2} \mathbf{u}^2 + e \right) = \frac{\partial}{\partial x_j} (u_i \sigma_{ij}) + \rho \mathbf{u} \cdot \mathbf{f} - \nabla \cdot \mathbf{q}. \quad (1.21)$$

Subtraction of  $u_i$  times (1.16) gives the *energy equation* in more standard form:

$$\rho \frac{De}{Dt} = \sigma_{ij} \frac{\partial u_i}{\partial x_j} - \nabla \cdot \mathbf{q}. \quad (1.22)$$

The Eulerian form of this equation is

$$\frac{\partial}{\partial t} (\rho (\frac{1}{2} \mathbf{u}^2 + e)) + \frac{\partial}{\partial x_j} Q_j = 0, \quad (1.23)$$

where the energy flux  $Q_j$  is given by

$$Q_j = \rho u_j (\frac{1}{2} \mathbf{u}^2 + e) - u_i \sigma_{ij} + q_j. \quad (1.24)$$

## 1.6 Entropy Equation, and Equation of Heat Transfer

Equation (1.22) may be written in two alternative forms by use of thermodynamic relations for the changes of state of a fluid element. Let  $\rho$  and  $T$  (temperature) be taken as independent variables of state. The laws of thermodynamics tell us that there exists a function  $s(\rho, T)$  of these variables (the entropy per unit mass) with the property

$$T ds = de + p d(1/\rho), \quad (1.25)$$

where  $p(\rho, T)$  is the thermodynamic pressure (given by an equation of state); in (1.25),  $ds$ ,  $de$  and  $d(1/\rho)$  are differential changes in  $s$ ,  $e$  and  $1/\rho$ , following an element of the fluid. It follows that

$$T \frac{Ds}{Dt} = \frac{De}{Dt} + p \frac{D}{Dt} \left( \frac{1}{\rho} \right) = \frac{De}{Dt} + \frac{p}{\rho} \nabla \cdot \mathbf{u}, \quad \text{from (1.10)}. \quad (1.26)$$

Hence, from (1.22) we derive the *entropy equation*,

$$\rho T \frac{Ds}{Dt} = p \nabla \cdot \mathbf{u} + \sigma_{ij} \frac{\partial u_i}{\partial x_j} - \nabla \cdot \mathbf{q}. \quad (1.27)$$

The thermodynamic relation (1.25) may be written in the alternative form

$$T ds = c_p dT - \beta \frac{T}{\rho} dp, \quad (1.28)$$

where  $c_p = T(\partial s/\partial T)_p$  is the specific heat at constant pressure, and  $\beta = \rho(\partial(1/\rho)/\partial T)_p$  is the coefficient of thermal expansion. Hence (1.27) may be written

$$\rho c_p \frac{DT}{Dt} - \beta \frac{T Dp}{Dt} = p \nabla \cdot \mathbf{u} + \sigma_{ij} \frac{\partial u_i}{\partial x_j} - \nabla \cdot \mathbf{q}; \quad (1.29)$$

this is the general *equation of heat transfer*.

It should be emphasised that the equations derived so far are of general validity for any continuum. We specialise to the case of a Newtonian fluid in the following section.

### 1.7 Constitutive Relations for a Newtonian Fluid

The stress tensor  $\sigma_{ij}$  may be expressed as the sum of an "isotropic part"  $\frac{1}{3}\sigma_{kk}\delta_{ij}$  and a "deviatoric part"

$$\sigma_{ij}^{(d)} = \sigma_{ij} - \frac{1}{3}\sigma_{kk}\delta_{ij}, \quad \sigma_{kk}^{(d)} = 0. \quad (1.30)$$

In a fluid at rest,  $p = -\frac{1}{3}\sigma_{kk}$ , and  $\sigma_{ij}^{(d)} = 0$ . In a fluid in motion, it is to be expected that both these relations will be modified by terms involving the state of motion, i.e. the velocity field. Most fluids in most normal circumstances are *Newtonian* in their response to stress, i.e.  $p + \frac{1}{3}\sigma_{kk}$  and  $\sigma_{ij}^{(d)}$  are linearly related to the velocity gradient tensor  $\partial u_i/\partial x_j$ ; the most general linear relations compatible with the tensor character of  $\sigma_{ij}$  and  $\partial u_i/\partial x_j$ , with the symmetry of  $\sigma_{ij}$ , and with the fact that  $\sigma_{kk}^{(d)} = 0$  by definition, are

$$p + \frac{1}{3}\sigma_{kk} = \lambda \nabla \cdot \mathbf{u}, \quad \sigma_{ij}^{(d)} = \mu \left( \frac{\partial u_i}{\partial x_j} + \frac{\partial u_j}{\partial x_i} - \frac{2}{3} \nabla \cdot \mathbf{u} \delta_{ij} \right), \quad (1.31)$$

where  $\lambda$  and  $\mu$  (which may be functions of  $\rho$  and  $T$ ) are the coefficients of bulk viscosity and shear viscosity respectively; these coefficients are both positive (see below).

The relations (1.31) are the *Newtonian constitutive relations* and they are basic to nearly all research work in fluid mechanics. They are of far wider generality than, for example, the similar linear relations for small deformations of an elastic solid. However, it should be remembered that, in restricting attention henceforth to the consequences of (1.31), we exclude from consideration (a) all long-range molecular effects which could lead to a non-local relation between  $\sigma_{ij}$  and  $\mathbf{u}(\mathbf{x}, t)$ ; (b) all memory (or elastic) effects which lead to a non-instantaneous relation between  $\sigma_{ij}$  and  $\partial u_i/\partial x_j$ ; (c) all effects dependent on lack of isotropy of the fluid sub-structure (such effects arise, for example in a suspension of fibres which will clearly tend to adopt a preferred orientation in a shear flow and which will then lead to departures from isotropy in the constitutive relation for the fluid suspension); and (d) all effects associated with extremely rapid rates of distortion which could

lead to the appearance of non-linear terms in the relation between  $\sigma_{ij}$  and  $\partial u_i / \partial x_j$ .

There is a further constitutive relation in the same category of phenomenological relations as (1.31), namely the linear relation between heat flux  $\mathbf{q}$  and temperature gradient  $\nabla T$ :

$$\mathbf{q} = -\kappa \nabla T, \quad (1.32)$$

where  $\kappa$ , also a function of  $\rho$  and  $T$ , is the thermal conductivity of the fluid.

We shall assume that variations of  $\rho$  and  $T$  are sufficiently weak for it to be reasonable to assume that coefficients such as  $\lambda$ ,  $\mu$  and  $\kappa$  are uniform throughout the fluid.

### 1.8 The Navier–Stokes Equation

From (1.30) and (1.31), it follows that

$$\frac{\partial}{\partial x_j} \sigma_{ij} = -\frac{\partial p}{\partial x_i} + \mu \nabla^2 u_i + (\lambda + \frac{1}{3}\mu) \frac{\partial}{\partial x_i} \nabla \cdot \mathbf{u}, \quad (1.33)$$

and hence the momentum equation (1.16) becomes

$$\rho \frac{D\mathbf{u}}{Dt} = -\nabla p + \mu \nabla^2 \mathbf{u} + (\lambda + \frac{1}{3}\mu) \nabla \nabla \cdot \mathbf{u} + \rho \mathbf{f}. \quad (1.34)$$

This equation, sometimes in conjunction with the equation of mass conservation, is known as the Navier–Stokes equation. For incompressible flow, for which  $\nabla \cdot \mathbf{u} = 0$ , it simplifies to

$$\rho \frac{D\mathbf{u}}{Dt} = -\nabla p + \mu \nabla^2 \mathbf{u} + \rho \mathbf{f}. \quad (1.35)$$

From (1.30) and (1.31), we have also that

$$\sigma_{ij} \frac{\partial u_i}{\partial x_j} = -p \nabla \cdot \mathbf{u} + \lambda (\nabla \cdot \mathbf{u})^2 + 2\mu e_{ij}^{(d)} e_{ij}^{(d)}, \quad (1.36)$$

where

$$e_{ij}^{(d)} = e_{ij} - \frac{1}{3} e_{kk} \delta_{ij}, \quad e_{ij} = \frac{1}{2} \left( \frac{\partial u_i}{\partial x_j} + \frac{\partial u_j}{\partial x_i} \right). \quad (1.37)$$

Moreover, from (1.32),

$$\nabla \cdot \mathbf{q} = -\kappa \nabla^2 T. \quad (1.38)$$

Hence the energy equation (1.22) becomes

$$\rho \frac{De}{Dt} = -p \nabla \cdot \mathbf{u} + \lambda (\nabla \cdot \mathbf{u})^2 + 2\mu e_{ij}^{(d)} e_{ij}^{(d)} + \kappa \nabla^2 T, \quad (1.39)$$

and the entropy equation (1.27) becomes

$$\rho T \frac{Ds}{Dt} = \lambda (\nabla \cdot \mathbf{u})^2 + 2\mu e_{ij}^{(d)} e_{ij}^{(d)} + \kappa \nabla^2 T. \quad (1.40)$$

The result that  $\lambda$ ,  $\mu$  and  $\kappa$  must be positive follows essentially from this equation applied to a volume of fluid thermally insulated from its surroundings. For let  $S_a$  be the (Lagrangian) insulating boundary on which  $\mathbf{q} \cdot \mathbf{n} = 0$ , i.e.  $\partial T / \partial n = 0$ ; then the rate of change of the total entropy of the fluid in the volume  $V$  inside  $S_a$  is

$$\frac{d}{dt} \int \rho s \, dV = \int \rho \frac{Ds}{Dt} \, dV = \int \left( \frac{\lambda}{T} (\nabla \cdot \mathbf{u})^2 + \frac{2\mu}{T} e_{ij}^{(d)} e_{ij}^{(d)} + \frac{\kappa}{T^2} (\nabla T)^2 \right) dV. \quad (1.41)$$

It is possible to conceive of an experiment in which any two of the quantities  $(\nabla \cdot \mathbf{u})^2$ ,  $e_{ij}^{(d)} e_{ij}^{(d)}$  and  $(\nabla T)^2$  vanish identically, but not the third. The thermodynamic result that the entropy of a thermally isolated system can only increase, coupled with the fact that  $T > 0$ , implies then that each of  $\lambda$ ,  $\mu$  and  $\kappa$  is positive. Physically, of course, the result appears obvious: heat tends to flow from regions of high temperature to regions of low temperature and this implies that  $\kappa > 0$ . Similarly molecular processes tend to transport momentum from regions of high fluid velocity to regions of low velocity. If the motion is purely solenoidal (i.e.  $\nabla \cdot \mathbf{u} = 0$ ) then shear viscosity is the agency by which momentum is transported and again the "high to low" direction of transfer requires that  $\mu > 0$ . If the motion is purely compressive, (i.e.  $e_{ij}^{(d)} \equiv 0$ ), then bulk viscosity is the agency and  $\lambda > 0$ .

Finally, the expression for energy flux in a Newtonian fluid from (1.24) and (1.30) – (1.32) takes the form

$$Q_j = \rho u_j \left( \frac{1}{2} \mathbf{u}^2 + h \right) - 2\mu u_i e_{ij}^{(d)} - \lambda u_j \nabla \cdot \mathbf{u} - \kappa \partial T / \partial x_j, \quad (1.42)$$

where

$$h = e + p/\rho \quad (1.43)$$

is the enthalpy per unit mass. Note particularly the form of the first term  $\rho u_j (\frac{1}{2} \mathbf{u}^2 + h)$ , which survives even when all molecular transport effects (represented by the other contributions) are negligible.

## Lecture 2 Some Exact Solutions of the Navier–Stokes Equations

### 2.1 Incompressibility

The equations derived in Lecture 1 are a complicated system of non-linear differential equations determining, in principle, the evolution of the fields

$\mathbf{u}$ ,  $p$ ,  $\rho$  and  $T$  (and all related variables such as  $\sigma_{ij}$ ,  $e$ ,  $s$ , etc.). The equations are considerably simplified if the flow is incompressible and the fluid is of uniform density; for then, not only do all effects associated with bulk viscosity disappear, but also the equation for  $T$  is effectively decoupled from the equations for  $\mathbf{u}$  and  $p$ ; these latter become simply

$$\rho \frac{D\mathbf{u}}{Dt} = -\nabla p + \mu \nabla^2 \mathbf{u} + \rho \mathbf{f}, \quad \nabla \cdot \mathbf{u} = 0. \quad (2.1)$$

If the body force  $\mathbf{f}$  is irrotational, then writing  $\mathbf{f} = -\nabla V$ , these equations further simplify to the form

$$\frac{D\mathbf{u}}{Dt} = -\nabla P + \nu \nabla^2 \mathbf{u}, \quad \nabla \cdot \mathbf{u} = 0, \quad (2.2)$$

where

$$P = p/\rho + V, \quad \nu = \mu/\rho, \quad \text{and} \quad \frac{D}{Dt} = \frac{\partial}{\partial t} + \mathbf{u} \cdot \nabla. \quad (2.3)$$

$\nu$  is called the kinematic viscosity; by analogy,  $P$  might be called the "modified kinematic pressure", modified in that it includes the effect of any body force potential, kinematic in that it is divided by  $\rho$ .

The incompressibility assumption  $\nabla \cdot \mathbf{u} = 0$  is known to be accurate in steady flows if the fluid velocity is everywhere small in magnitude compared with the speed of sound  $c_s$  in the fluid; and in unsteady flows, provided the time-scale of the phenomenon under consideration is large compared with the time for a sound wave to traverse the region of interest. Neglect of compressibility effects is equivalent to filtering out sound waves from the governing equations; in the incompressibility limit, sound waves travel at infinite speed, and effects can be transmitted instantaneously from one point in a fluid to another. One shouldn't of course worry unduly about this apparently unphysical behaviour; one must just trust that the behaviour becomes "physical" again if compressibility effects in all their complexity are restored to the governing equations. In any event, for better or for worse, we shall for the most part neglect compressibility effects in all that follows.

## 2.2 Rectilinear Flows

A rectilinear flow, as the name suggests, is one in which the streamlines are *straight*. For such a flow of an incompressible fluid the velocity is constant in magnitude and direction following a streamline, i.e.  $(\mathbf{u} \cdot \nabla)\mathbf{u} \equiv 0$ . Hence (2.2) becomes

$$\frac{\partial \mathbf{u}}{\partial t} = -\nabla P + \nu \nabla^2 \mathbf{u}, \quad \nabla \cdot \mathbf{u} = 0. \quad (2.4)$$

If the flow is everywhere parallel to, say, the  $x$ -axis, then  $\mathbf{u} = (u(y, z, t), 0, 0)$  and evidently  $\partial P/\partial y = \partial P/\partial z = 0$ , and  $\partial P/\partial x = -G(t)$ , say. We then have

$$\frac{\partial u}{\partial t} = G(t) + \nu \nabla^2 u. \quad (2.5)$$

The following flows, in which  $u = u(y, t)$  only, are typical of flows governed by this equation.

*i) Poiseuille flow;  $G = \text{const.}$ ,  $u = 0$  on  $y = 0, b$*

This is pressure driven flow in a two-dimensional channel; note the “no-slip” condition  $u = 0$  on the walls  $y = 0, b$ . The steady solution of (2.5) is simply

$$u(y) = \frac{G}{2\nu} y(y - b), \quad (2.6)$$

the well-known “parabolic profile” (figure 2.1a). The total flux in the channel per unit width in the  $z$ -direction is

$$Q_1 = \int_0^b u \, dy = \frac{Gb^3}{12\nu}. \quad (2.7)$$

*ii) Couette flow;  $G = 0$ ,  $u = 0$  on  $y = 0$ ,  $u = U$  on  $y = b$*

The steady solution of (2.5) is, trivially, (figure 2.1b),

$$u(y) = Uy/b, \quad (2.8)$$

and the flux in this case is

$$Q_2 = \frac{1}{2}Ub. \quad (2.9)$$

*iii) Flow due to an oscillating plane boundary  $G = 0$ ,  $u = 0$  on  $y = 0$ ,*

$$u = R(u_0 e^{int}) \text{ on } y = b$$

The solution of (2.5) is

$$u(y, t) = R \left( u_0 \frac{\sin \lambda y}{\sin \lambda b} e^{int} \right) \quad (2.10)$$

where

$$\lambda = \sqrt{n/2\nu} (1 - i). \quad (2.11)$$

The nature of this solution depends critically on the value of the parameter  $m = (n/\nu)^{1/2}b$ . If  $m \ll 1$ ,

$$u(y, t) \sim R(u_0(y/b)e^{int}), \quad (2.12)$$

i.e. we have at each instant a linear velocity profile (figure 2.1c) determined instantaneously by the motion of the boundary.

If  $m \gg 1$ , by contrast, we have

$$u(y, t) \sim u_0 \cos(nt + k(y - b)) e^{-k(b-y)}, \quad (2.13)$$

where  $k = \sqrt{n/v}$ . In this case (figure 2.1d), viscous effects diffuse only a small distance  $O(\sqrt{v/n})$  into the fluid.

iv) *Flow due to impulsive motion of a boundary (Rayleigh problem)*

$$G = 0, u(y, t) = 0 \text{ for } t < 0, u(0, t) = U \text{ for } t > 0, u(\infty, t) = 0$$

For dimensional reasons, the solution to this problem must have the form

$$u = Uf(\eta), \quad \eta = y/2\sqrt{vt}. \quad (2.14)$$

Substitution in (2.5) leads to an ordinary differential equation for with solution, satisfying  $f(0) = 1, f(\infty) = 0$ ,

$$f(\eta) = 1 - \operatorname{erf} \eta, \quad \operatorname{erf} \eta = \frac{2}{\sqrt{\pi}} \int_0^\eta e^{-\xi^2} d\xi. \quad (2.15)$$

The solution describes the diffusion of a velocity discontinuity (or "vortex sheet") initially concentrated on  $y = 0$ ; the thickness of the sheet at time  $t$  is evidently  $O(\sqrt{vt})$  (figure 2.1e).

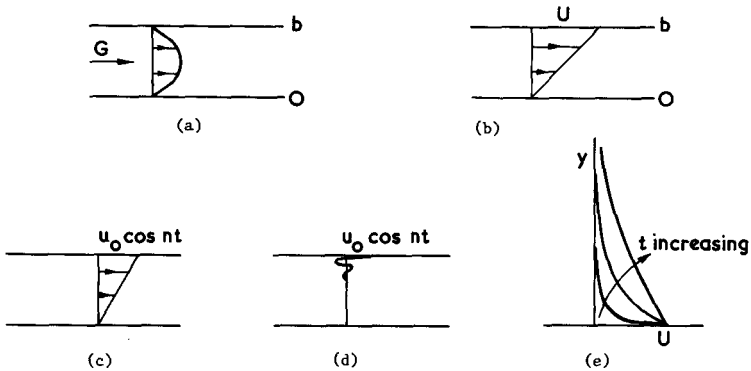


**Figure 2.1** Typical velocity profiles for rectilinear flow: (a) Poiseuille flow; (b) Couette flow; (c) oscillating boundary  $m \ll 1$ ; (d)  $m \gg 1$ ; (e) Rayleigh problem

### 2.3 Flow Between Rotating Cylinders

Suppose that fluid is contained between two long coaxial circular cylinders of radii  $a$  and  $b$  rotating with angular velocities  $\Omega_1$  and  $\Omega_2$  about their

common axis (figure 2.2). The equations of motion admit a steady solution of the form

$$\mathbf{u} = (0, v(r), 0) = v(r)\hat{\mathbf{e}}_\theta \quad (2.16)$$

in cylindrical polar coordinates  $(r, \theta, z)$ ; we use  $\hat{\mathbf{e}}_r, \hat{\mathbf{e}}_\theta, \hat{\mathbf{e}}_z$  to denote unit vectors in the  $(r, \theta, z)$  directions respectively. The streamlines of the flow (2.16) are circular; moreover

$$(\mathbf{u} \cdot \nabla)\mathbf{u} = -\frac{v^2}{r}\hat{\mathbf{e}}_r, \quad \nabla^2\mathbf{u} = \hat{\mathbf{e}}_\theta \left( \nabla^2 - \frac{1}{r^2} \right) v. \quad (2.17)$$

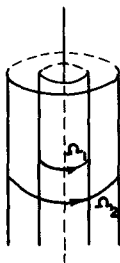


Figure 2.2 Flow between rotating cylinders

Hence from (2.2)

$$\frac{dP}{dr} = \frac{v^2}{r} \quad \text{and} \quad \left( \nabla^2 - \frac{1}{r^2} \right) v = 0. \quad (2.18)$$

The solution for  $v(r)$  satisfying the boundary conditions

$$v(a) = \Omega_1 a, \quad v(b) = \Omega_2 b \quad (2.19)$$

is

$$v = Ar + \frac{B}{r} \quad (2.20)$$

where

$$A = \frac{\Omega_1 a^2 - \Omega_2 b^2}{a^2 - b^2}, \quad B = \frac{(\Omega_1 - \Omega_2)a^2 b^2}{b^2 - a^2}. \quad (2.21)$$

Note that if  $a = 0$  then  $B = 0$  and  $A = \Omega_2$  and, as expected, the fluid rotates as if rigid with angular velocity  $\Omega_2$ . If  $b = \infty$  and the fluid is at rest "at infinity", then  $v = \Omega_1 a^2/r$ ; this is an *irrotational flow* ( $\nabla \wedge \mathbf{u} = 0$ ); a small arrow suspended in the fluid would remain fixed in direction in this flow while swept round on a circular streamline.

The simple flow described by (2.20) and (2.21) is unstable (and therefore unrealisable in the laboratory) if  $\Omega_1$  is increased beyond a certain critical value (other parameters being kept constant); the nature of the instability, and the behaviour of the flow when  $\Omega_1$  is *much* greater than the critical value for the onset of instability, are topics of great interest, to which I shall return in a later lecture. I should just point out at this stage that the existence of a steady solution of the equations of motion for given steady boundary conditions is no guarantee that the corresponding flow will be realised in practise; its stability is a matter of primary importance. Similarly, an unsteady solution such as (2.8) may be unrealisable due to instability; but the analytical treatment of the stability of a basically unsteady flow poses severe problems that are by no means as yet fully understood.

## 2.4 The Round Jet

If the body force distribution  $\mathbf{f}$  is steady and concentrated at a single point in a fluid of infinite extent, then a jet-type flow is generated with an axis of symmetry determined by the direction of the point force. The point force is of course an idealisation, but it is realised approximately when fluid is pumped at high speed  $U$  from a circular tube of small radius  $\delta$  into an expanse of the same fluid. If  $U \rightarrow \infty$  and  $\delta \rightarrow 0$  in such a way that  $U\delta^2 \rightarrow 0$  and  $U\delta$  remains finite, then in the limit we have a point source of momentum, and zero source of mass. Taking  $\rho\mathbf{f} = \mathbf{F}\delta(\mathbf{x})$ , the steady momentum balance, from (1.17), is given by

$$\int_S (\rho u_i u_j - \sigma_{ij}) n_j dS = F_i, \quad (2.22)$$

where  $S$  is any surface surrounding the point  $\mathbf{x} = 0$ .

Let  $(r, \theta, \varphi)$  be spherical polar coordinates based on the axis of symmetry, with  $r = |\mathbf{x}|$ , and let  $\mathbf{u} = (u, v, 0)$  in these coordinates. The incompressibility condition  $\nabla \cdot \mathbf{u} = 0$  is satisfied through the introduction of the *Stokes stream function*  $\psi(r, \theta)$  such that

$$u = \frac{1}{r^2 \sin \theta} \frac{\partial \psi}{\partial \theta}, \quad v = -\frac{1}{r \sin \theta} \frac{\partial \psi}{\partial r}. \quad (2.23)$$

The streamlines of the flow are then given by  $\psi = \text{const}$ . The form of  $\psi(r, \theta)$  for this flow is constrained by dimensional considerations. The only dimensional quantities appearing in the definition of the problem are  $F$ ,  $\rho$  and  $\nu$ , with dimensions  $MLT^{-2}$ ,  $ML^{-3}$  and  $L^2T^{-1}$  respectively; note that (i) the quantity

$$R = \left(\frac{F}{\rho}\right)^{1/2} \frac{1}{\nu} \quad (2.24)$$

is dimensionless and (ii) it is not possible to construct out of  $F$ ,  $\rho$  and  $\nu$  a single quantity having the dimensions of a length, i.e. *there is no natural length-scale in the problem*. It follows that  $\psi$ , which has dimensions  $L^3 T^{-1}$  must be expressible in the form

$$\psi = r\nu f(\theta, R) \tag{2.25}$$

for some function  $f$ .

This function satisfies a fourth-order non-linear ordinary differential equation obtained by substituting (2.23) and (2.25) in the curl of the Navier-Stokes equation (2.2a). It is an astonishing fact that this fourth order equation can be integrated four times to give the solution to the problem:

$$f(\theta, R) = \frac{2 \sin^2 \theta}{1 + c - \cos \theta}, \tag{2.26}$$

where  $c$  is a constant of integration; (the other three constants of integration are all determined by the condition that the velocity be finite for  $r \neq 0$  on  $\theta = 0$  and on  $\theta = \pi$ );  $c$  depends on  $R$  in a way that is determined by the condition (2.22):

$$\frac{1}{2\pi} R^2 = 8(1 + c) + \frac{32(1 + c)}{3c(2 + c)} + 4(1 + c)^2 \log \frac{c}{2 + c}. \tag{2.27}$$

The right-hand side of (2.27) is a monotonic decreasing function of  $c$ , which behaves like  $8/c$  as  $c \rightarrow \infty$  and like  $16/c$  as  $c \rightarrow 0$  (figure 2.3).

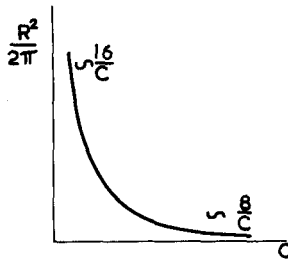


Figure 2.3 The function  $R(c)$

The character of the flow described by (2.25) – (2.27) depends on the value of the parameter  $R$  (the *Reynolds number* of the flow). If  $R \ll 1$ , then  $c \gg 1$ , and

$$\psi \sim \frac{2r\nu}{c} \sin^2 \theta = \frac{F}{8\pi\mu} r \sin^2 \theta. \tag{2.28}$$

The velocity field determined by this stream-function is symmetric about the plane  $\theta = \pi/2$  (figure 2.4a), and has an  $r^{-1}$  type of singularity at  $r = 0$ , known as a *stokeslet*. (Contrast the  $r^{-3}$  singularity associated with a dipole.)

As  $R$  increases, the flow becomes asymmetric about the plane  $\theta = \pi/2$ , and for  $R \gg 1$  this asymmetry is very marked (figure 2.4b). In this limit,  $c \ll 1$ , and  $f$  is sharply peaked in the neighbourhood of  $\theta = 0$  where  $\cos \theta \approx 1$ . In this neighbourhood,

$$f \sim \frac{2\theta^2}{c + \frac{1}{2}\theta^2} \quad \text{and} \quad u \sim \frac{4v}{r(c + \frac{1}{2}\theta^2)}, \quad (2.29)$$

and the velocity is large in a conical region whose angle is of order  $c^{1/2} \sim 32\pi(\rho/F)^{1/2}v$ .

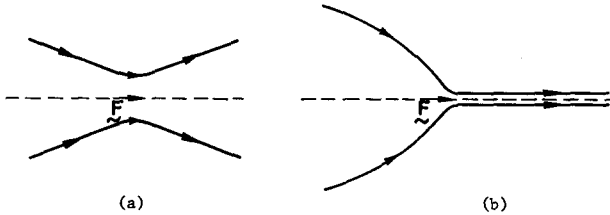


**Figure 2.4** Flow due to the application of a point force  $F$ : (a)  $R \ll 1$ , the stokeslet; (b)  $R \gg 1$ , the circular jet

### Lecture 3 Flows in which Inertia Forces are Negligible†

#### 3.1 The Reynolds Number

A steady flow of a viscous fluid bounded only by surfaces on which the velocity is prescribed is characterised by a balance between inertia forces, pressure forces and viscous forces. Let  $U$  be a typical velocity and let  $L$  be a typical length-scale (over which the velocity varies by an amount of order  $U$ ); then

$$(\mathbf{u} \cdot \nabla)\mathbf{u} = 0 \left( \frac{U^2}{L} \right), \quad |\nabla^2 \mathbf{u}| = 0 \left( \frac{U}{L^2} \right), \quad (3.1)$$

†I was influenced in my choice of some of the topics in this chapter by G. I. Taylor's film "Low Reynolds Number Flow" which was shown during an afternoon discussion session.

and so the ratio of the inertia force to the viscous force is

$$\frac{|\mathbf{u} \cdot \nabla \mathbf{u}|}{|\nu \nabla^2 \mathbf{u}|} = 0 \left( \frac{UL}{\nu} \right). \quad (3.2)$$

This is of course a very preliminary estimate, and there may be regions of the flow in which it is quite wrong. However it would seem reasonable to proceed on the assumption that, at least in a first approximation, inertia forces will be negligible provided

$$R \equiv \frac{UL}{\nu} \ll 1. \quad (3.3)$$

$R$  is the *Reynolds number* characterising the flow. Two flows are said to be *dynamically similar* if (i) they are geometrically similar both as regards the configuration and instantaneous velocity distribution of the boundaries and (ii) they have the same Reynolds numbers. In this situation, the flows are identical if the space variables are scaled on  $L$  and the velocity variables scaled on  $U$ .

There are circumstances when the criterion (3.3) is unnecessarily stringent for the neglect of inertia forces. For example, we know that the inertia force is identically zero for any rectilinear flow. In a flow which is *nearly* rectilinear, (3.1a) will in general be an overestimate of  $|\mathbf{u} \cdot \nabla \mathbf{u}|$ . It turns out in this situation that inertia forces are negligible provided

$$R\alpha \ll 1 \quad (3.4)$$

where  $\alpha$  is a measure of the small angle between an actual streamline of the flow and a streamline of the rectilinear flow to which it approximates.

In an air or water flow, when  $U$  is of the order of centimetres per second, the Reynolds number is small only if  $L$  is extremely small ( $\ll 1$  mm. in air,  $\ll 0.1$  mm. in water). Almost the only problems of practical interest at this sort of length-scale are those associated with the motion of small particles (or drops or bubbles) suspended in the fluid. In a viscous fluid such as glycerine,  $R$  is small when  $U \sim 1$  cm./sec. provided  $L \ll 10$  cm.; laboratory experiments in which the flow may be readily visualised are clearly possible in these conditions. Extremely viscous fluids, such as pitch ( $\nu \sim 10^{10}$  cm<sup>2</sup>/sec.) invariably flow at very small Reynolds number. Ice flows provide a natural example of low Reynolds number flows of quite large length-scale. Extremely slow thermal convection in the Earth's mantle may provide another example of low Reynolds number flow on an even larger length-scale ( $L \sim 10^7$  cm.,  $U \sim 10^{-3}$  cm./sec.,  $\nu \sim 10^{10}$  cm<sup>2</sup>/sec.,  $R \sim 10^{-6}$ !).

In an *unsteady* flow, it may happen that  $\mathbf{u} \cdot \nabla \mathbf{u}$  is negligible in the equation of motion, but that  $\partial \mathbf{u} / \partial t$  is not. For example, in a periodic flow with fre-

quency  $n$ ,  $\partial \mathbf{u} / \partial t = 0(nU)$ , so that

$$\frac{|\partial \mathbf{u} / \partial t|}{|\nu \nabla^2 \mathbf{u}|} = 0 \left( \frac{nL^2}{\nu} \right). \quad (3.5)$$

The flow is *quasi-steady* (cf. §2.2(iii)) if

$$m \equiv \frac{nL^2}{\nu} \ll 1. \quad (3.6)$$

Dynamical similarity of two unsteady flows requires (in addition to geometrical similarity) that they have the same value of  $m$  as well as the same value of  $R$ .

We shall suppose in the following sections that both the criteria (3.3) and (3.6) are satisfied, so that the total inertia force  $\rho \mathbf{D}\mathbf{u}/\mathbf{D}t$  in the equation of motion is negligible, and we shall explore some of the consequences.

### 3.2 Uniqueness, Minimum Dissipation, Reversibility and Reciprocity

The *Stokes equations* are just the Navier–Stokes equations without the inertia term, viz.

$$\nabla p = \mu \nabla^2 \mathbf{u}, \quad \nabla \cdot \mathbf{u} = 0. \quad (3.7)$$

Equivalently, in terms of  $\sigma_{ij}$  and the rate of strain tensor

$$e_{ij} = \frac{1}{2} \left( \frac{\partial u_i}{\partial x_j} + \frac{\partial u_j}{\partial x_i} \right), \quad \frac{\partial}{\partial x_j} \sigma_{ij} = 0, \quad \sigma_{ij} = -p\delta_{ij} + 2\mu e_{ij}, \quad e_{kk} = 0. \quad (3.8)$$

#### i) Uniqueness

The solution of (3.7) subject to a boundary condition  $\mathbf{u} = \mathbf{U}(\mathbf{x})$  on the surface  $S$  of the volume  $V$  occupied by the fluid is unique; this may be proved by showing that

$$2\mu \int_V \tilde{e}_{ij} \tilde{e}_{ij} dV = \int_V \tilde{\sigma}_{ij} \tilde{e}_{ij} dV = 0, \quad (3.9)$$

where the tilde  $\sim$  indicates the difference between two fields satisfying (3.8), and  $\tilde{\mathbf{u}} = 0$  on  $S$ . The theorem is interesting if only because there is *no* such theorem for the full Navier–Stokes equation; indeed there is at least one well-known example of a geometry (flow between rotating cylinders) for which two quite distinct steady flows are possible solutions of the Navier–Stokes equations satisfying the same boundary conditions (only one of these flows generally being stable). The uniqueness theorem for Stokes flows is of practical value in that it provides a justification for more or less any method of finding a solution to a particular problem.

ii) *Minimum dissipation*

A closely related theorem is the following: let  $(\mathbf{u}, p)$  satisfy (3.7) and  $\mathbf{u} = \mathbf{U}(\mathbf{x})$  on  $S$ , and let  $(\mathbf{u}', p')$  satisfy merely  $\nabla \cdot \mathbf{u}' = 0$  and  $\mathbf{u}' = \mathbf{U}(\mathbf{x})$  on  $S$ . Then the rate of viscous dissipation associated with the  $\mathbf{u}$ -field, (see equations (1.37), (1.39)),

$$\Phi = 2\mu \int_V e_{ij} e_{ij} dV, \quad (3.10)$$

is less than the corresponding expression for the  $\mathbf{u}'$ -field (unless  $\mathbf{u}'$  is identical with  $\mathbf{u}$ ). In other words, the Stokes flow has a smaller dissipation than any other kinematically possible flow satisfying the same boundary conditions. In particular, since the Stokes flow is only an approximation to the real flow, the rate of dissipation of energy that is actually realised in a flow must be greater than that predicted by the Stokes solution. This result is interesting in that it puts a lower bound on the rate of working of external torques and forces required to maintain the motion of fluid boundaries.

iii) *Reversibility*

The linearity of the equations (3.7) and of the boundary condition  $\mathbf{u} = \mathbf{U}(\mathbf{x})$  on  $S$  clearly implies a linear relation of the form

$$u_i(\mathbf{x}) = \int_S G_{ij}(\mathbf{x}, \xi) U_j(\xi) dS(\xi) \quad (3.11)$$

where  $G_{ij}(\mathbf{x}, \xi)$  is determined solely by the instantaneous configuration of the fluid boundaries. Hence if the boundary motion is instantaneously reversed ( $\mathbf{U}(\xi) \rightarrow -\mathbf{U}(\xi)$ ) then the fluid velocities are everywhere reversed:

$$\mathbf{u}(\mathbf{x}) \rightarrow -\mathbf{u}(\mathbf{x}).$$

iv) *Reciprocity*

Let  $(u_i, \sigma_{ij})$  and  $(u'_i, \sigma'_{ij})$  be the velocity and stress fields corresponding to two Stokes flows in a region bounded by a surface  $S$ . Then it follows almost immediately from (3.8) and similar equations for the dashed fields that

$$\int_S \sigma_{ij} u'_j n_i dS = \int_S \sigma'_{ij} u_j n_i dS. \quad (3.12)$$

As an application of this result, let  $(u_i, \sigma_{ij})$  be the velocity and stress fields due to the motion of a particle of arbitrary shape with velocity  $U_i$ , and let  $(u'_i, \sigma'_{ij})$  correspond to velocity  $U'_i$  of the same particle. Assuming that  $u_i$  and  $u'_i$  are  $O(r^{-1})$  and that  $\sigma_{ij}$  and  $\sigma'_{ij}$  are  $O(r^{-2})$  as  $r \rightarrow \infty$  (cf. the velocity field of §2.4 associated with the application of a point force to the fluid), there is no contribution to the integrals in (3.12) from the surface at infinity. Moreover  $u'_j = U'_j$  on  $S$  and  $\int_S \sigma_{ij} n_i dS$  is the force  $F_j$  on the particle when it moves

with velocity  $U_j$ ; hence (3.12) becomes

$$U'_j F_j = U_j F'_j. \quad (3.13)$$

Slightly modified arguments lead to the similar results

$$\Omega'_j G_j = \Omega_j G'_j, \quad \Omega'_j G_j = U_j F'_j, \quad (3.14)$$

where  $G_j$  is the torque experienced by a particle which rotates with angular velocity  $\Omega_j$ , and  $G'_j$  corresponds to  $\Omega'_j$  for the same particle.

### 3.3 Motion of a Particle of Arbitrary Shape †

Suppose that a particle of arbitrary shape (surface  $S$ ) moves in an arbitrary manner in a viscous fluid. At a given instant suppose that its centre of volume ( $\mathbf{x} = 0$ ) moves with velocity  $\mathbf{U}$  and that its angular velocity is  $\boldsymbol{\Omega}$ . Then

$$\mathbf{u} = \mathbf{U} + \boldsymbol{\Omega} \wedge \mathbf{x} \text{ on } S, \quad \text{and } \mathbf{u} \rightarrow 0 \text{ at } \infty. \quad (3.15)$$

The solution to the Stokes equations subject to these boundary conditions is unique, and we can then calculate (in principle)  $e_{ij}$  and  $\sigma_{ij}$  and thence the force and torque on the particle:

$$F_i = \int_S \sigma_{ij} n_j \, dS, \quad G_i = \int_S \epsilon_{ijk} x_j \sigma_{ke} n_e \, dS. \quad (3.16)$$

The linearity of the problem implies that  $\mathbf{F}$  and  $\mathbf{G}$  will be linearly related to  $\mathbf{U}$  and  $\boldsymbol{\Omega}$ , i.e.

$$F_i = -\mu(A_{ij}U_j + B_{ij}\Omega_j), \quad G_i = -\mu(C_{ij}U_j + D_{ij}\Omega_j), \quad (3.17)$$

where  $A_{ij}, \dots, D_{ij}$  depend only on the size and shape of the particle. The results (3.13) and (3.14) immediately imply that

$$A_{ij} = A_{ji}, \quad D_{ij} = D_{ji}, \quad C_{ij} = B_{ji}. \quad (3.18)$$

(For example, to prove the third of these let  $\mathbf{G}$  be the torque on the particle when it translates without rotation, and let  $\mathbf{F}$  be the force on the particle when it rotates without translation, and apply (3.14b).)

#### *Translation without rotation*

If  $\boldsymbol{\Omega} = 0$ , then

$$F_i = -\mu A_{ij}U_j. \quad (3.19)$$

---

†For a very detailed treatment of the material of this section, see Happel and Brenner (1965).

Since  $A$  is symmetric, there exist three mutually orthogonal axes fixed in the particle with respect to which  $A$  is diagonal; since  $A$  has the dimensions of length, we write, with respect to these axes,

$$A_{ij} = a \begin{pmatrix} \lambda^{(1)} & \cdot & \cdot \\ \cdot & \lambda^{(2)} & \cdot \\ \cdot & \cdot & \lambda^{(3)} \end{pmatrix} = a \operatorname{diag} \{ \lambda^{(1)}, \lambda^{(2)}, \lambda^{(3)} \}, \quad (3.20)$$

where  $\lambda^{(1)}, \lambda^{(2)}, \lambda^{(3)}$  are dimensionless numbers determined solely by the shape of the particle. Hence the components of  $\mathbf{F}$  relative to these principle axes are

$$\mathbf{F} = -\mu a (\lambda^{(1)} U_1, \lambda^{(2)} U_2, \lambda^{(3)} U_3). \quad (3.21)$$

Since  $-\mathbf{F} \cdot \mathbf{U}$  is the work done by the particle on the fluid, and this is certainly positive (being equal to the instantaneous rate of viscous dissipation in the fluid), the  $\lambda$ 's are all positive.

A case of particular interest is the particle with *cubic symmetry* (i.e. a particle which occupies a region of space which is invariant under the group of rotations of the cube); the cube itself of course exhibits this symmetry, as does a sphere. In this case  $A_{ij}$  is isotropic, so that

$$A_{ij} = \lambda a \delta_{ij}, \quad (3.22)$$

where  $\lambda$  is a number of order unity, and so

$$\mathbf{F} = -\lambda \mu a \mathbf{U}. \quad (3.23)$$

It is a remarkable consequence of this result that a particle with cubic symmetry will fall without rotation through a viscous fluid at a terminal speed  $U$  independent of the orientation of the particle relative to the vertical. A moment's reflection (perhaps more than a moment!) will convince you that the same is true for a particle exhibiting the same degree of symmetry as any of the other regular solids (tetrahedron, octahedron etc.). Note that, for a sphere (which, with its exceptional degree of symmetry, is amenable to elementary analysis—see §3.4),  $\lambda = 6\pi$ .

For certain other shapes of particles, the directions of the principle axes will be evident for reasons of symmetry. For example, for an ellipsoidal particle, the principle axes of  $A_{ij}$  are clearly the principle axes of the ellipsoid. The detailed solution for this case was obtained by Jeffery (1922); an interesting feature of the solution is that for a long thin ellipsoid of revolution,  $\lambda^{(1)} = \lambda^{(2)} = 2\lambda^{(3)}$  where the 3-axis is along the axis of symmetry; this means that the resistance to motion parallel to its length is half that perpendicular to its length; this result is in fact true for any "long thin" particle (Tillett, 1970).

In addition to the force given by (3.19), the arbitrary particle experiences

a torque, even when  $\Omega = 0$ , given by

$$G_i = -\mu C_{ij} U_j, \quad (3.24)$$

Note that since  $\mathbf{U}$  is a polar vector and  $\mathbf{G}$  an axial vector,  $C_{ij}$  is a pseudotensor, and is non-zero only for particles which exhibit a lack of reflexional symmetry; a helical particle may be regarded as the prototype. Clearly a helical particle constrained to move parallel to its axis without rotation will experience a torque

$$G = -\mu a^2 \lambda' U \quad (3.25)$$

about the same axis, the sign of  $\lambda'$  depending on whether the helix is right-handed (giving  $\lambda' < 0$ ) or left-handed ( $\lambda' > 0$ ).

#### *Rotation without translation*

If  $\mathbf{U} = 0$ , then firstly

$$F_i = -\mu B_{ij} \Omega_j = -\mu C_{ji} \Omega_j, \quad (3.26)$$

The helical particle referred to above will experience a force

$$F = -\mu a^2 \lambda' \Omega, \quad (3.27)$$

parallel to the rotation  $\Omega$ . Some microorganisms generate a propulsive force by sending helical waves down their tails in order to exploit this mechanism!

The torque, when  $\mathbf{U} = 0$ , is given by

$$G_i = -\mu D_{ij} \Omega_j \quad (3.28)$$

and relative to the principle axes of  $D_{ij}$  (which need not coincide with those of  $A_{ij}$ !),

$$\mathbf{G} = -\mu a^3 (d^{(1)} \Omega_1, d^{(2)} \Omega_2, d^{(3)} \Omega_3). \quad (3.29)$$

Again, for particles of cubic symmetry,

$$\mathbf{G} = -\mu a^3 \lambda'' \Omega \quad (3.30)$$

where  $\lambda''$  is of order unity. For a sphere,  $\lambda'' = 8\pi$ .

### 3.4 The Translating Sphere

Suppose now that a sphere of radius  $a$  moves with velocity  $\mathbf{U}$  through a viscous fluid and that  $R \equiv Ua/\nu \ll 1$  so that, at any rate in the first instance, inertia forces may be neglected. The force on the sphere is given by (3.23); consequently the sphere exerts on the fluid a force

$$\mathbf{F}_1 = -\mathbf{F} = \lambda \mu a \mathbf{U}. \quad (3.31)$$

From the considerations of §2.4, we would therefore expect the stream

function  $\psi(r, \theta)$  for the resulting flow to include a "stokeslet" ingredient of the form

$$\psi_S = Sr \sin^2 \theta, \quad S = \lambda a U / 8\pi. \quad (3.32)$$

There is another well-known flow whose stream-function is proportional to  $\sin^2 \theta$ , viz. the flow due to a source dipole at  $r = 0$ , for which

$$\psi_d = \frac{D}{r} \sin^2 \theta, \quad (3.33)$$

where  $D$  is the dipole strength. The flow corresponding to  $\psi_d$  is irrotational and is certainly a possible solution of the Stokes equations. One might therefore hazard a guess that the flow due to the translating sphere has a stream-function of the form

$$\psi = \psi_S + \psi_d. \quad (3.34)$$

(Remember that, by the uniqueness theorem, the end justifies the means; there are of course more systematic procedures that lead to the same conclusions.)

The constants  $S$  and  $D$  must be determined from the boundary conditions on the sphere:

$$u = \frac{1}{r^2 \sin \theta} \frac{\partial \psi}{\partial \theta} = U \cos \theta, \quad v = -\frac{1}{r \sin \theta} \frac{\partial \psi}{\partial r} = -U \sin \theta \quad (3.35)$$

on  $r = a$ . These conditions lead to

$$S = \frac{3}{4} U a, \quad D = -\frac{1}{4} U a^3, \quad (3.36)$$

and comparison with (3.32) shows that

$$\lambda = 6\pi, \quad \mathbf{F} = -6\pi\mu a \mathbf{U}, \quad (3.37)$$

as mentioned in §3.3. This is the Stokes drag formula. It is frequently expressed in non-dimensional form in terms of a *drag coefficient*

$$C_D = \frac{|\mathbf{F}|}{\pi \rho U^2 a^2} = \frac{6}{R}. \quad (3.38)$$

This is of course only asymptotically valid for  $R \ll 1$ . The actual measured drag on a sphere when  $R = O(1)$  is somewhat greater than that given by (3.38) (consistent with the minimum dissipation theorem).

It would perhaps be misleading to leave this topic without mentioning a fundamental difficulty which was first treated by Oseen (1910), but which was only fully and finally resolved by Kaplun and Lagerstrom (1957) and Proudman and Pearson (1957). The difficulty is that the ratio of the inertia force to the viscous force at a large distance  $r$  from the sphere is  $O(Rr/a)$ ,

so that, no matter how small  $R$  may be, inertia forces predominate at a great distance. Proudman and Pearson used a technique now known as the method of matched asymptotic expansion, whereby different expansions for  $\psi(r, \theta)$  based on the small parameter  $R$  are used in the "inner region"  $r \ll a/R$  and the "outer region"  $r \gg a$ , and terms in the two expansions are successively identified in the region of common validity where  $a \ll r \ll a/R$ . This technique leads in principle to any number of terms of the asymptotic expansion for  $C_D$  of which (3.38) provides the first. Proudman and Pearson obtained the improved formula

$$C_D \sim \frac{6}{R} \left( 1 + \frac{3}{8}R + \frac{9}{40}R^2 \log R + O(R^2) \right), \quad (3.39)$$

which is in fact in reasonable agreement with measurements up to  $R \approx 1$ .

The difficulty referred to in the preceding paragraph is much more severe in the analogous two-dimensional problem of a circular cylinder moving perpendicular to its axis through viscous fluid. In this case, the Stokes equations have no solution satisfying the appropriate boundary conditions on the cylinder *and* at infinity and some consideration of inertia effects is necessary even to obtain the leading term in the expansion analogous to (3.39). The following asymptotic formula, analogous to (3.39), was obtained by Kaplun (1957) for the force  $F$  per unit length of cylinder:

$$C_D = \frac{F}{2\rho U^2 a} \sim \frac{16\pi}{R} \epsilon (1 + a_2 \epsilon^2 + O(\epsilon^3)), \quad (3.40)$$

where

$$\epsilon = \frac{1}{\log 8/R + \frac{1}{2} - \gamma}, \quad \gamma \doteq 0.58 \text{ (Euler's constant)}, \quad a_2 \doteq -0.87.$$

The complexity of this formula is indicative of the complexity of the underlying analysis.

### 3.5 Flow Near a Sharp Corner

Flow sufficiently near a sharp corner is invariably dominated by viscous forces, since the velocity certainly falls to zero as the corner is approached. The structure of the flow has a universal form sufficiently near the corner, and this form is so peculiar that it seems to deserve mention. We restrict attention to plane flow in the angle between rigid planes  $\theta = \pm\alpha$ , the flow having the symmetry indicated in figure (3.1). It is natural to use polar coordinates  $(r, \theta)$  and a stream-function  $\psi(r, \theta)$  in terms of which the velocity

components are

$$u = \frac{1}{r} \frac{\partial \psi}{\partial \theta}, \quad v = -\frac{\partial \psi}{\partial r}. \quad (3.41)$$

The vorticity  $\omega = \nabla \wedge \mathbf{u}$  is then given by

$$\omega = -\nabla^2 \psi \mathbf{k} \quad (3.42)$$

where  $\mathbf{k}$  is a unit vector parallel to the corner. The Stokes equations (3.7) imply that  $\nabla^2 \omega = 0$ , so that, from (3.42),

$$\nabla^4 \psi \equiv \nabla^2(\nabla^2 \psi) = 0. \quad (3.43)$$

This is the *biharmonic equation*.

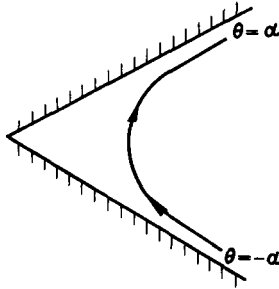


Figure 3.1 Flow in a corner

We anticipate that, sufficiently near  $r = 0$ ,

$$\psi \sim r^\lambda f(\theta) \quad \text{for some } \lambda. \quad (3.44)$$

Substitution in (3.43) gives a fourth-order ordinary differential equation for  $f(\theta)$  with general solution

$$f(\theta) = A \cos \lambda \theta + B \sin \lambda \theta + C \cos(\lambda - 2)\theta + D \sin(\lambda - 2)\theta. \quad (3.45)$$

The particular symmetry of the flow implies that  $f(\theta) = f(-\theta)$ , i.e. that  $B = D = 0$ . Moreover both velocity components must vanish on  $\theta = \pm\alpha$ , so that  $f(\alpha) = f'(\alpha) = 0$ . These conditions give two linear homogeneous equations for  $A$  and  $C$ ; the determinantal condition for a non-trivial solution reduces to

$$\sin 2(\lambda - 1)\alpha = -(\lambda - 1) \sin 2\alpha, \quad (3.46)$$

The interesting feature of (3.46), pointed out by Dean and Montagnon (1949), is that if  $2\alpha$  is less than a critical angle  $2\alpha_c$  (approximately  $146^\circ$ ) there is no real solution for  $\lambda$ . There are however complex solutions; (3.44) is then complex, but since the problem is linear we may focus attention on its real part. The question remains to interpret the meaning of a complex  $\lambda$  in terms of the structure of the flow.

Putting  $\lambda = p + iq$ , we have

$$\psi \sim R(r^{p+iq}f(\theta)) = R(r^p e^{iq \log r} f(\theta)), \quad (3.47)$$

and so the transverse velocity on  $\theta = 0$  is

$$v(r, 0) = - \left( \frac{\partial \psi}{\partial r} \right)_{\theta=0} \sim cr^{p-1} \sin(q \log r + \epsilon), \quad (3.48)$$

where  $c$  and  $\epsilon$  are constants which are presumably determined by conditions far from the corner. As  $r \rightarrow 0$ ,  $v(r, 0)$  oscillates infinitely rapidly; at first sight this appears most remarkable in a region where viscous forces might be expected to smooth out velocity gradients; but in fact the factor  $r^{p-1}$  always implies such a rapid damping of  $|v|$  as  $r \rightarrow 0$  that not more than two or three of the oscillations will ever be physically significant. The solution (3.44) with  $\lambda$  complex describes an infinite sequence of geometrically and dynamically similar eddies (figure 3.2), having a sort of triangular structure. The values of  $p$  and  $q$  for different values of  $\alpha$  can be obtained numerically from (3.46) (for details, see Moffatt 1964). For example, when  $\alpha = 15^\circ$ ,  $p \approx 8$ ,  $q \approx 4$ . As the corner is approached the intensity from one eddy to the next falls by a factor  $e^{\pi(p-1)/q}$  and this is of order 300 or greater for all  $\alpha$ . This explains why it is difficult to observe more than one or two eddies in practice. Of course the steady flow would really take an infinite time to establish starting from a state of rest. If a cylinder is rotated at say one revolution per 10 seconds, the  $n$ th eddy in the sequence will appear after a

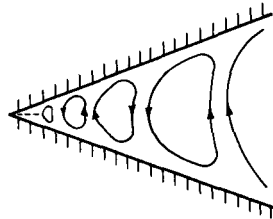


Figure 3.2 Viscous corner eddies

time of order  $10 \times (300)^n$  seconds. Work this out for  $n = 4$ , and you'll see why the fourth eddy hasn't yet been observed!

### 3.6 Flow in a Thin Film

It was mentioned above that inertia forces should be negligible in any nearly rectilinear flow. Suppose for example that fluid is contained in the gap between a fixed surface  $y = 0$  and a moving surface  $y = h(x, t)$  where  $|\partial h/\partial x| \ll 1$ . Let  $(U, V)$  be the velocity components on the moving surface, satisfying  $V = \partial h/\partial t + U\partial h/\partial x$ , and let  $\psi(x, y)$  be the stream-function for the flow in the gap. Since  $|\partial\psi/\partial y| \gg |\partial\psi/\partial x|$  and *a fortiori*  $|\partial^2\psi/\partial y^2| \gg |\partial^2\psi/\partial x^2|$  when conditions vary slowly in the  $x$ -direction, the biharmonic equation  $\nabla^4\psi = 0$  degenerates to the approximate form  $\partial^4\psi/\partial y^4 = 0$ , which integrates to give

$$\frac{\partial^3\psi}{\partial y^3} \left( = \frac{\partial^2 u}{\partial y^2} \right) = -\frac{G(x, t)}{\mu}. \quad (3.49)$$

By comparison with (2.4), it is clear that we must identify  $G(x, t)$  with the local pressure gradient  $-\partial p/\partial x$ , which must in this approximation be independent of the transverse coordinate  $y$ . Two further integrations of (3.49) with boundary conditions  $u = 0$  on  $y = 0$ ,  $u = U$  on  $y = h(x, t)$  lead to the Poiseuille–Couette profile

$$u(x, y, t) = -\frac{G(x, t)}{2\mu}y(y-h) + U\frac{y}{h}. \quad (3.50)$$

The flux across the section  $x = \text{const.}$  (cf. (2.7) and (2.9)) is then

$$Q(x, t) = \int_0^{h(x,t)} u(x, y, t) dy = \frac{G(x, t)}{12\mu}h^3 + \frac{1}{2}Uh. \quad (3.51)$$

Now it is evident from mass conservation that

$$\frac{\partial Q}{\partial x} = -\frac{\partial h}{\partial t} = U\frac{\partial h}{\partial x} - V, \quad (3.52)$$

and hence, from (3.51), with  $G = -\partial p/\partial x$ ,

$$\frac{\partial}{\partial x} \left( h^3 \frac{\partial p}{\partial x} \right) = 6\mu \left[ h \frac{\partial U}{\partial x} + U \frac{\partial h}{\partial x} + 2 \frac{\partial h}{\partial t} \right]. \quad (3.53)$$

This is *Reynolds' equation* which determines in principle the pressure distribution  $p(x, t)$  in the gap if  $h$  and  $U$  are prescribed.

If the moving surface has the more general form  $y = h(x, z, t)$  and if its

velocity components are  $(U, V, W)$  with

$$V = \frac{\partial h}{\partial t} + U \frac{\partial h}{\partial x} + W \frac{\partial h}{\partial y} \quad (3.54)$$

then the pressure  $p(x, z, t)$  in the gap is determined by the slightly more general equation

$$\nabla \cdot (h^3 \nabla p) = 6\mu \left[ h \nabla \cdot \mathbf{U} + \mathbf{U} \cdot \nabla h + 2 \frac{\partial h}{\partial t} \right]. \quad (3.55)$$

### *The thrust bearing*

A simple illustration of the application of (3.55) is provided by the “thrust bearing”, alternatively called the “squeeze film”, in which viscous fluid is contained between two parallel surfaces that are squeezed together. Think for example of what happens when a hammer strikes a drop of viscous fluid on a table (figure 3.3): the fluid shoots out with a high radial velocity and the hammer is rapidly brought to rest. For this problem,  $\nabla \cdot \mathbf{U} = 0$  and  $\mathbf{U} \cdot \nabla h = 0$ , and (3.55) with  $p = p(r, t)$  becomes simply

$$\frac{1}{r} \frac{\partial}{\partial r} r \frac{\partial p}{\partial r} = 2p = \frac{12\mu}{h^3} \frac{\partial h}{\partial t}. \quad (3.56)$$

While the drop (of volume  $V$ ) remains entirely within the gap between hammer and table, its radius  $a(t)$  is given by  $\pi a^2 h = V$ , and the solution of (3.56) satisfying  $p = p_0$  (atmospheric) on  $r = a$  is

$$p = p_0 + \frac{3\mu}{h^3} \frac{\partial h}{\partial t} (r^2 - a^2). \quad (3.57)$$

The force  $F$  applied to the hammer (including its weight  $W$ ) then satisfies

$$F = \int_0^a (p - p_0) 2\pi r \, dr = \frac{3\mu V^2}{8\pi} \frac{d}{dt} \left( \frac{1}{h^4} \right). \quad (3.58)$$

If  $F = \text{const.}$ , this integrates to give

$$h = \left( \frac{3\mu V^2}{8\pi F} \right)^{1/4} (t - t_0)^{-1/4}, \quad (3.59)$$

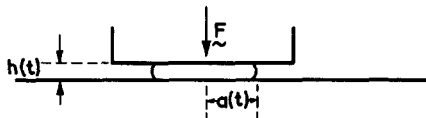


Figure 3.3 Hammer and drop; the squeeze film

where  $t_0$  is a (virtual) origin of time. The build-up of pressure in the gap is such that the hammer never quite reaches the table!

### Journal bearing

A further example of the application of the thin film approach is provided by the problem of lubrication in a journal bearing, which is of course of great practical importance. Fluid is contained in the small gap between the fixed outer cylinder  $r = a(1 + \epsilon)$  and the inner cylinder  $r = a(1 + \lambda\epsilon\cos\theta)$  which rotates with angular velocity  $\Omega$  (figure 3.4). The gap is small provided  $\epsilon \ll 1$ . The parameter  $\lambda$  ( $0 < \lambda < 1$ ) is a measure of the eccentricity of the two cylinders.

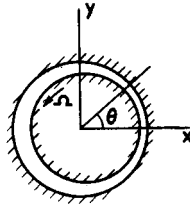


Figure 3.4 Lubrication in a journal bearing

The gap between the cylinders is

$$h(\theta) \approx a\epsilon(1 - \lambda \cos \theta), \quad (3.60)$$

and equation (3.51) for the flux round the annulus becomes

$$Q = -\frac{h^3}{12\mu a} \frac{dp}{d\theta} + \frac{1}{2} \Omega a h. \quad (3.61)$$

(The fact that the fixed surface is curved rather than flat clearly makes no difference in the thin film approximation, and we merely replace  $\partial/\partial x$  by  $(1/a)\partial/\partial\theta$  in this geometry.) Since  $\int_0^{2\pi} (dp/d\theta) d\theta = 0$ , the pressure being single-valued, (3.61) gives

$$\int_0^{2\pi} \frac{Q}{h^3} d\theta = \int_0^{2\pi} \frac{\Omega a}{2h^2} d\theta \quad (3.62)$$

i.e.

$$Q = \frac{\Omega a^2 \epsilon}{2} \frac{I_2}{I_3}, \quad \text{where} \quad I_n(\lambda) = \int_0^{2\pi} \frac{d\theta}{(1 - \lambda \cos \theta)^n}. \quad (3.63)$$

Equation (3.61) then determines  $dp/d\theta$  in the gap. Note that

$$\left. \begin{array}{l} \frac{dp}{d\theta} < 0 \text{ in some neighbourhood (depending on } \lambda) \text{ of } \theta = 0, \\ \text{and } \frac{dp}{d\theta} > 0 \text{ in some neighbourhood (depending on } \lambda) \text{ of } \theta = \pi \end{array} \right\} \quad (3.64)$$

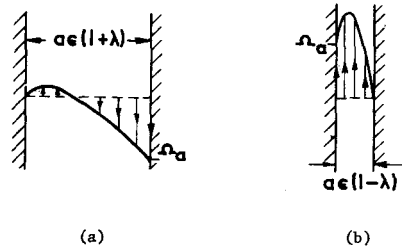


Figure 3.5 Velocity profiles in journal bearing: (a)  $\theta = \pi$ ; (b)  $\theta = 0$

The qualitative form of the resulting velocity profiles in these regions is indicated in figure (3.5). If the eccentricity is large then the adverse pressure gradient near  $\theta = \pi$  is sufficiently large that a region of back-flow (in what may loosely be described as a “separation bubble”) appears adjacent to the outer cylinder; the condition for this (which may easily be derived from the results of this section) is

$$\lambda > \frac{1}{2}(\sqrt{13} - 3) \doteq 0.30. \quad (3.65)$$

The force on the inner cylinder per axial unit length is

$$F_i = \oint \sigma_{ij} n_j dl = \oint -pn_i dl + 2\mu \oint e_{ij} n_j dl = F_i^{(p)} + F_i^{(v)}, \quad (3.66)$$

the integral being taken round the inner cylinder, and the superscripts  $(p)$  and  $(v)$  indicating contributions to the force from the pressure distribution and from the viscous stress respectively. Now  $h$  is an even function of  $\theta$ , and therefore, by (3.61), so is  $dp/d\theta$ . Hence  $p(\theta)$  is an odd function of  $\theta$ , and so, with Cartesian coordinates as in figure (3.4),  $F_x^{(p)} = 0$ , and

$$\begin{aligned} F_y^{(p)} &= -\int_0^{2\pi} p \sin \theta d\theta = -\int_0^{2\pi} \cos \theta dp/d\theta d\theta \\ &= -12\mu a \int_0^{2\pi} \left( \frac{\Omega a}{2h^3} - \frac{Q}{h^3} \right) \cos \theta d\theta = -6\mu a (\Omega a K_2 - Q K_3) \end{aligned} \quad (3.67)$$

where

$$K_n(\lambda) = \int_0^{2\pi} \frac{\cos \theta}{(1 - \lambda \cos \theta)^n} d\theta = \frac{1}{\lambda} (I_n - I_{n-1}). \quad (3.68)$$

Hence, using (3.63a),

$$F_y^{(p)} = - \frac{6\mu\Omega a}{\epsilon^2 \lambda} \frac{I_2^2 - I_1 I_3}{I_3}. \quad (3.69)$$

Likewise, by symmetry,  $F_x^{(v)} = 0$ , and

$$F_y^{(v)} = - \int_0^{2\pi} \mu \left( \frac{\partial v}{\partial r} - \frac{v}{r} \right) \cos \theta a d\theta, \quad (3.70)$$

where  $v$  is the  $\theta$ -component of velocity round the annulus. [The components of a tensor in curvilinear coordinates are always troublesome; that we have  $e_{r,\theta} = \frac{1}{2}(\partial v/\partial r - v/r)$  is in part evident from the fact that it vanishes as it should when  $v \propto r$ .] Now

$$\left| \frac{\partial v}{\partial r} - \frac{v}{r} \right| = 0 \left( \frac{\Omega a}{\epsilon a} \right), \quad (3.71)$$

and so

$$F_y^{(v)} = 0 \left( \frac{\mu\Omega a}{\epsilon} \right) = 0(\epsilon) F_y^{(p)}. \quad (3.72)$$

Hence, with  $\epsilon \ll 1$ , the viscous contribution to the force is negligible.

The integrals  $I_n(\lambda)$  may be evaluated by contour integration. In particular,

$$I_1(\lambda) = \frac{2\pi}{(1 - \lambda^2)^{1/2}}, \quad I_2(\lambda) = \frac{2\pi}{(1 - \lambda^2)^{3/2}}, \quad I_3(\lambda) = \frac{\pi(2 + \lambda^2)}{(1 - \lambda^2)^{5/2}}, \quad (3.73)$$

and the formulae (3.63) and (3.69) reduce to

$$Q = \frac{\Omega a^2 \epsilon (1 - \lambda^2)}{2 + \lambda^2}, \quad (3.74)$$

and

$$F_y^{(p)} = \frac{12\pi\mu\Omega a\lambda}{\epsilon^2(1 - \lambda^2)^{1/2}(2 + \lambda^2)}. \quad (3.75)$$

The parameter  $\lambda$  can thus adjust itself so that the upward force on the inner cylinder is sufficient to support any external load.

At high rates of rotation, the pressure can fall below the vapour pressure in the low pressure region around  $\theta = \pi/2$ , with the consequence that

vapour cavities form spontaneously in the lubricant. These cavities generally have a “finger” structure, and tend to be periodic (although unsteady and rather irregular) in the  $z$ -direction. Theoretical analysis of such a phenomenon is naturally extremely difficult. The problem is an important one however, because the practical consequences of cavitation are severe; when a cavity collapses on a solid boundary, a pressure singularity occurs (softened only by compressibility effects—Hunter, 1960) which tends to erode the boundary. Cavitation can be prevented only by maintaining a high ambient pressure in the lubricant, by keeping it in a suitably pressurised container sealed from the atmosphere.

## Lecture 4 High Reynolds Number Flow: The Euler Limit

### 4.1 The General Character of Laminar Flow at High Reynolds Number

When  $R \gg 1$ , we may expect inertia forces to predominate over viscous forces throughout the bulk of the fluid. However, we have seen from particular exact solutions of the Navier–Stokes equations that in the limit  $R \rightarrow \infty$  ( $\nu \rightarrow 0$ ) a flow normally adjusts itself so that viscous forces remain of the same order of magnitude as inertia forces in regions of the fluid typically  $O(\nu^{1/2})$  in volume relative to the whole volume. In these regions the velocity gradients are large ( $O(\nu^{-1/2})$ ) and this is just sufficient for the viscous term in the equation of motion to remain  $O(1)$  as  $\nu \rightarrow 0$ . These singular regions may occur either on solid boundaries (as in the examples of §2.2) or in the interior of the fluid (as in the jet problem considered in §2.4); in the former case, they are known as “boundary layers”, and in the latter as “free shear layers”.

The problem of high Reynolds number flow involves a complicated interaction between the flows in the singular regions and the flow outside these singular regions where the effects of viscosity are almost negligible. In this lecture we shall focus attention on the flow outside the singular regions, and we shall consider the structure of boundary layers and their interaction with the “exterior flow” in lecture 5.

For given boundary conditions, the velocity field  $\mathbf{u}$  will depend upon the parameter  $\nu$ . As  $\nu$  decreases, neglecting for the moment the important question of the stability of the flows considered,  $\mathbf{u}(\mathbf{x}, t; \nu)$  may be expected to vary continuously and to approach a limit

$$\mathbf{u}_E(\mathbf{x}, t) = \lim_{\nu \rightarrow 0} \mathbf{u}(\mathbf{x}, t; \nu). \quad (4.1)$$

This is the Euler limit, which will in general fail to satisfy the no-slip condition on solid boundaries, and which may exhibit shear discontinuities

(i.e. vortex sheets) in the fluid interior;  $\mathbf{u}_E$  satisfies the Euler equation

$$\frac{\partial \mathbf{u}_E}{\partial t} + \mathbf{u}_E \cdot \nabla \mathbf{u}_E = -\nabla P, \quad \nabla \cdot \mathbf{u}_E = 0, \quad (4.2)$$

where, as before, we suppose that body force potentials are absorbed in the definition of  $P$ . We shall consider equation (4.2) in the following sections, and shall drop the suffix  $E$ , unless the context requires its retention.

## 4.2 Kelvin's Theorem and Related Results

The circulation  $K = \oint_C \mathbf{u} \cdot d\mathbf{x}$  round any closed Lagrangian circuit  $C$  may be shown from (4.2) to be a conserved quantity. Since

$$K = \int_S \boldsymbol{\omega} \cdot d\mathbf{S}, \quad \boldsymbol{\omega} = \nabla \wedge \mathbf{u}, \quad (4.3)$$

where  $S$  spans  $C$ , it follows that the flux of vorticity across any open surface  $S$  is constant. This leads to the result that vortex lines "move with the fluid" and that stretching of vortex tubes leads to proportionate intensification of vorticity, a process that is of key importance in the phenomenon of turbulence. A formal proof of the result requires consideration of the inviscid vorticity equation (the curl of 4.2), viz

$$\frac{\partial \boldsymbol{\omega}}{\partial t} = \nabla \wedge (\mathbf{u} \wedge \boldsymbol{\omega}), \quad (4.4)$$

and its Lagrangian solution (due to Cauchy),

$$\omega_i(\mathbf{x}, t) = \omega_j(\mathbf{a}, 0) \frac{\partial x_i}{\partial a_j}, \quad (4.5)$$

where, as in the notation of §1.3,  $\mathbf{a}$  is the position at time  $t = 0$  of the particle that arrives at the point  $\mathbf{x}$  at time  $t$ .

A localised vorticity distribution  $\boldsymbol{\omega}(\mathbf{x})$  in a fluid of infinite extent gives rise to a velocity field  $\mathbf{u}(\mathbf{x})$  given by (cf. the Biot-Savart law for the relation between electric current and magnetic field)

$$\mathbf{u}(\mathbf{x}) = \frac{1}{4\pi} \int \frac{\boldsymbol{\omega}(\mathbf{x}') \wedge (\mathbf{x} - \mathbf{x}')}{|\mathbf{x} - \mathbf{x}'|^3} d^3\mathbf{x}'. \quad (4.6)$$

At a large distance from the region in which the vorticity is localised, the leading term in the asymptotic expansion of (4.6) is

$$\mathbf{u}(\mathbf{x}) \sim \nabla \varphi, \quad \varphi = \frac{1}{4\pi} (\boldsymbol{\mu} \cdot \nabla) \frac{1}{r} \quad (4.7)$$

where

$$\boldsymbol{\mu} = \frac{1}{2} \int \mathbf{x}' \wedge \boldsymbol{\omega}(\mathbf{x}') d^3 \mathbf{x}'. \quad (4.8)$$

Equation (4.7) represents the velocity field associated with a source dipole of strength  $\boldsymbol{\mu}$ . The vector  $\rho \boldsymbol{\mu}$  may also be identified with the impulsive force required to establish the motion associated with the vorticity field  $\boldsymbol{\omega}(\mathbf{x})$ ; it may be verified from (4.4) that  $d\boldsymbol{\mu}/dt = 0$ , and this may be interpreted as a statement of conservation of the linear momentum  $\rho \boldsymbol{\mu}$  of the disturbance. The corresponding expression for angular momentum (also conserved) is

$$\mathbf{h} = \frac{1}{2} \rho \int \mathbf{x} \wedge (\mathbf{x} \wedge \boldsymbol{\omega}) d^3 \mathbf{x}. \quad (4.9)$$

The vectors  $\boldsymbol{\mu}$  and  $\mathbf{h}$  are conserved even when viscosity is included in the equations of motion. There are two further quantities which are invariant only in so far as viscous effects are negligible. The first is the kinetic energy of the disturbance,

$$T = \frac{1}{2} \int \rho \mathbf{u}^2 d^3 \mathbf{x}. \quad (4.10)$$

The second is the *helicity*

$$I = \int \mathbf{u} \cdot \boldsymbol{\omega} d^3 \mathbf{x}, \quad (4.11)$$

which is a topological invariant related to the degree of knottedness (or topological complexity) of the vorticity field (Moffatt, 1969); the fact that vortex lines move and deform continuously with the fluid ensures that the topological character of the vorticity field is certainly conserved.

A flow that is two-dimensional has a stream-function  $\psi(x, y)$  and vorticity  $\boldsymbol{\omega} = -\nabla^2 \psi \mathbf{k}$  where  $\mathbf{k} = (0, 0, 1)$ . The equation (4.4) reduces to

$$\frac{D\boldsymbol{\omega}}{Dt} \equiv \frac{\partial \boldsymbol{\omega}}{\partial t} + \mathbf{u} \cdot \nabla \boldsymbol{\omega} = 0, \quad (4.12)$$

and the condition for steady flow is that  $\boldsymbol{\omega}$  should be constant on streamlines  $\psi = \text{const.}$

Analogously, for a flow that is axisymmetric and without swirl, the vortex lines are circles about the axis of symmetry, and (4.4) reduces to

$$\frac{D}{Dt} \left( \frac{\boldsymbol{\omega}}{r \sin \theta} \right) = 0, \quad (4.13)$$

where  $(r, \theta, \varphi)$  are spherical polar coordinates. This simply expresses the fact that the vorticity on a circular vortex line that moves with the fluid is proportional to its radius  $r \sin \theta$ . The condition for steady flow is now that  $\boldsymbol{\omega}/r \sin \theta = \text{const.}$  on streamlines.

A well-known example of an axisymmetric flow with localised vorticity is

provided by “Hill’s spherical vortex” for which the Stokes stream function is

$$\psi(r, \theta) = \left. \begin{aligned} &\frac{3}{4}Ur^2 \left(1 - \frac{r^2}{a^2}\right) \sin^2 \theta \quad (r < a), \\ &-\frac{1}{2}U \left(r^2 - \frac{a^3}{r}\right) \sin^2 \theta \quad (r > a). \end{aligned} \right\} \quad (4.14)$$

The velocity field associated with this stream function (see 3.35) is continuous across the spherical surface  $r = a$ . The vorticity  $\omega = (0, 0, \omega)$  is given by

$$\omega = \left. \begin{aligned} &\frac{15U}{2a^2}r \sin \theta \quad (r < a) \\ &0 \quad (r > a) \end{aligned} \right\} \quad (4.15)$$

and so clearly satisfies (4.13). The flow outside the sphere  $r = a$  is the (unique) irrotational flow past a sphere with uniform velocity  $-U$  at  $\infty$ . The streamlines  $\psi = \text{const.}$  are sketched in figure (4.1).

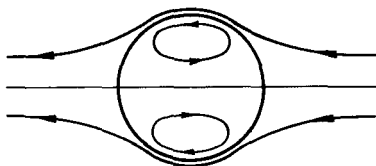


Figure 4.1 Hill’s spherical vortex

Relative to axes fixed in the fluid at infinity, the vortex “propagates” with speed  $U$ . The energy and momentum of the associated flow are given, from (4.8) and (4.10) by

$$T = \frac{10}{7}\pi\rho a^3U^2, \quad \rho\mu = 2\pi\rho a^3U. \quad (4.16)$$

The angular momentum  $\mathbf{h}$  and helicity  $I$  are both zero.

### 4.3 Irrotational Flow

If  $\omega = \nabla \wedge \mathbf{u} \equiv 0$ , then the flow is *irrotational* and there exists a scalar potential  $\phi$  such that  $\mathbf{u} = \nabla\phi$ . However, if the region occupied by fluid is not simply-connected, then  $\phi$  need not be single-valued; the prototype example is provided by the irrotational flow mentioned in §2.3,

$$\mathbf{u} = (0, \Omega a^2/r, 0) \quad (4.17)$$

generated in a viscous fluid of infinite extent by the rotation of a circular cylinder of radius  $a$  with angular velocity  $\Omega$ . The circulation round any

closed curve  $C$  is

$$K = \oint_C \mathbf{u} \cdot d\mathbf{x} = 2n\pi\Omega a^2, \quad (4.18)$$

where  $n$  is the number of times that  $C$  circulates round the cylinder before it closes on itself. Clearly  $\phi$  increases by  $2\pi n\Omega a^2$  in traversing  $C$ .

Irrotational flow occurs in a variety of situations. Firstly if bodies are accelerated impulsively from rest in fluid at rest, vorticity is generated only at the solid boundaries (essentially by the process described in §2.2 (iv)) in a boundary layer of thickness  $O(\nu t)^{1/2}$ . Outside the boundary layer the flow is irrotational. For example, if a sphere is jerked into motion with speed  $U$ , the stream-function at the instant  $t = 0+$  relative to axes fixed in space but with origin instantaneously at the centre of the sphere is

$$\Psi(r, \theta) = \frac{Ua^3}{2r} \sin^2 \theta \quad (4.19)$$

no matter how viscous the fluid may be! Of course, at subsequent instants, vorticity diffuses (and is convected) into the fluid and this drastically modifies the flow pattern.

Secondly, in a *steady* flow past an obstacle, if the flow upstream is uniform (and therefore irrotational), the vorticity on every streamline that comes from "upstream infinity" must be zero in the Euler limit. In particular, the assumption of irrotational flow is certainly a good one in the neighbourhood of the front part of a bluff body in a uniform stream.

Thirdly, flows which are not significantly influenced by solid boundaries are frequently irrotational to a good approximation. For example, gas bubbles, rising in liquids, that are at the same time large enough for the Reynolds number to be large, yet small enough to be kept approximately spherical by surface tension, generate the irrotational flow (4.19) outside a very weak viscous boundary layer on the surface  $r = a$ .

For these reasons, an understanding of irrotational flow theory is really a necessary preliminary to a study of boundary-layer theory. It is of course possible to over-emphasise the irrotational aspects of fluid dynamics; but one must be careful also not to underestimate the power of irrotational theory in a variety of problems of practical importance.

With  $\mathbf{u} = \nabla \phi$  and  $\nabla \cdot \mathbf{u} = 0$ , we have Laplace's equation

$$\nabla^2 \phi = 0, \quad (4.20)$$

and standard techniques are available for finding solutions for reasonably simple geometries. We note the following for future reference:

i) *Flow past a circular cylinder with circulation*

$$\phi = U \left( r + \frac{a^2}{r} \right) \cos \theta + \frac{\kappa}{2\pi} \log r. \quad (4.21)$$

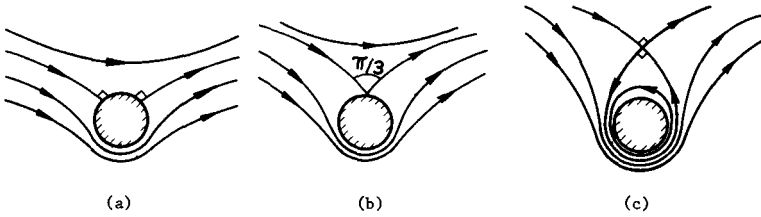


**Figure 4.2** Flow past a circular cylinder with circulation (a)  $\kappa < 4\pi Ua$ ; (b)  $\kappa = 4\pi Ua$ ; (c)  $\kappa > 4\pi Ua$

The streamlines for this flow for various values of the circulation are indicated in figure 4.2.

ii) Flow past a wedge  $\theta = 0, \pi(2 - \beta)$  (figure 4.3a)

$$\varphi = Cr^\lambda \cos \lambda\theta, \quad \lambda = \frac{2}{2 - \beta} \tag{4.22}$$

iii) Flow round a corner  $\theta = \pi(1 + \beta), 0$  (figure 4.3b)

$$\varphi = Cr^\lambda \cos \lambda\theta, \quad \lambda = \frac{1}{1 + \beta} \tag{4.23}$$

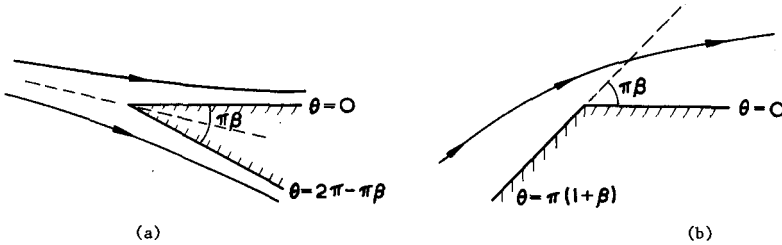


**Figure 4.3** Irrotational flows with rectilinear boundaries (a) wedge flow; (b) flow round a corner

### 4.4 The Pressure Distribution in Irrotational Flow

The Euler equation (4.2) may be written in the alternative form

$$\frac{\partial \mathbf{u}}{\partial t} = -\nabla(P + \frac{1}{2}\mathbf{u}^2) + \mathbf{u} \wedge \boldsymbol{\omega}. \tag{4.24}$$

When  $\boldsymbol{\omega} \equiv 0$  and  $\mathbf{u} = \nabla\varphi$ , this integrates to give

$$P + \frac{1}{2}\mathbf{u}^2 + \dot{\varphi} = F(t). \tag{4.25}$$

The pressure (eqn. 2.3) is then given by

$$p = p_0 - \frac{1}{2}\rho\mathbf{u}^2 - \rho\dot{\varphi} - V \tag{4.26}$$

where  $V$  is the body force potential, and  $p_0$  is a reference pressure where  $\mathbf{u} = 0$  and  $V = 0$ .

This formula enables that force  $\mathbf{F} = - \int_S p \mathbf{n} \, dS$  on a body immersed in an irrotational flow to be calculated: we shall not linger over the details, but merely note the following:

i) the contribution from  $V$  to  $\mathbf{F}$  is merely the buoyancy force when  $V = -\mathbf{g} \cdot \mathbf{x}$  and  $\mathbf{g}$  is the acceleration due to gravity;

ii) there is no contribution to  $\mathbf{F}$  from the term  $-(1/2)\rho\mathbf{u}^2$  if  $\mathbf{u} = o(r^{-2})$  at infinity (e.g. the velocity derived from the stream function (4.19)). There is a contribution however in the important problem of two-dimensional flow past a cylinder with circulation  $\kappa$ . The force is perpendicular to  $\mathbf{U}$  and has magnitude  $\rho U \kappa$ ; this is independent of the shape of cross-section of the cylinder.

iii) There is always a contribution from the term  $-\rho\dot{\phi}$ ; this is evidently linearly related to the acceleration of the body  $\dot{\mathbf{U}}$ , and may therefore be written

$$F_i^{(a)} = -\rho V_0 c_{ij} \dot{U}_j, \quad (4.27)$$

where  $V_0$  is the volume of the body and  $c_{ij}$  is a symmetric tensor determined entirely by the shape of the body. Just as in the case of the tensor  $A_{ij}$  in §3.3,  $c_{ij}$  is isotropic if the body has at least the degree of symmetry of one of the regular solids; in this case  $c_{ij} = c\delta_{ij}$  say, and

$$\mathbf{F}^{(a)} = -\rho V_0 c \dot{\mathbf{U}}. \quad (4.28)$$

The coefficient  $\rho V_0 c$  is the *virtual mass* of the body, corresponding to the increased inertia of the joint body-fluid system, due to the presence of the fluid, in response to an applied force. For a sphere,  $c = 1/2$ , while for a cylinder  $c = 1$  (and  $\mathbf{F}^{(a)}$  and  $V_0$  are both "per unit length" in this case).

It is perhaps worth noting that if a body experiences an angular acceleration  $\dot{\Omega}$  as well as a linear acceleration  $\dot{\mathbf{U}}$ , then again by analogy with §3.3, it will experience a force and couple

$$\begin{aligned} F_i^{(a)} &= -\rho V_0 (c_{ij} \dot{U}_j + d_{ij} a \Omega_j), \\ G_i^{(a)} &= -\rho V_0 a (d_{ji} \dot{U}_j + e_{ij} a \dot{\Omega}_j), \end{aligned} \quad (4.29)$$

where  $a$  is a typical dimension of the body and  $d_{ij}$  and  $e_{ij}$  ( $=e_{ji}$ ) are further dimensionless tensors determined entirely by the shape of the body. The cross term involving  $d_{ij}$  is for example responsible for the thrust generated when a propellor is subject to angular acceleration.

## Lecture 5 Boundary-Layer Theory

### 5.1 The Euler Limit and the Prandtl Limit

In order to simplify matters, we shall concentrate on steady flow at high Reynolds number past a cylindrical body. For such a flow, the stream function  $\psi(x, y)$  satisfies the equation

$$-\frac{\partial(\psi, \nabla^2 \psi)}{\partial(x, y)} = \nu \nabla^4 \psi. \quad (5.1)$$

This is the curl of eqn. (2.2) (the vorticity equation) which has in this geometry only one component in the  $z$ -direction. We have seen that the Euler limit defined by

$$\psi_E(x, y) = \lim_{\nu \rightarrow 0} \psi(x, y; \nu) \quad (5.2)$$

satisfies

$$\frac{\partial(\psi_E, \nabla^2 \psi_E)}{\partial(x, y)} = 0, \quad (5.3)$$

so that  $\nabla^2 \psi_E = f(\psi_E)$ ; and if the vorticity upstream vanishes, then  $\nabla^2 \psi_E = 0$  on all streamlines starting far upstream. Solution of this equation subject to  $\psi_E = \text{const.}$  on the body cannot at the same time satisfy the no-slip condition on the body; this suggests that we look more closely at the flow in the immediate neighbourhood of the body surface.

It is customary in boundary-layer analysis to let  $x$  and  $y$  be coordinates tangential and normal to the boundary (figure 5.1). These coordinates are not strictly Cartesian; but provided the boundary curvature is finite, the error involved in treating them as Cartesian (as far as the flow in the thin layer near the boundary is concerned) is negligible. Just as in the "thin layer" analysis of §3.6, we have also that, near the surface,

$$\left| \frac{\partial \psi}{\partial y} \right| \gg \left| \frac{\partial \psi}{\partial x} \right|, \quad \left| \frac{\partial^2 \psi}{\partial y^2} \right| \gg \left| \frac{\partial^2 \psi}{\partial x^2} \right|, \quad \nabla^2 \psi \approx \frac{\partial^2 \psi}{\partial y^2}, \quad (5.4)$$

and so (5.1) becomes

$$-\frac{\partial(\psi, \psi_{yy})}{\partial(x, y)} = \nu \psi_{yyyy}, \quad (5.5)$$

which integrates with respect to  $y$  to give

$$\psi_y \psi_{xy} - \psi_x \psi_{yy} = G(x) + \nu \psi_{yyy}, \quad (5.6)$$

or, in terms of the tangential and normal velocity components,  $u = \psi_y$ ,

$$v = -\phi_x,$$

$$u \frac{\partial u}{\partial x} + v \frac{\partial u}{\partial y} = G(x) + \nu \frac{\partial^2 u}{\partial y^2}. \quad (5.7)$$

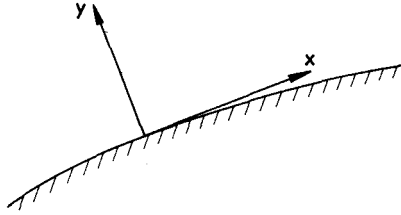


Figure 5.1 Coordinates for boundary layer analysis

This is the *boundary-layer equation* (Prandtl, 1905). Just as in thin film theory,  $G(x)$  must be identified with the pressure gradient

$$G(x) = -\frac{1}{\rho} \frac{dp}{dx}, \quad (5.8)$$

which, in the boundary-layer approximation, is independent of the normal coordinate  $y$ .

Equations (5.5) and (5.6) may be obtained more formally from (5.1) by first “stretching” the normal coordinate: let

$$\hat{y} = y/\nu^{1/2}, \quad \hat{\psi} = \psi/\nu^{1/2}, \quad (5.9)$$

and let

$$\psi_p(x, y) = \lim_{\nu \rightarrow 0} \hat{\psi}(x, \hat{y}; \nu). \quad (5.10)$$

Substituting (5.9) in (5.1) and taking the limit  $\nu \rightarrow 0$ , we obtain

$$-\frac{\partial(\psi_p, \partial^2 \psi_p / \partial \hat{y}^2)}{\partial(x, \hat{y})} = \frac{\partial^4 \psi_p}{\partial \hat{y}^4}. \quad (5.11)$$

This is just eqn. (5.5) again in terms of the scaled variables;  $\psi_p(x, \hat{y})$  is the *Prandtl limit* of the stream function of the flow.

It is significant that only a scaling proportional to  $\nu^{1/2}$  leads to equation (5.11). If instead of (5.9) we write

$$\hat{y} = y/\nu^q, \quad \hat{\psi} = \psi/\nu^q, \quad (5.12)$$

(so that  $u = \partial\psi/\partial y = \partial\hat{\psi}/\partial\hat{y}$ ) and go through the formal limiting procedure  $\nu \rightarrow 0$  after making this substitution, we obtain the Euler equation if  $q < \frac{1}{2}$ , the boundary-layer equation if  $q = \frac{1}{2}$ , and the “lubrication” equation  $\partial^4 \hat{\psi} / \partial \hat{y}^4 = 0$  if  $q > \frac{1}{2}$ .

This provides the clue to the matching principle:

$$\lim_{y \rightarrow 0} \frac{\partial \psi_E}{\partial y} = \lim_{\hat{y} \rightarrow \infty} \frac{\partial \psi_p}{\partial \hat{y}} = U(x), \text{ say.} \quad (5.13)$$

$U(x)$  is the tangential streaming velocity on the boundary  $y = 0$  as determined by the Euler limit; the solution of the boundary-layer equation (5.11) (or equivalently (5.5)) must match to this as the boundary-layer variable  $\hat{y} = y/\nu^{1/2}$  tends to infinity. We may usefully think of an overlap region  $y = 0(\nu^q)$  where  $\frac{1}{2} < q < 1$ , in which both Euler limit and Prandtl limit provide valid limiting forms for the exact stream-function.

In practice, this means that we must solve (5.6) subject to the conditions that both velocity components vanish on the boundary, i.e.

$$\psi = \frac{\partial \psi}{\partial y} = 0 \quad \text{on} \quad y = 0, \quad (5.14)$$

and the matching condition

$$\frac{\partial \psi}{\partial y} \rightarrow U(x) \quad \text{as} \quad y/\nu^{1/2} \rightarrow \infty. \quad (5.15)$$

From (5.6) and (5.15),  $G(x)$  and  $U(x)$  are evidently related by

$$G(x) = U \frac{dU}{dx}. \quad (5.16)$$

If  $G(x) > 0$ , the pressure gradient tends to accelerate the flow and is described as *favourable*; if  $G(x) < 0$ , it tends to retard the flow, and is described as *adverse*.

## 5.2 Reduction of the Boundary-Layer Equation by Dimensional Arguments

The fact that the parameter  $\nu$  can be scaled out of the boundary-layer equation (5.6) by the transformation (5.9) is of great significance; the problem then becomes

$$\hat{\psi}_{\hat{y}} \hat{\psi}_{\hat{x}\hat{y}} - \hat{\psi}_{\hat{x}} \hat{\psi}_{\hat{y}\hat{y}} = U \frac{dU}{dx} + \hat{\psi}_{\hat{y}\hat{y}\hat{y}}, \quad (5.17)$$

$$\hat{\psi} = \hat{\psi}_{\hat{y}} = 0 \quad \text{on} \quad \hat{y} = 0, \quad \hat{\psi}_{\hat{y}} \rightarrow U(x) \quad \text{as} \quad \hat{y} \rightarrow \infty. \quad (5.18)$$

The parameter  $\nu$  no longer appears in the statement of the problem, and the solution  $\hat{\psi}(x, \hat{y})$  must therefore also be independent of  $\nu$ . (No such simplification is possible for the full Navier–Stokes equations.)

If the velocity  $U(x)$  involves only one dimensional parameter (in addition

to  $x$  itself), then dimensional arguments may be used to great effect to reduce (5.17) to an ordinary differential equation. Suppose that the dimensional parameter is  $\alpha$  with dimensions  $L^q T^r$ . Then the only possibility for  $U(x)$  is

$$U(x) = \alpha^{-1/r} x^{1+q/r} = Ax^m \text{ say,} \tag{5.19}$$

where for the moment we restrict attention to the situation  $A > 0$ , and the only dimensional possibility for  $\hat{\psi}(x, y)$  is

$$\hat{\psi}(x, y) = (Ax^{m+1})^{1/2} f(\eta) \text{ where } \eta = y(Ax^{m-1})^{1/2}. \tag{5.20}$$

Substitution of (5.19) and (5.20) in (5.17) and (5.18) leads after some simplification to the *Falkner-Skan equation*

$$f''' + \frac{1}{2}(m + 1)ff'' + m(1 - f'^2) = 0, \tag{5.21}$$

and the boundary conditions

$$f(0) = f'(0) = 0, \quad f'(\infty) = 1. \tag{5.22}$$

Equation (5.19) represents a rather severe limitation in the type of problem covered by *similarity solutions* of the type (5.20); and yet the problems covered by different values of the parameter  $m$  are sufficiently varied to make a careful study of the problem (5.21), (5.22) well worthwhile. When  $m = 0$ , we have flow without pressure gradient past a flat plate aligned with the stream (figure 5.2a). When  $m = 1$ , we have "stagnation point flow" against a plate placed perpendicular to an incident stream (figure 5.2b); this models the flow in the neighbourhood of the front stagnation point of any bluff cylindrical body placed in a stream. When  $0 < m < 1$ , we have symmetrical flow past a wedge of angle  $\pi\beta$  where  $m = \beta/(2 - \beta)$  (figure 5.2c, and compare equation (4.22) with  $m = \lambda - 1$ ). When  $-1/2 < m < 0$ , we have flow round a corner, artificial to the extent that we are concerned with viscous effects only downstream of the corner and any boundary layer upstream of the corner must be ignored (figure 5.2d, and compare equation (4.23) with  $m = \lambda - 1$ ).

The solution of equation (5.21) for given  $m$  subject to the boundary conditions (5.22) may be obtained numerically by a Runge-Kutta procedure:

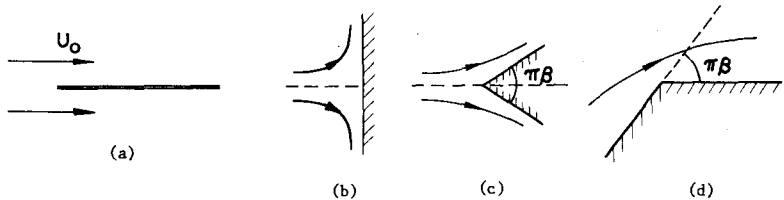


Figure 5.2 Boundary layer flows represented by solutions of the Falkner-Skan equation for different values of the parameter  $m$ : (a)  $m = 0$ ; (b)  $m = 1$ ; (c)  $0 < m < 1$ ; (d)  $-1/2 < m < 0$

guess the value of  $f''(0)$ , compute step-by-step using (5.21); if  $f'(\eta) \rightarrow \infty$  decrease  $f''(0)$  and repeat; if  $f'(\eta) \rightarrow -\infty$ , increase  $f''(0)$  and repeat; the guess for  $f''(0)$  can be improved until  $f'(\eta) \rightarrow 1$  as  $\eta \rightarrow \infty$  with arbitrary accuracy. Some sample velocity profiles obtained by this procedure are sketched in figure 5.3.

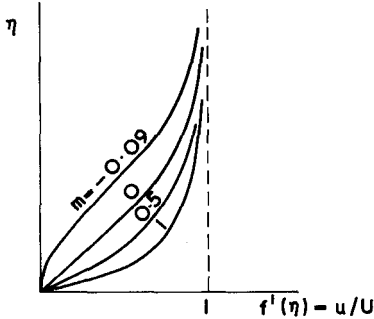


Figure 5.3 Sketch of velocity profiles given by solutions of the Falkner-Skan equation

Certain results are known concerning the third-order non-linear two-point boundary-value problem given by (5.21) and (5.22). These results, which can be proved analytically, but are also evident in computational work are as follows:

i) For  $m > 0$ , there exists a unique solution to the problem; in particular the boundary layers for the problems sketched in figures (5.2) (a), (b) and (c) are uniquely determined.

ii) For  $m_c < m < 0$ , where  $m_c \doteq -0.09$ , there exist two solutions, but only one of these satisfies the conditions  $0 < f' < 1$  which might be expected to apply to a "well-behaved" or "realisable" boundary layer profile; the other solution actually has  $f''(0) < 0$ , implying reversed velocity near the boundary.

iii) For  $m = m_c$ , the two solutions of (ii) coalesce and  $f''(0) = 0$ , implying zero stress on the wall. This corresponds to the flow of figure 5.2(d), when the flow turns through an angle of approximately  $20^\circ$ .

iv) For  $m < m_c$ , there is no solution satisfying  $0 < f' < 1$ ; since  $G(x) = U dU/dx = mA^2x^{2m-1}$ , this suggests that a boundary layer cannot subsist under an external stream which decelerates too rapidly (i.e. which is subjected to too great an adverse pressure gradient).

Note that the outer edge of the boundary layer may be defined by  $\eta = \eta_1$  say, where  $|f'(\eta_1) - 1|$  is some suitably small number (e.g. 0.01). In terms of  $x$  and  $y$ , from (5.20), this becomes  $y = \delta(x)$  where

$$\delta(x) = \eta_1 \left( \frac{v}{A} \right)^{1/2} x^{(1-m)/2}. \quad (5.23)$$

The particular cases  $m = 0$  and  $m = 1$  deserve further comment.

*The flat plate ( $m = 0$ )*

The boundary layer growth in this case is parabolic. The computed value of  $f''(0)$  is 0.33. The tangential stress on the plate is therefore

$$(\sigma_{xy})_{y=0} = \mu \left( \frac{\partial u}{\partial y} \right)_{y=0} = C \rho U^2 \left( \frac{v}{Ux} \right)^{1/2}, \quad C = 0.33. \quad (5.24)$$

The total force (per unit length in the  $z$ -direction) on a plate of length  $l$  parallel to the flow is  $F = 2 \int_0^l (\sigma_{xy})_{y=0} dx$ , so that (neglecting small corrections from effects near the edges where the boundary layer approximation  $\partial/\partial y \gg \partial/\partial x$  breaks down),

$$\frac{F}{\rho U^2 l} = 1.33 R^{-1/2}, \quad R = \frac{Ul}{v}. \quad (5.25)$$

Note the decrease of the drag coefficient with increasing Reynolds number.

The velocity profile with  $m = 0$  (known as the *Blasius* profile) is remarkably linear out to about  $\eta = 0.8$ . In fact from (5.21) (with  $m = 0$ ) and (5.22), it is evident that  $f'''(0) = f^{(iv)}(0) = 0$ , and that the Taylor series for  $f'(\eta)$  has the form

$$f'(\eta) = c\eta - \frac{c^2}{48}\eta^4 + 0(\eta^7). \quad (5.26)$$

*Stagnation point flow ( $m = 1$ )*

In this case (from (5.23)),  $\delta = \text{const.}$ , i.e. the boundary layer does not grow. The solution of the boundary layer equation is actually in this case an exact solution of the full Navier–Stokes equations, the terms neglected in the boundary layer approximation being identically zero.

### 5.3 Flow in a Diverging Channel; an Example of the Non-Existence of a Boundary Layer

If  $m = -1$ , then  $U(x) = A/x$ , corresponding to flow from a line source  $Q$  at the intersection of two planes intersecting at an angle  $\beta$  where  $A\beta = Q$ . The Falkner–Skan equation in this case becomes

$$f''' + f'^2 - 1 = 0. \quad (5.27)$$

Multiply this by  $f''$ , integrate from 0 to  $\infty$  and use  $f'(0) = 0, f'(\infty) = 1, f''(\infty) = 0$ ; we obtain

$$\frac{1}{2}(f''(0))^2 = -\frac{2}{3}, \quad (5.28)$$

which is clearly impossible†. There is therefore *no solution* of the boundary layer problem for this geometry; the fluid simply refuses to behave in the “obvious” manner (figure 5.4a); the flow decelerates too rapidly for the boundary layer to be possible. It may well then be asked what *is* the correct Euler limit for this flow. It so happens that the exact solution for the problem can be obtained, since on dimensional grounds the exact stream function  $\psi(r, \theta)$  must have the form  $\psi = Qf(\theta)$ ; the equation for  $f(\theta)$  is of course non-linear, but it can be integrated in terms of elliptic integrals. As the Reynolds number  $R = Q/\nu$  increases, different solutions become possible; for a typical solution the velocity profile exhibits oscillations (figure 5.4b), the number of oscillations being  $O(R^{1/2})$  as  $R \rightarrow \infty$ . In this way, the flow arranges itself so that viscous effects remain important throughout the whole body of fluid in the limit  $\nu \rightarrow 0$ .

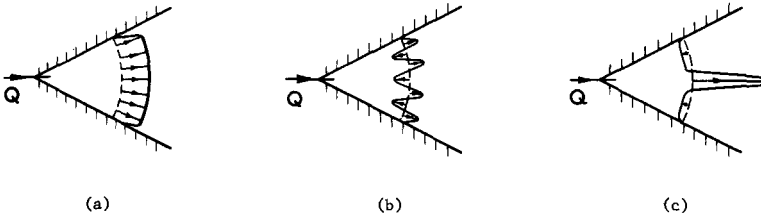


Figure 5.4 Flow in a diverging channel: (a) wrong!; (b) Euler limit; (c) observed flow (usually turbulent)

It is perhaps not surprising that such a flow is not in fact realised in practice. The *observed* flow (figure 5.4c) depends on conditions near the source  $Q$ , and almost invariably is turbulent and has a jet-like structure with entrainment from the sides.

## 5.4 Flow in a Converging Channel

If the line source of §5.3 is replaced by a line sink  $-Q$ , then with

$$\psi = \left( \nu \frac{Q}{\beta} \right)^{1/2} f(\eta), \quad \eta = \left( \frac{Q}{\nu \beta} \right)^{1/2} \frac{y}{x}, \quad (5.29)$$

†I am indebted to Prof. L. E. Fraenkel for illuminating discussions that I have had with him on the subject matter of Sections 5.2–5.4, and in particular for his drawing my attention to this simple proof of non-existence.

the Falkner–Skani problem becomes

$$f''' + f'^2 - 1 = 0, \quad f(0) = f'(0) = 0, \quad f'(\infty) = -1. \quad (5.30)$$

The crucial change is in the sign of  $f'(\infty)$ . Putting  $F = f'$ , and multiplying by  $F'$ , we integrate once to give

$$\frac{1}{2}F'^2 + \frac{1}{3}F^3 - F = \text{const.} = \frac{2}{3}. \quad (5.31)$$

This integrates again to give

$$F = 2 - 3 \tanh^2 \left( \frac{\eta}{\sqrt{2}} + C \right), \quad (5.32)$$

where  $C$  is a constant of integration satisfying

$$\tanh C = \pm\sqrt{\frac{2}{3}}, \quad \text{i.e. } C \doteq \pm 3.04. \quad (5.33)$$

The two choices for  $C$  correspond to two possible boundary layer structures (figure 5.5). Both structures appear as limiting forms (as  $R \rightarrow \infty$ ) of alternative exact solutions of the Navier–Stokes equations. The form (a) is the “normal” boundary layer profile that is generally observed in the sink flow geometry; the form (b) is “abnormal” in that it involves reversed flow at the wall; it could however presumably arise as the result of suitably imposed conditions at  $r = 0$ .

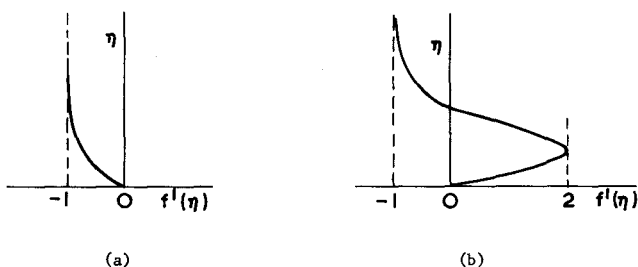


Figure 5.5 Possible boundary layer structures for sink flow

The analogous three-dimensional problem (flow due to a point sink  $Q_1$  at the vertex of a cone) is superficially similar, but is in fact far more difficult due to the existence of a natural length scale  $Q_1/\nu$  for the problem, (and the non-existence of a natural Reynolds number). If  $r \gg Q_1/\nu$ , then viscous forces dominate and inertia forces are negligible. If  $r \ll Q_1/\nu$  inertia forces dominate, and a boundary-layer structure is to be expected. However the flow outside the boundary layer on the inner surface of the cone certainly need not be irrotational since all the fluid comes from a region where viscous

forces have established a vorticity distribution. The problem has been studied by Ackerberg (1965) but there are some outstanding difficulties that have not yet been fully resolved.

### 5.5 Impulsive Motion of a Cylinder

We now turn to the important question of the growth of a boundary layer on a body which accelerates from rest in a fluid initially at rest. Suppose that, at  $t = 0$ , a cylinder, boundary  $C$ , is jerked into motion with velocity  $-U$  and that this velocity is subsequently maintained. Relative to axes moving with the cylinder, the fluid "at infinity" appears to have the velocity  $+U$ . At  $t = 0+$ , the flow is irrotational since vorticity is confined to the singular sheet on  $C$ , i.e.  $\mathbf{u} = \nabla\phi$  where  $\phi$  is the unique solution of

$$\nabla^2\phi = 0, \quad \phi \sim U \cdot \mathbf{x} \text{ at } \infty, \quad \frac{\partial\phi}{\partial n} = 0 \text{ on } C. \quad (5.34)$$

For  $t > 0$ , the vortex sheet on  $C$  diffuses into the fluid and modifies the flow pattern. With the usual boundary layer coordinates, the boundary layer equation is

$$\frac{\partial u}{\partial t} + u \frac{\partial u}{\partial x} + v \frac{\partial u}{\partial y} = U \frac{dU}{dx} + v \frac{\partial^2 u}{\partial y^2}, \quad (5.35)$$

where  $U(x) = (\partial\phi/\partial x)_{y=0}$ . The form of the solution to the Rayleigh problem (when  $U(x) = \text{const.}$ —see equation 2.14) suggests that in this case we look for a solution of (5.35) in the form of a series based on the boundary-layer variable  $\eta = y/2\sqrt{vt}$ , viz,

$$u(x, y, t) = \sum_{n=0}^{\infty} t^n g_n(x) f_n(\eta), \quad (5.36)$$

where

$$g_0(x) = U(x), \quad f_0(\eta) = \text{erf } \eta, \quad (5.37)$$

and the expansion for  $v$  is given by  $\partial v/\partial y = -\partial u/\partial x$ . Substitution in (5.35) and equating successive powers of  $t$  leads in principle to the determination of the functions  $g_n(x)$  and  $f_n(\eta)$ . In particular,  $g_1(x) = U dU/dx$ , and

$$f_1(\eta) = \frac{1}{2}(2\eta^2 - 1)(\text{erf } \eta)^2 + \frac{3}{\sqrt{\pi}}\eta e^{-\eta^2} \text{erf } \eta + 1 - \frac{4}{3\pi}e^{-\eta^2} + \frac{2}{\pi}e^{-2\eta^2} \quad (5.38)$$

$$+ \alpha(2\eta^2 + 1) + \beta \left[ \frac{1}{2\sqrt{\pi}}(2\eta^2 + 1) \text{erf } \eta + \eta e^{-\eta^2} \right],$$

where

$$\alpha = -\left(1 + \frac{2}{3\pi}\right) \doteq -1.2, \quad \beta = \frac{1}{\sqrt{\pi}}\left(1 + \frac{4}{3\pi}\right) \doteq 0.8. \quad (5.39)$$

Expressions for subsequent functions  $f_n(\eta)$  become rapidly more complicated!

The first two terms alone of (5.36) give

$$u = Uf_0(\eta) + tU \frac{dU}{dx} f_1(\eta), \quad (5.40)$$

and the corresponding stress on the boundary  $y = 0$  is

$$(\sigma_{xy})_{y=0} = \mu \left(\frac{\partial u}{\partial y}\right)_{y=0} = \frac{\mu U}{\sqrt{\pi\nu t}} \left[1 + \left(1 + \frac{4}{3\pi}\right)tU'\right], \quad (5.41)$$

using (5.37) – (5.39). In a region of deceleration ( $U' < 0$ ), this becomes negative (indicating reversed flow near the boundary) after a time  $t_r$  given by

$$t_r(-U') = \frac{1}{1 + 4/3\pi} \doteq 0.702. \quad (5.42)$$

If a typical dimension of the cylinder is  $a$ , so that  $U' = 0(U/a)$ , this means that reversed flow in the boundary layer develops after a time of order  $a/U$ , which is the time for the cylinder to move through a distance  $a$ . The inclusion of further terms of the series (5.36) does not significantly modify this conclusion.

In the case of a circular cylinder, from eqn. (4.21) with  $\kappa = 0$ ,  $U(x) = 2U_\infty \sin x/a$ , where  $x$  is the tangential distance from the front stagnation point. Hence  $-U'(x) = -2(U_\infty/a) \cos x/a$  is maximal at the rear stagnation point ( $x = \pi a$ ), and this is where reversed flow in the boundary layer starts.

In the case of an elliptic cylinder of semi-axes  $a$  and  $b$  (with the  $b$ -axis parallel to  $U$ ), the irrotation flow (which may be analysed by complex variable methods) has the property that  $-(dU/dx)$  has its maximum value at the rear stagnation point  $R$  only if  $(a/b)^2 < 4/3$ . As  $a/b$  increases from

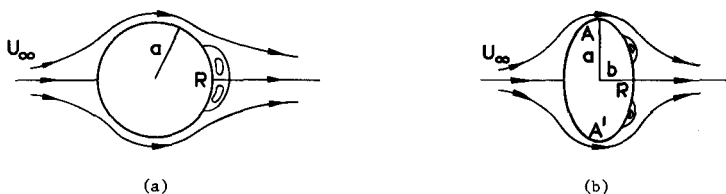


Figure 5.6 Development of reversed flow in the boundary layer: (a)  $t \approx 0.4a/U_\infty$ ; (b)  $t \approx 0.4b/U_\infty$

$-\sqrt{4/3}$ , the points where  $-dU/dx$  is a maximum move steadily from  $R$  towards the points  $A$  and  $A'$  (figure 5.6b). Immediately after reversed flow starts, there must appear separation bubbles on the surface as indicated in figures 5.6(a) and (b).

## 5.6 Boundary Layer Separation

The Prandtl limit streamlines and velocity profiles near a point of zero stress  $P$  in a decelerating flow ( $U' < 0$ ) have the form indicated in figures 5.7(a). Separation occurs if a streamline  $\psi_E = \text{const.}$  of the Euler limit leaves the surface at a point  $S$  (figure 5.7(b)). Mathematically,  $S$  is a singular point of the boundary layer equation (5.17), since we must have

$$\frac{\partial \hat{\psi}}{\partial x} \rightarrow \infty \text{ as } x \rightarrow x_S. \quad (5.43)$$



**Figure 5.7** Zero stress and separation: (a) velocity profiles and streamlines  $\psi_p = \text{const.}$  near a point of zero stress (b) streamlines  $\psi_E = \text{const.}$  near a separation point  $S$

The problem of separation has recently been reviewed by Brown and Stewartson (1969) who conclude that it is likely that

$$\hat{\psi} \sim (x - x_S)^{1/2}, \quad \text{so that} \quad \frac{\partial \hat{\psi}}{\partial x} \sim (x - x_S)^{-1/2} \text{ as } x \rightarrow x_S. \quad (5.44)$$

“Zero stress” and “separation” are believed to be closely related phenomena, and it seems likely that separation is always triggered by a zero stress point (and reversed flow in the boundary layer) a short distance ( $o(1)$  as  $\nu \rightarrow 0$ ) upstream.

Three examples of separating flows are sketched in figure 5.8. In each case, separation occurs because if it did not, then a boundary layer would have to penetrate into a region of rapidly increasing pressure (decreasing velocity) and this it cannot do. Note that the eddies downstream of separation are frequently unsteady and of very complex structure. Separation leads to increased viscous dissipation in the eddying regions and a consequent

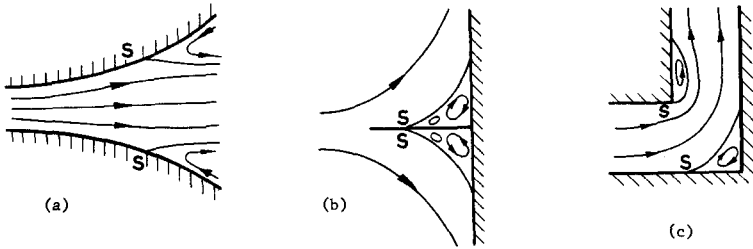


**Figure 5.8** Examples of separating flows: (a) diverging channel (diffuser); (b) effect of splitter plate on stagnation point flow; (c) flow round a sharp corner

loss of efficiency; it is therefore a phenomenon that engineers frequently try to avoid.

In some circumstances, separation cannot be completely avoided but can be controlled to a certain extent. For example, in flow past a bluff body, separation can be delayed (i.e. pushed towards the rear end of the body) by (a) suction upstream of separation to decrease the rate of growth of the boundary layer, (b) tangential injection of fast moving fluid at the boundary, (c) the forced onset of turbulence in the boundary layer which leads to a beneficial exchange of momentum between inner and outer parts of the boundary layer (hence the dimples on a golf-ball!).

### 5.7 Flow Past Streamlined Cylinders (Airfoils)

The most natural method of avoiding separation however is to make the body streamlined, i.e. slowly varying in the flow direction and with no sharp edges except the sharp “trailing edge” (figure 5.9). How does such an *airfoil* generate lift at high Reynolds number? If it is jerked into motion with velocity  $-U$  as in §5.5 (or more realistically accelerated from rest to this velocity) then for  $t = 0+$ , the flow is the unique irrotational flow sketched in figure 5.9a (cf. the flow pattern of figure (4.2a)—the two flows are related by a conformal mapping). Now irrotational flow round the sharp corner  $T$  would have infinite velocity at  $T$  (check this from eqn. (4.23)); this is clearly unrealistic and the flow separates at  $T$  forming a region of reversed flow and closed streamlines between  $T$  and the stagnation point  $A$  (figure 5.9b). Try drawing a knife at an angle through a glass of water (with pepper sprinkled on the surface to make the motion clearly visible) and you will see the effect. The vorticity emanating from the boundary layer above the section  $TA$  is then swept away by a process that is physically clear (vortex lines move with the fluid!) but mathematically somewhat obscure, leaving an equal and opposite net circulation  $\kappa$  round the airfoil (the total circulation round a very large circuit enclosing the whole region of disturbed fluid remaining zero).

What is the magnitude of  $\kappa$ ? Clearly just such as to make the flow leave smoothly from the trailing edge (Joukowski's hypothesis), since otherwise we still have trouble with the infinite velocity round  $T$ . If  $l$  is the span of the airfoil, then dimensionally,  $\kappa = O(Ul\alpha)$ , where  $\alpha$  is the angle of incidence,† and the lift (i.e. the component of force perpendicular to  $U$ ) is (§4.4)

$$L = \rho U \kappa = O(\rho U^2 l) \quad \text{per unit length of airfoil} \quad (5.45)$$

The drag, by contrast, (c.f. eqn. (5.25)) is clearly

$$D = O(R^{-1/2})\rho U^2 l, \quad R = Ul/v. \quad (5.46)$$

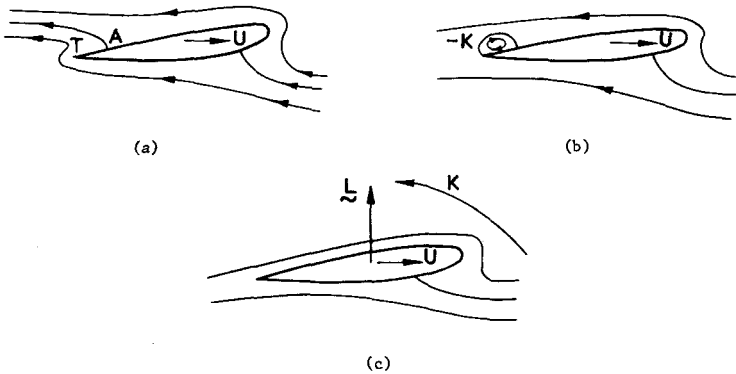


Figure 5.9 Development of lift on accelerated airfoil

It is an extraordinary fact, and yet the fact that underlies the phenomenal success of the science of aerodynamics, that the drag on the streamlined airfoil of figure (5.9) is equal to the drag on a cylinder of circular cross-section and of radius  $O(R^{-1/2})l$ ; with  $R^{1/2} \approx 500$  (above which the boundary-layer flow becomes unstable) the dramatic effect of successful streamlining is apparent.

## 5.8 A Mechanism for Lift Production for Hovering Insects

I would like to close this chapter by making brief reference to a fascinating mechanism of lift production believed to be exploited by the tiny insect *Encarsia formosa* (Weis-Fogh, 1973; Lighthill, 1973) whose wing chord is approximately 0.22 mm. Slow movie films show that the periodic motion of

†By symmetry,  $\kappa$  vanishes when  $\alpha = 0$ , and a linear relation between  $\kappa$  and  $\alpha$  is to be expected for small  $\alpha$ ; for large  $\alpha$ , the flow separates near the leading edge and the theory of §4.4 is no longer valid; there is a dramatic reduction in lift ("stalling").

the insect's wings consists essentially of a "clap" behind the back, followed by an "angular opening" or "fling", followed by a "sweep" of both wings, as illustrated in figure 5.10. During stage (b), contact between the wings is maintained at the "hinge" point: air rushes into the increasing angle  $2\alpha$  and gives rise to the circulation indicated. If the insect succeeds in passing to stage (c) at the moment when the pressure is continuous across the hinge, a state of affairs that is nearly attained when  $2\alpha \gtrsim 120^\circ$  (Lighthill, 1973), then the circulation survives round each wing and gives an *immediate* lift force  $\rho U \kappa$  on inviscid theory. This is to be contrasted with the situation in airfoil theory where the process of vortex shedding leads to a time delay of order  $l/U$  between the impulsive acceleration and the generation of maximum lift. The fact that the insect *does* hover is a tribute to the efficiency of the mechanism! Viscous effects modify the numbers involved, but not the essential nature of the lift process.

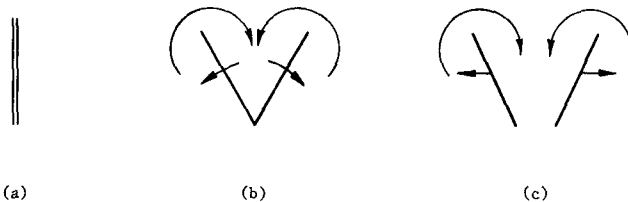


Figure 5.10 Motion of the wings of *Encarsia formosa*: (a) clap; (b) fling; (c) sweep

The lift force  $mg$  on the insect implies the application of an equal and opposite "point" force to the air; for *Encarsia formosa* the ratio  $mg/\rho v^2$  is about 900 (Lighthill, 1973) and the "round jet" theory of §2.4 is therefore applicable in the determination of the velocity field far from the beating wings.

## Lecture 6 Instability of Steady Flow

### 6.1 General Remarks

Problems of hydrodynamic stability and of transition from laminar to turbulent flow are of key interest, and it would be a grave omission not to give them some place, however inadequate, in this course of lectures, if only to provide some sort of bridge between the foregoing lectures and Professor Orszag's parallel course on turbulence. It is not a bridge that can be crossed with any confidence, although the theory of linear instability in its present highly developed form (see e.g. Lin's *Theory of Hydrodynamic*

*Stability* and Chandrasekhar's *Hydrodynamic and Hydromagnetic Stability*) provides reasonably secure foundations at least on the laminar bank (la rive droite?—la turbulence est sûrement sur la rive gauche!)

When a flow is unstable, a typical amplitude  $a(t)$  of a velocity or pressure fluctuation grows exponentially, like  $e^{\sigma t}$ , where  $\sigma = \sigma_r + i\sigma_i$ ,  $\sigma_r > 0$ , on the basis of *linear theory* (in which squares and products of quantities proportional to  $a(t)$  are neglected). It frequently happens that, when  $\sigma_r = 0$ ,  $\sigma_i = 0$  also, so that the onset of instability is characterised by the possible existence of a *steady* neutrally stable perturbation superposed on the basic flow. In some circumstances in theoretical work, it can be proved that  $\sigma_i = 0$  when  $\sigma_r = 0$ ; in other circumstances, it merely cannot be disproved, and it is then a natural assumption, at most consistent with observation, and dignified with the title of the "principle of exchange of stabilities".

When  $a(t) \propto e^{\sigma t}$ ,  $\sigma_r > 0$ , the amplitude rapidly passes out of the domain of validity of linearised theory and some account of non-linear interactions is necessary. An excellent recent review of non-linear stability theory is available (Stuart, 1971) from which I shall draw freely in the discussion that follows. Non-linear effects may be discussed in general terms in the context of the Landau equation (see e.g. Landau and Lifshitz, 1959: §27),

$$\frac{1}{2} \frac{d}{dt} |a|^2 = \sigma_r |a|^2 - \alpha |a|^4 + O(|a|^6), \quad (6.1)$$

which may be thought of as the formal result of expanding all perturbations in powers of  $a(t)$  and truncating at the cubic level. The coefficients  $\sigma_r$  and  $\alpha$  are in principle functions of the various dimensionless parameters that characterise the flow, e.g. a Reynolds number  $R$ , i.e.

$$\sigma_r = \sigma_r(R), \quad \alpha = \alpha(R). \quad (6.2)$$

If  $\sigma_r$  passes smoothly from negative to positive values as  $R$  increases through a *critical Reynolds number*  $R_c$ , then

$$\sigma_r = \sigma'_r(R_c)(R - R_c) + O(R - R_c)^2, \quad (6.3)$$

where  $\sigma'_r(R_c) > 0$ . In general  $\alpha(R_c) \neq 0$  and may in principle be either positive or negative.

Suppose first that  $\alpha(R_c) > 0$ . Then for  $0 < R - R_c < \epsilon$  where  $\epsilon$  is small, unstable solutions of (6.1) will stabilise at an equilibrium amplitude  $a_e$  given by

$$|a_e|^2 = \frac{\sigma_r(R)}{\alpha(R)} \approx \frac{\sigma'_r(R_c)(R - R_c)}{\alpha(R_c)}, \quad (6.4)$$

it being reasonable to suppose that for sufficiently small  $\epsilon$ , the  $O(|a|^6)$  terms in (6.1) are negligible. Solutions of (6.1) then remain permanently within its

domain of validity, in contrast to the linearised theory in which  $|a|^4$  is neglected. According to (6.4), instability of the basic flow will be characterised by the appearance of a steady secondary motion of amplitude proportional to  $(R - R_c)^{1/2}$  which interacts with the original flow in such a way as to render the joint flow stable to further perturbation. Two well-known problems which exhibit this behaviour are the circular Couette problem considered in §2.3 above, and the Bénard problem (thermal convection between horizontal plane boundaries heated from below).

If  $\alpha(R_c) < 0$ , then the term in  $|a|^4$  in (6.1) does not tend to stabilise the growth of perturbations (although conceivably subsequent terms in the expansion may do so). On the other hand, even at *subcritical* Reynolds numbers  $R < R_c$ , at which  $\sigma_r < 0$  and perturbations decay on linear theory, there will exist a threshold amplitude, given by (6.4) again, with the property that perturbations of amplitude greater than  $|a_c|$  will grow while those of amplitude less than  $|a_c|$  will decay. Poiseuille flow in a channel (§2.3) exhibits this behaviour: the critical Reynolds number, based on the half-width and the maximum velocity, is around 6000, but transition to turbulence occurs for this flow at Reynolds numbers of 2000 or even less depending on the level of disturbance present.

The threshold effect is more striking in flows such as plane Couette flow and Poiseuille flow in a pipe of circular section, which are stable on linear theory at all Reynolds numbers, i.e. for which no critical Reynolds number exists. These flows can indeed be kept laminar at exceedingly high Reynolds numbers (of order  $10^5$  in the case of pipe flow) provided great care is taken to minimise random disturbances; but under "normal" conditions, the flows exhibit transition to turbulence at Reynolds numbers of order  $10^4$ , and this can only be interpreted in terms of the non-linear threshold mechanism.

## 6.2 Centrifugal Instability

Consider first a velocity field with circular streamlines of the general form

$$\mathbf{u} = (0, v(r), 0) \quad \text{in cylindrical polars } (r, \theta, z), \quad (6.5)$$

with pressure  $p(r)$  given by

$$dp/dr = \rho v^2/r. \quad (6.6)$$

The centrifugal force  $\rho v^2/r$  tends to expand a ring of fluid of radius  $r$ ; suppose that it expands to radius  $r_1 = r + \delta r$ , its angular momentum remaining constant, so that its velocity is now  $rv/r_1$ . The centrifugal force acting on the ring will now be  $\rho(rv/r_1)^2/r_1$ , and if this is greater than the local restoring pressure gradient  $\rho v^2/r_1$ , the ring will continue to expand. The condition for instability (Rayleigh's criterion) is therefore  $r^2 v^2/r_1^3 > v^2/r_1$ , or

$$|rv(r)| > |r_1 v(r_1)|. \quad (6.7)$$

Note that conservation of angular momentum for the moving ring is equivalent to conservation of the circulation round it; this holds (§4.2) only in so far as viscosity is negligible. Viscosity tends to eliminate any local excess of circulation and thus tends to stabilise the flow; nevertheless any flow in which the circulation decreases rapidly outwards may be expected to be unstable to axisymmetric perturbations. The argument does not of course exclude the possibility of *non-axisymmetric* instabilities in flows in which the circulation is an *increasing* function of  $r$ .

In the case of circular Couette flow (§2.3), the circulation decreases outwards if  $\Omega_1 a^2 > \Omega_2 b^2 > 0$ , and in particular if the inner cylinder is rotating and the outer one at rest. (The situation when the cylinders rotate in opposite directions presents particular difficulties.) In this case, and when the gap  $d = b - a$  is small compared with  $a$ , the linearised problem for the determination of the growth rate  $\sigma$  reduces to (Stuart 1963)

$$\left. \begin{aligned} (D^2 - \lambda^2)(D^2 - \lambda^2 - \sigma)^2 \bar{v} + \lambda^2 T \bar{v} &= 0, \\ \bar{v} = D^2 \bar{v} = D(D^2 - \lambda^2 - \sigma) \bar{v} &= 0 \text{ at } \zeta = \pm \frac{1}{2}. \end{aligned} \right\} \quad (6.8)$$

Here,  $\zeta = d^{-1}(r - \frac{1}{2}(a + b))$ ,  $R(\bar{v}(\zeta)e^{i\lambda z/d}e^{\sigma t/d^2})$  is the perturbation to the velocity component  $v(r)$ ,  $D = d/d\zeta$ , and

$$T = \frac{a^4 \Omega_1^2}{v^2} \left(\frac{d}{a}\right)^3. \quad (6.9)$$

$T$  is the *Taylor number*; in the small gap approximation and when  $\Omega_2 = 0$ , it is the sole dimensionless parameter determining the stability characteristics of the flow. It may be interpreted (Stuart, 1963) as the ratio of the destabilising centrifugal force to the stabilising viscous force; and instability is therefore to be expected if  $T$  exceeds a critical value  $T_c$  determined by solution of the problem (6.8) with  $\sigma = 0$ . This linear eigenvalue problem (which may be treated by variational methods) in fact gives a neutral stability curve  $T = T(\lambda)$  (figure 6.1a) with a well defined minimum

$$T_c = 1708 \text{ at } \lambda = \lambda_c = 3.13. \quad (6.10)$$

The qualitative character of the neutrally stable disturbance when  $T = T_c$  is sketched in figure 6.1b—see Taylor (1923) for the original photographs of this striking phenomenon. Note that the small convection cells are as near square in cross-section as makes no difference.

When  $T$  is a little greater than  $T_c$ , the amplitude of the cellular motion is, by the general considerations of §6.1, proportional to  $(T - T_c)^{1/2}$ . This cellular motion tends to redistribute the angular momentum of the mean flow in such a way as to restore a situation of neutral stability, i.e.  $-(rv(r))'$  is decreased except near the cylindrical boundaries where viscous forces are better able to resist the instability. There is an increase in the gradient of  $v/r$  at the inner boundary and the torque required to maintain the motion

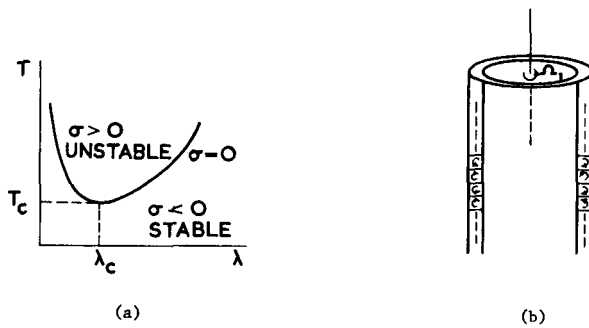


Figure 6.1 Onset of instability in circular Couette flow: (a) neutral stability curve; (b) structure of Taylor vortices

of the inner cylinder is greater than it would be if the Taylor vortices were not present; that this must be so is evident from the minimum dissipation theorem of §3.2 which is applicable whenever, as in the present context, the inertia term  $\mathbf{u} \cdot \nabla \mathbf{u}$  in the undisturbed flow is derivable from a potential which may be absorbed in the pressure term. The torque  $G$  is the simplest quantity to measure experimentally, and its variation with  $T$  is indicated in the qualitative sketch in figure 6.2a.

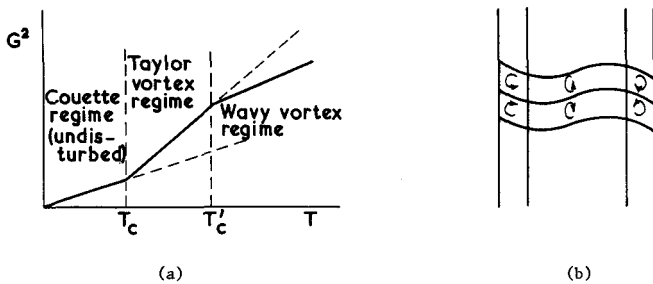


Figure 6.2 (a) Qualitative variation of  $G^2$  with  $T$ ; (b) Wavy vortices ( $m = 3$ )

When  $T$  is increased further, the Taylor vortices themselves are observed to become unstable to wavy disturbances (figure 6.2b) proportional to  $e^{im\theta} e^{i\omega t}$  at a second critical Taylor number  $T'_c > T_c$ ;  $T'_c$ ,  $\omega$  and the integer  $m$  depend on just how small the parameter  $d/a$  is. The fact that  $\omega \neq 0$  means that the waves propagate round the inner cylinder. In the experiments of Coles (1965),  $d/a \sim 0.8$ ,  $T'_c \sim 1.25T_c$  and  $m = 4$  at the first appearance of waves on the vortices. No convincing theoretical reason for the selection of the value  $m = 4$  appears to be yet available; however Eagles (1974) has

shown that interaction of a wavelike disturbance (with  $m = 4$ ) with the basic flow plus Taylor vortices leads to a *reduction* in the theoretical torque (consistent with experiment) below the level predicted when waves are not present. This suggests that the flow actually realised at high Taylor number will *not* be such as to maximise the flux of angular momentum from the inner cylinder (contrast the thermal convection situation envisaged by Malkus and Veronis, 1958).

When  $T$  is increased far beyond  $T_c$  (to values of order  $100T_c$  and greater) the flow observed by Coles (1965) exhibits a behaviour that is tantalising in its variety and complexity. First the number  $n$  of vortices along the axial length and the wave-number  $m$  make jumps in a manner that is repeatable from one experiment to the next, but that depends on the way the function  $\Omega_1(t)$  is increased with time; there is moreover a hysteresis effect whereby different values of the pair  $(m, n)$  for given  $\Omega_1$  may be arrived at by different paths in the  $\Omega_1 - t$  plane. These flows are certainly laminar and stable (although time-periodic on account of the factor  $e^{i\omega t}$ ) and it is therefore quite certain that there can be no general uniqueness theorem for laminar solutions of the Navier–Stokes equations subject to a prescribed steady velocity distribution on a closed bounding surface; (the possible uniqueness of *steady* solutions would not appear to be quite ruled out by these considerations).

When  $T$  is further increased, further instability modes are excited, and the flow pattern gradually becomes more irregular evolving into fully developed turbulence when  $T$  is very large. Even when the flow is fully turbulent however, vestiges of the Taylor vortex pattern make sporadic appearances, suggesting that the mean velocity field is in some sense neutrally stable to perturbations of Taylor vortex type.

The behaviour is strikingly different when the inner cylinder is at rest and the outer cylinder rotates. In this case the flow is stable on linear theory, but the threshold mechanism discussed in §7.1 leads to what Coles (1965) describes as *catastrophic transition* to a flow regime characterised by helical bands of turbulence which rotate at an angular speed somewhat less than  $\Omega_2$ . This means that fluid particles near to the outer cylinder appear to pass both from the laminar to the turbulent region at the “trailing edge” of the turbulent band, and from the turbulent to the laminar region at the “leading edge”. The suggestion that a fluid particle may find itself following at one moment a random path in the turbulent region and at the next moment a non-random path in the laminar region is most striking but has as yet attracted no theoretical explanation (but see Phillips, 1972; Townsend, 1966 for relevant discussion of the turbulent—non-turbulent interface in a different context).

It will be evident from the above remarks that circular Couette flow provides a stability problem of almost infinite variety and challenge. The

phenomenon of the appearance of new solutions of the Navier–Stokes equations as a parameter such as  $T$  increases (*bifurcation*) and the stability of these solutions pose questions of considerable delicacy, answers to which will be provided presumably only through the use of sophisticated weapons of non-linear functional analysis—see Stuart (1971) for further discussion of theoretical approaches and for detailed references.

## Lecture 7 The Dynamo Problem

### 7.1 The Self-Excited Disc Dynamo

The magnetic fields of the Earth and of the Sun are believed to be associated with electric currents in the conducting fluid regions of these bodies which are maintained by some kind of inductive action due to motion of the fluid across the self-same magnetic field. This sort of bootstrap action is perhaps best illustrated with reference to the so-called homopolar disc dynamo (figure 7.1a). The electrically conducting disc rotates about its axis with angular velocity  $\Omega$ , and a conducting wire makes sliding contact with the rim of the disc and with its axis as shown; the wire is twisted into a circle in its passage from the rim to the axis so that any current flowing in the wire gives rise to a magnetic field with a non-zero flux  $\Phi$  across the disc. The rotation of the disc in the presence of this flux generates a radial current which clearly flows along the wire. If the value of  $\Omega$  is just right, then the value of the current  $I$  will be just compatible with the flux  $\Phi$  that it produces and a steady field will result. Note two crucial features of this intriguing device: (i) there is a concentrated shear (a  $\delta$ -function) at the sliding contact at the rim; and (ii) the device lacks reflexional symmetry; the wire must be twisted in a definite sense relative to the rotation vector if the flux produced is to have the appropriate sign for dynamo action; if the sense of

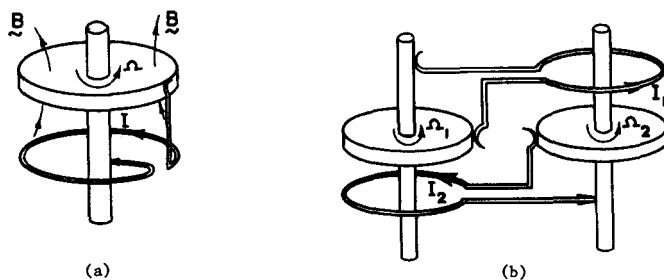


Figure 7.1 (a) Self-exciting disc dynamo; (b) Coupled disc dynamo

twist is reversed, the field rapidly decays to zero. Of course a torque is required to maintain the rotation of the disc, the rate of working of this torque being equal in the steady state to the rate of Joule dissipation in the conductor.

A more elaborate gadget is illustrated in figure 7.1b (Allan, 1958; see also Hide and Roberts, 1961). Two identical discs rotate with angular velocities  $\Omega_1$  and  $\Omega_2$ , and these drive currents  $I_1$  and  $I_2$  respectively. The current  $I_1$  creates a flux  $MI_1$  across disc 2, where  $M$  is the mutual inductance between the loop of  $I_1$  and the rim of disc 2; similarly for the flux across disc 1. If  $R$  is the net resistance in each circuit, and  $L$  the self-inductance, then

$$\left. \begin{aligned} L \frac{dI_1}{dt} + RI_1 &= M\Omega_1 I_2 \\ L \frac{dI_2}{dt} + RI_2 &= M\Omega_2 I_1 \end{aligned} \right\} \quad (7.1)$$

Suppose further that each disc is subjected to a constant torque  $G$ ; then the equations of motion of the disc are

$$\left. \begin{aligned} C \frac{d\Omega_1}{dt} &= G - MI_1 I_2 \\ C \frac{d\Omega_2}{dt} &= G - MI_2 I_1 \end{aligned} \right\} \quad (7.2)$$

where  $C$  is the moment of inertia of each disc, the term  $MI_1 I_2$  representing the additional torque due to the Lorentz force  $\mathbf{j} \wedge \mathbf{B}$  in each disc. The coupled equations (7.1) and (7.2) have some interesting properties which in some ways model the long-term behaviour of the Earth's magnetic field, and which therefore merit discussion.

First note that from (7.2),  $\Omega_1 - \Omega_2 = \text{const.}$  Denoting this constant by  $\Omega$ , let

$$\omega_1 = \Omega y_1, \quad \omega_2 = \Omega y_2, \quad \tau = (R/L)t. \quad (7.3)$$

and, with  $I = (CR\Omega/ML)^{1/2}$ , let

$$I_1 = Ix_1, \quad I_2 = Ix_2. \quad (7.4)$$

The equations then take the simplified form

$$\left. \begin{aligned} \dot{x}_1 + x_1 &= m^2 y_1 x_2 \\ \dot{x}_2 + x_2 &= m^2 y_2 x_1 \\ \dot{y}_1 &= g^2 - x_1 x_2 \\ y_2 - y_1 &= 1, \end{aligned} \right\} \quad (7.5)$$

where  $m^2 = M\Omega/R$  and  $g^2 = GL/CR\Omega$ . These equations have two possible

steady solutions satisfying  $x_1 x_2 = g^2$  and  $y_1 y_2 = m^{-4}$ . If  $A$  satisfies

$$A^2 - \frac{1}{A^2} = m^2, \quad (7.6)$$

then these two solutions are given by

$$x_1 = \pm Ag, \quad x_2 = \pm g/A, \quad y_1 = A^2/m^2, \quad y_2 = 1/A^2 m^2. \quad (7.7)$$

It may be verified that both solutions are neutrally stable on a *linear* perturbation analysis.

Solutions to the equations may be computed starting from arbitrary initial conditions. If these initial conditions are sufficiently near to either of the solutions (7.7), then the solution remains permanently in that neighbourhood; but if the initial conditions are chosen arbitrarily, the solution behaves in a much more interesting manner. The behaviour is best visualised in the phase plane of the variables  $(x_1, x_2)$  (figure 7.2a) in which the steady states are represented by the points  $S_1$  and  $S_2$ . The point  $(x_1(t), x_2(t))$  in general circulates a number of times round  $S_1$ , then flicks over to a neighbourhood of  $S_2$  which it circulates a number of times before returning to the neighbourhood of  $S_1$  when the process is repeated. Figure 7.2b shows the corresponding typical variation of the function  $x_1(t)$ . The magnetic field associated with  $I_1(t)$  will of course exhibit corresponding *reversals* when  $x_1(t)$  changes sign.

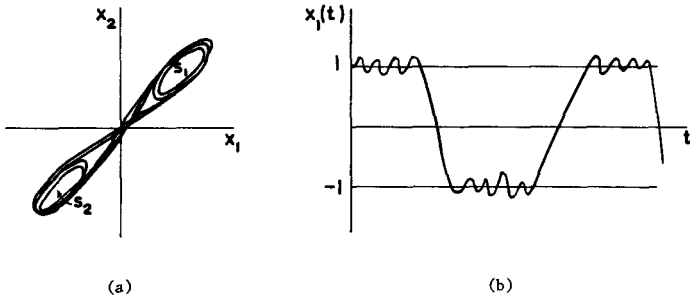


Figure 7.2 Behaviour of coupled disc dynamos: (a) typical phase diagram when  $A = 2$ ,  $g = 1/2$ ; (b) typical variation of  $x_1(t)$  when  $A = 2$ ,  $g = 1/2$

The Earth's main dipole is known to have reversed in polarity a large number of times and at rather random intervals during its long history. The evidence is primarily paleomagnetic (Bullard, 1968) and the indications are that the gap between reversals is typically of order  $10^6$  years, while the duration of a reversal "event" is typically of order  $10^4$  years. The two time-scales evident in a graph of the form of figure 7.2b and the qualitative similarity of the curve to the curve for the Earth's dipole moment  $\mu(t)$  make the coupled disc dynamo a suggestive model for processes that may be

important in the Earth's core. It is however a challenging problem as yet unsolved to effect a simplification of the complicated magnetohydrodynamics of the Earth's core (by judicious averaging procedures) to the level of coupled ordinary differential equations remotely resembling (7.5).

## 7.2 The Induction Equation

The magnetic field  $\mathbf{B}(\mathbf{x}, t)$ , current density  $\mathbf{j}(\mathbf{x}, t)$ , and electric field  $\mathbf{E}(\mathbf{x}, t)$  are related in a moving conductor by the equations

$$\nabla \cdot \mathbf{B} = 0, \quad \frac{\partial \mathbf{B}}{\partial t} = -\nabla \wedge \mathbf{E}, \quad \mu_0 \mathbf{j} = \nabla \wedge \mathbf{B}, \quad \mathbf{j} = \sigma(\mathbf{E} + \mathbf{u} \wedge \mathbf{B}), \quad (7.8)$$

where  $\sigma$  is the electrical conductivity, and  $\mu_0$  is the usual permeability constant. In these equations, we neglect displacement current, since we are concerned with phenomena whose time-scale is large compared with the time for a light wave to cross the region of interest. In this (MHD) approximation, light waves are filtered out of the equations; in a sense the approximation is analogous to the incompressibility assumption in conventional fluid dynamics in which sound waves are similarly filtered out.

Elimination of  $\mathbf{j}$  and  $\mathbf{E}$  from (7.3) yields the *induction equation*

$$\frac{\partial \mathbf{B}}{\partial t} = \nabla \wedge (\mathbf{u} \wedge \mathbf{B}) + \lambda \nabla^2 \mathbf{B}, \quad (7.9)$$

where  $\lambda = (\mu_0 \sigma)^{-1}$  is the *magnetic diffusivity* (or sometimes *resistivity*) of the medium. This equation is comparable in structure with the vorticity equation

$$\frac{\partial \boldsymbol{\omega}}{\partial t} = \nabla \wedge (\mathbf{u} \wedge \boldsymbol{\omega}) + \nu \nabla^2 \boldsymbol{\omega}, \quad (7.10)$$

the major difference being that  $\boldsymbol{\omega}$  is further constrained by the relation  $\boldsymbol{\omega} = \nabla \wedge \mathbf{u}$ , whereas  $\mathbf{B}$  can be prescribed independently of  $\mathbf{u}$  at any initial instant. Nevertheless there are certain immediate consequences of the analogy, of which the following are perhaps the most important:

i) When  $\lambda = 0$ , the lines of force of the  $\mathbf{B}$ -field (i.e. the “ $\mathbf{B}$ -lines”) are frozen in the fluid (Alfvén's theorem); flux tubes move with constant strength, and stretching of magnetic lines of force implies proportionate intensification.

ii) The counterpart of the helicity (§4.2) is the quantity

$$I_m = \int \mathbf{A} \cdot \mathbf{B} \, dV, \quad (7.11)$$

where  $\mathbf{A}$  is the vector potential of the magnetic field—i.e.  $\mathbf{B} = \nabla \wedge \mathbf{A}$ . That  $I_m$  is an invariant for a localised magnetic field distribution when  $\lambda = 0$  was

proved by Woltjer (1956); the invariant has the same topological interpretation as the helicity in the vorticity context.

The analogy with vorticity led Batchelor (1950) to the conclusion that the magnetic energy density  $(1/2\mu_0)\langle \mathbf{B}^2 \rangle$  would increase in a conducting fluid in turbulent motion provided  $\lambda < \nu$ , on the grounds that the quantity  $\langle \omega^2 \rangle$  is in approximate statistical equilibrium so that if  $\lambda = \nu$ ,  $\langle \mathbf{B}^2 \rangle$  may be expected to be in statistical equilibrium also; if  $\lambda < \nu$ , the increase in  $\langle \mathbf{B}^2 \rangle$  due to line stretching may then be expected to predominate over the decrease in  $\langle \mathbf{B}^2 \rangle$  due to ohmic dissipation. Batchelor further argued that  $\frac{1}{2}\langle \mathbf{B}^2 \rangle$  would increase to the level of the energy density of the small-scale components of the turbulence, since line stretching in turbulence is essentially a small-scale process. Although plausible, the Batchelor criterion  $\lambda < \nu$  has never been established beyond doubt, and potent counter-arguments have been produced (e.g., Saffman, 1963); the trouble is that increase in  $\langle \mathbf{B}^2 \rangle$  is inevitably associated with increase in  $\langle \mathbf{j}^2 \rangle$  also so that there is an accelerated diffusion effect associated with the term  $-\lambda\langle \mathbf{j}^2 \rangle$  in the magnetic energy equation which can be of crucial importance. (A simple example by way of illustration will be described in the following section.) The question is evidently a delicate one (Kraichnan and Nagarajan, 1967), but has to some extent been successfully bypassed by more recent developments, which I shall describe in Lecture 8.

### 7.3 Field Exclusion by Differential Rotation

The subtle long-term influence of weak diffusion is well illustrated by the problem of the distortion of an initially uniform magnetic field  $\mathbf{B}_0$  by a localised differential rotation of the form

$$\mathbf{u} = (0, r\omega(r), 0) \quad (7.12)$$

in cylindrical polars  $(r, \theta, z)$ , where  $\omega(r)$  is everywhere finite and tends to zero as  $r \rightarrow \infty$ . We suppose that the field is undisturbed at infinity, so that (figure 7.3)

$$\mathbf{B} \sim \mathbf{B}_0(\cos \theta, -\sin \theta, 0) \text{ as } r \rightarrow \infty. \quad (7.13)$$

It would be inappropriate here to give the full details for the solution of this problem, and a qualitative description will suffice (see R. L. Parker, 1966; Weiss, 1966 for details).

Let  $\omega_0$  represent a typical angular velocity and  $a$  a typical eddy dimension. We suppose that the *magnetic Reynolds number*  $R_m = \omega_0 a^2 / \lambda$  is large, implying that the induction term  $\nabla \wedge (\mathbf{u} \wedge \mathbf{B})$  dominates over the diffusion term  $\lambda \nabla^2 \mathbf{B}$ . For small values of  $t$ , the field is locally rotated by the eddy, and the  $\theta$ -component of the field grows linearly with time in the neighbourhood of the region where the gradient of angular velocity is non-zero. As  $t$  increases,

the field is distorted into a tight double spiral in which the field gradients become large; when these are so large that diffusion becomes significant, loops of field break off and decay with time as they rotate. The flux across the rotating region decreases systematically and ultimately approaches zero. The sequence of events is represented in the qualitative sketches of figure 7.3.

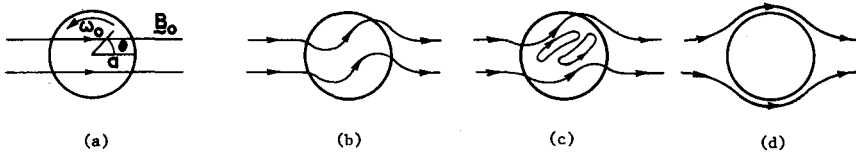


Figure 7.3 Qualitative sketch of the process of flux expulsion when  $R_m = \omega_0 a^2 / \lambda \gg 1$ : (a)  $t = 0$ ; (b)  $\omega_0 t \approx 1$ ; (c)  $\omega_0 t \gg 1$ ; (d)  $\omega_0 t \rightarrow \infty$ .

The ultimate steady state is adequately represented in the particular case when

$$\left. \begin{aligned} \omega(r) &= \omega_0, & (r < a), \\ &0, & (r > a), \end{aligned} \right\} \quad (7.14)$$

i.e. we have rigid body rotation of the cylindrical region  $r < a$ . First note that since the field merely satisfies  $\nabla^2 \mathbf{B} = 0$  for  $r > a$ , it does not depend on the conductivity of the medium outside the cylinder and the problem is the same as if this medium were insulating. Relative to axes rotating with the cylinder, the field is rotating with angular velocity  $-\omega_0$ ; regarding this as the superposition of two alternating fields at right angles and in quadrature ( $\pi/2$  out of phase) it is evident that for  $R_m \gg 1$  the field will only penetrate into the conductor a distance  $\delta = O(aR_m^{-1/2})$  (the skin effect). Inside this skin, the field is effectively zero, i.e. it is almost totally excluded from the rotating region. Note the analogy between this skin (or magnetic boundary layer) and the boundary layers treated in Lecture 5.

A detailed analysis shows that  $\langle \mathbf{B}^2 \rangle$  increases to a value  $O(B_0^2 R_m)$  before diffusion becomes important, and that  $\langle \mathbf{B}^2 \rangle$  decreases to  $O(B_0^2 R_m^{-1})$  as  $t \rightarrow \infty$ , where the average  $\langle \dots \rangle$  is an average over the region  $r < a$ . Note the dramatic difference between the limiting processes

$$\lim_{t \rightarrow \infty} \lim_{R_m \rightarrow \infty} \quad \text{and} \quad \lim_{R_m \rightarrow \infty} \lim_{t \rightarrow \infty}$$

a property that no doubt extends also to the much more difficult turbulent problem referred to in §7.2.

### 7.4 Generation of Toroidal Field by Differential Rotation

Suppose now that, at time  $t = 0$ ,

$$\mathbf{B} = B_r(r, z)\hat{\mathbf{e}}_r + B_z(r, z)\hat{\mathbf{e}}_z, \quad (7.15)$$

in cylindrical polars  $(r, \varphi, z)$ , and that

$$\mathbf{u} = r\omega(r, z)\hat{\mathbf{e}}_\varphi. \quad (7.16)$$

The field  $\mathbf{B}$  is purely *poloidal*, while  $\mathbf{u}$  is purely *toroidal*. The motion tends to generate a toroidal component  $B_\varphi$  of magnetic field; in fact the inductive term  $\nabla \wedge (\mathbf{u} \wedge \mathbf{B})$  reduces to  $\hat{\mathbf{e}}_\varphi r(\mathbf{B} \cdot \nabla)\omega$ , so that the  $\varphi$ -component of (7.9) becomes

$$\frac{\partial B_\varphi}{\partial t} = r(\mathbf{B} \cdot \nabla)\omega + \lambda \left( \nabla^2 - \frac{1}{r^2} \right) B_\varphi. \quad (7.17)$$

If  $(\mathbf{B} \cdot \nabla)\omega = 0$ , i.e. if  $\omega$  is constant on  $\mathbf{B}$ -lines, then  $B_\varphi$  remains equal to zero (Ferraro's law of isorotation); clearly variation of  $\omega$  along  $\mathbf{B}$ -lines is necessary to distort  $\mathbf{B}$ -lines out of meridian planes.

Consider the particularly simple situation when  $\mathbf{B}$  is uniform and parallel to the  $z$ -axis, i.e.  $B_r = 0$ ,  $B_z = B_0$ , and when  $\omega = \omega(R)$  where  $r = R \sin \theta$ ; then

$$r(\mathbf{B} \cdot \nabla)\omega = B_0 R \omega'(R) \sin \theta \cos \theta. \quad (7.18)$$

For small values of  $t$ , diffusion is again negligible, and from (7.17) the field  $B_\varphi$  grows linearly with time:

$$B_\varphi = B_0 R \omega'(R) t \sin \theta \cos \theta. \quad (7.19)$$

Note that symmetry of  $\omega$  about the plane  $z = 0$  ( $\theta = \pi/2$ ) implies antisymmetry of  $B_\varphi$ . Physically, it is as if the lines of forces were locally gripped by the fluid and "cranked" round the  $z$ -axis (figure 7.4).

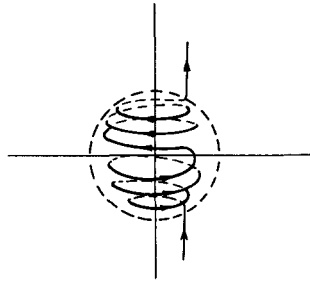


Figure 7.4 Distortion of a typical line of force by local differential rotation

For  $t \rightarrow \infty$ , a steady state again develops. In this steady state,

$$B_\phi = \frac{B_0}{\lambda} f(R) \sin \theta \cos \theta \quad (7.20)$$

where

$$f(R) = -\frac{1}{R^3} \int_0^R s^4 \omega(s) ds, \quad (7.21)$$

a result that may be verified by straight substitution in (7.17). Note that the distortion of the field will be localised only if  $\omega(s) = o(s^{-2})$  as  $s \rightarrow \infty$ . If  $\omega(s) = o(s^{-5})$  as  $s \rightarrow \infty$ , then  $f(R) = 0(R^{-3})$  as  $R > \infty$ .

In the particular case of rigid body rotation in a spherical region  $R < a$ , i.e.

$$\left. \begin{aligned} \omega(R) &= \omega_0 & (R < a) \\ &0 & (R > a) \end{aligned} \right\} \quad (7.22)$$

we have

$$\left. \begin{aligned} B_\phi &= -\frac{R_m}{5} B_0 \left(\frac{R}{a}\right)^2 \sin \theta \cos \theta, & (R < a) \\ &-\frac{R_m}{5} B_0 \left(\frac{a}{R}\right)^3 \sin \theta \cos \theta, & (R > a) \end{aligned} \right\} \quad (7.23)$$

where  $R_m = \omega_0 a^2 / \lambda$ . Note particularly the linear dependence of the perturbation field on  $R_m$  (in contrast to the situation of §7.3). There is no suggestion of flux expulsion here; flux expulsion evidently occurs only when the vorticity associated with the swirling motion is perpendicular to the convected magnetic field.

### 7.5 The 3-Sphere Dynamo

Perhaps the simplest example of localised dynamo action in a simply-connected region of fluid of uniform conductivity is provided by a 3-sphere dynamo of figure 7.5 (Gibson, 1968; Venezian, 1967). Let  $A, B, C$  be the points with Cartesian co-ordinates  $(d, 0, 0), (0, d, 0), (0, 0, d)$ , and let  $S_A, S_B, S_C$  be spheres of equal radii  $a \ll d$  centred at  $A, B$  and  $C$ . Suppose that the conductivity of the spheres and of the surrounding medium is  $\sigma$ . Suppose that  $S_A$  rotates with angular velocity  $(0, 0, \omega)$ ,  $S_B$  with angular velocity  $(\omega, 0, 0)$  and  $S_C$  with angular velocity  $(0, \omega, 0)$ , and that outside the spheres,  $\mathbf{u} \equiv 0$ . This defines a kinematically possible (though dynamically implausible) velocity field in a fluid of infinite extent.

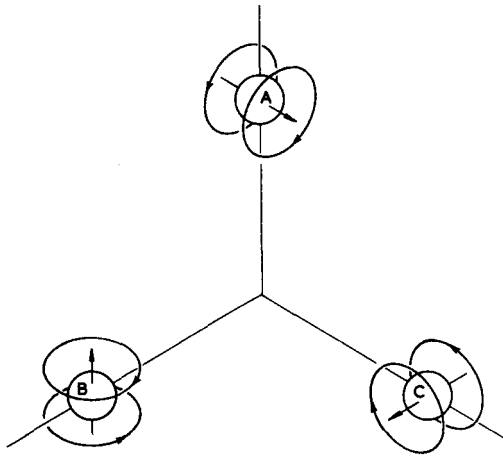


Figure 7.5 The 3-sphere dynamo (Venezian, 1967)

We know from §7.4 that, if there is a locally uniform magnetic field  $(0, 0, B)$  in the neighbourhood of  $S_A$ , then the rotation of  $S_A$  will generate a toroidal field which (from 7.23) in the neighbourhood of  $S_C$  is  $(0, B_1, 0)$  where

$$B_1 = kR_m B (a/R)^3, \quad (7.24)$$

where  $R_m = \omega a^2 / \lambda$ ,  $R = \sqrt{2} d$  and  $k = \frac{1}{10}$  (since  $\theta \approx \pi/4$ ).

If

$$R_m = \frac{1}{k} (R/a)^3 \quad (7.25)$$

then  $B_1 = B$ . Similarly, the rotation of  $S_C$  generates a field which in the neighbourhood of  $S_B$  is  $(B, 0, 0)$  and the rotation of  $S_B$  generates the field  $(0, 0, B)$  that we started with in the neighbourhood of  $S_A$ . The condition (7.25) is evidently the condition for steady dynamo action, valid when  $R \gg a$  (and so requiring  $R_m \gg 1$ ).

Actually the value  $k = \frac{1}{10}$  is not correct for a rather subtle reason. Weak spatial gradient of the field  $B$ , of order  $Ba/R$ , in the neighbourhood of  $S_A$  leads to a perturbation field in the neighbourhood of  $S_C$  of order  $(Ba/R)(a/R)^2 = B(a/R)^3$ . The net effect (Gibson, 1968) is simply to modify the critical value of  $k$  (from  $\frac{1}{10}$  to  $-\frac{1}{3}$ !) for steady dynamo action.

It should be mentioned that the 3-sphere dynamo is an elaboration of the celebrated 2-sphere dynamo of Herzenberg (1958) which was the first example, rigorously established, of the possibility of steady dynamo action

in a simply-connected *bounded* region. The 3-sphere dynamo (unlike the 2-sphere dynamo) can function in a medium of infinite extent; moreover the mutual interaction of the three spheres is rather simpler to comprehend than the corresponding interaction for the 2-sphere case (which involves consideration of the images of the two spheres outside the conducting region).

## Lecture 8 Turbulence and Mean-Field Electrodynamics

### 8.1 Motivation

We have seen in § 7.4 that there is a simple mechanism whereby toroidal field may be generated out of poloidal field, in an axisymmetric system *viz.* the distortion of field lines by differential rotation about the axis of symmetry. Dynamo action in a spherical system, such as the Earth or the Sun requires that there should be a second mechanism whereby poloidal field may be regenerated out of toroidal field. It is physically clear that no axisymmetric motion is capable of providing this mechanism; and indeed it was proved by Cowling (1934) (the famous “anti-dynamo theorem”) that sustained dynamo action is impossible in an axisymmetric system; the poloidal field may be amplified for a time by poloidal motions, but ultimately the magnetic field in such a system, and in the absence of external sources, must decay to zero. A full discussion of this theorem and of related results is given in Roberts (1967).

The crucial second physical mechanism was put forward by Parker (1955), although some years elapsed before the mathematical foundations were clarified (Steenbeck, Krause and Radler, 1966†; Moffatt, 1970*a*; Parker, 1970; a large number of further references are given in the review article *Dynamo Theory* by Roberts, 1971). Parker introduced the concept of a “local cyclonic event”, *i.e.* an eddy of limited extent and duration and in which the local rotation (or vorticity) bears a definite relation (as say in a right-handed screw) to the local velocity vector. The effect of such an event on a **B**-line is indicated in figure 8.1. The **B**-line is locally distorted and twisted, and the loop that is formed is the same as would be generated by a current **j** parallel to **B** (and note that  $\mathbf{j} \cdot \mathbf{B} < 0$  when  $\mathbf{u} \cdot \boldsymbol{\omega} > 0$ ). The inference is that a random superposition of such cyclonic events with  $\langle \mathbf{u} \cdot \boldsymbol{\omega} \rangle > 0$  will lead to an average current distribution antiparallel to the local magnetic field.

Now consider this effect in the spherical geometry (figure 8.2). In a rotating thermally convecting system, such as the Earth or the Sun, a

†An important series of papers by these authors has been translated into English by Roberts and Stix (1971).

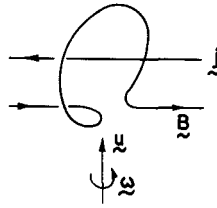


Figure 8.1 Effect of cyclonic event on a B-line

cyclonic event corresponds to the rising of a blob of fluid with a local excess of buoyancy. Local entrainment and conservation of angular momentum leads to positive values of  $\mathbf{u} \cdot \boldsymbol{\omega}$  in the northern hemisphere and negative values in the southern hemisphere. The Parker effect then generates a symmetric toroidal current distribution  $\mathbf{j}_T$  out of the antisymmetric toroidal field distribution  $\mathbf{B}_T$ . With the current  $\mathbf{j}_T$  is associated a poloidal field  $\mathbf{B}_P$ . (It has been pointed out by Weiss (1971) that this poloidal field must have an X-type (rather than an O-type) neutral point on the equatorial plane; the O-type neutral points are shifted into the northern or southern hemispheres where the Parker mechanism sidesteps Cowling's anti-dynamo theorem.)

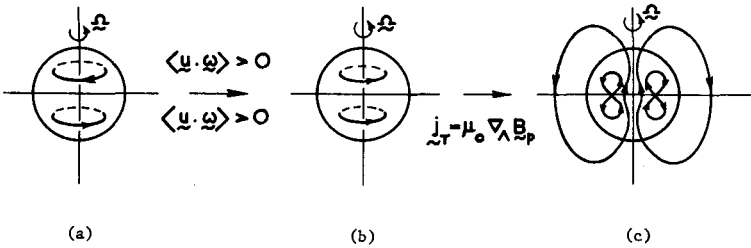


Figure 8.2 Regeneration of poloidal field from toroidal field by Parker's mechanism

It should be clear from these introductory remarks that the Parker mechanism is at least plausible as the second crucial ingredient of the dynamo process. In the following sections we shall show how the mechanism emerges from an appropriate averaging procedure starting from the induction equation; we shall then show how this effect leads to dynamo action, and conclude with a brief discussion of the possible influence of Lorentz forces in controlling the ultimate level of the amplified magnetic field.

## 8.2 The Mean Electromotive Force Generated in Homogeneous Turbulence (Steenbeck, Krause, Rädler, 1966)

Let us neglect for the moment any mean velocity in the fluid. Let  $\mathbf{u}(\mathbf{x}, t)$  be an incompressible turbulent velocity field, homogeneous in space and stationary in time (an idealisation of course), with  $\langle \mathbf{u} \rangle = 0$ , where we use angular brackets to denote an ensemble average. Suppose that at some reference instant  $t = 0$ , the magnetic field is non-random, and that its length-scale  $L$  is very large compared with any length-scale  $l$  characterising the turbulence (e.g. the integral length scale). For  $t > 0$ , we may then write

$$\mathbf{B}(\mathbf{x}, t) = \mathbf{B}_0(\mathbf{x}, t) + \mathbf{b}(\mathbf{x}, t), \quad \langle \mathbf{b} \rangle = 0, \quad (8.1)$$

where  $\mathbf{B}_0 = \langle \mathbf{B} \rangle$  is the ensemble average field on a scale  $L$  and  $\mathbf{b}$  is the fluctuation field, generated by the inductive motion  $\mathbf{u}$ , on a scale of order  $l$ .

The average of the induction equation (7.9) is clearly

$$\frac{\partial \mathbf{B}_0}{\partial t} = \nabla \wedge \mathcal{E} + \lambda \nabla^2 \mathbf{B}_0 \quad (8.2)$$

$$\text{where } \mathcal{E} = \langle \mathbf{u} \wedge \mathbf{b} \rangle. \quad (8.3)$$

$\mathcal{E}$  is the mean electromotive force (emf) that is generated by the turbulence, and a central aim of any theory must be to calculate its value in terms of the statistical properties of the velocity field.

Subtraction of (8.2) from (7.9) gives an equation for the fluctuation field  $\mathbf{b}(\mathbf{x}, t)$ , viz.

$$\frac{\partial \mathbf{b}}{\partial t} = \nabla \wedge (\mathbf{u} \wedge \mathbf{B}_0) + \nabla \wedge (\mathbf{u} \wedge \mathbf{b} - \langle \mathbf{u} \wedge \mathbf{b} \rangle) + \lambda \nabla^2 \mathbf{b}. \quad (8.4)$$

Coupled with the initial condition  $\mathbf{b}(\mathbf{x}, 0) = 0$ , this equation establishes a *linear relation* between  $\mathbf{b}$  and  $\mathbf{B}_0$  and hence between  $\langle \mathbf{u} \wedge \mathbf{b} \rangle$  and  $\mathbf{B}_0$ .

We now exploit the assumption that the scale  $L$  of  $\mathbf{B}_0$  is large, i.e. that  $\mathbf{B}_0$  is slowly varying. If  $\mathbf{B}_0$  were uniform, then  $\mathcal{E}$  would also necessarily be uniform, and the most general linear relation between  $\mathcal{E}$  and  $\mathbf{B}_0$  would be simply

$$\mathcal{E}_i = A_{ij} B_{0j}, \quad (8.5)$$

where  $A_{ij}$  is a second-rank pseudo-tensor ("pseudo" because  $\mathcal{E}$  is a polar vector and  $\mathbf{B}_0$  an axial vector). When  $\mathbf{B}_0$  is not quite uniform, (8.5) must provide the first term of an expansion of the form

$$\mathcal{E}_i = A_{ij} B_{0j} + C_{ijk} \frac{\partial B_{0j}}{\partial x_k} + E_{ijkl} \frac{\partial^2 B_{0j}}{\partial x_k \partial x_l} + \dots \quad (8.6)$$

Note that any term involving *time* derivatives of  $\mathbf{B}_0$  can be re-expressed in terms of space derivatives via (8.2) and (8.3). The pseudo-tensors  $A, C, E, \dots$  are determined in principle solely by the statistical properties of the  $\mathbf{u}$ -field and by the parameter  $\lambda$  (which appears in eqn. (8.4) determining  $\mathbf{b}(\mathbf{x}, t)$ ).

If the statistical properties of the turbulence are invariant under rotations of the axis of reference, then the pseudo-tensors  $A, C, E, \dots$  must exhibit the same invariance; in particular

$$A_{ij} = \alpha \delta_{ij}, \quad C_{ijk} = \beta \epsilon_{ijk}, \quad (8.7)$$

where  $\alpha$  is a pseudo-scalar and  $\beta$  a pure scalar. The parameter  $\alpha$  changes sign under a change from a right-handed to a left-handed frame of reference, and can therefore be non-zero only in turbulence in which there is a basic *lack of reflexional symmetry*. Turbulence whose statistical properties are invariant under rotations, but not under reflexions, of the frame of reference, may be described as *pseudo-isotropic*. A simple measure of the lack of reflexional symmetry in a turbulent flow is the mean helicity  $\langle \mathbf{u} \cdot \boldsymbol{\omega} \rangle$  (recall §4.2). In conventional (e.g. wind-tunnel) turbulence,  $\langle \mathbf{u} \cdot \boldsymbol{\omega} \rangle$  is almost invariably zero from symmetry considerations; but  $\langle \mathbf{u} \cdot \boldsymbol{\omega} \rangle$  may be non-zero in turbulence in a rotating environment such as the Earth or Sun, and when  $\langle \mathbf{u} \cdot \boldsymbol{\omega} \rangle \neq 0$ ,  $\alpha$  will in general be non-zero also.

From (8.6) and (8.7), we have in the pseudo-isotropic case

$$\boldsymbol{\varepsilon} = \alpha \mathbf{B}_0 - \beta \nabla \wedge \mathbf{B}_0 + \dots, \quad (8.8)$$

and substitution of just these two terms of the expansion in (8.2) gives the mean-field equation

$$\frac{\partial \mathbf{B}_0}{\partial t} = \alpha \nabla \wedge \mathbf{B}_0 + (\lambda + \beta) \nabla^2 \mathbf{B}_0. \quad (8.9)$$

The parameter  $\beta$  evidently plays the part of an *eddy diffusivity*. Subsequent terms of the expansion (8.8) lead to terms involving third and higher derivatives of  $\mathbf{B}_0$  in (8.9), and these are of no importance when the scale  $L$  of  $\mathbf{B}_0$  is very large.

The values of the parameters  $\alpha$  and  $\beta$  are of crucial importance in (8.9); they can be evaluated in the limiting cases  $\lambda \rightarrow \infty$  and  $\lambda \rightarrow 0$  (§§8.3 and 8.4 below), but no general derivation valid for arbitrary  $\lambda$  is yet available (or is likely to be available for a very long time in view of the great difficulty of the problem). The appearance of a component of electromotive force parallel to  $\mathbf{B}_0$  in (8.8) (the term  $\alpha \mathbf{B}_0$ ) is of crucial importance for dynamo theory, and has been described as the  *$\alpha$ -effect* by Steenbeck, Krause and Radler (1966). Actually, Parker used the symbol  $\Gamma$  in 1955 for the constant of proportionality in the relation between toroidal emf and toroidal magnetic field; but the term  *$\alpha$ -effect* is now established in the literature and seems to have come to stay!

### 8.3 The Diffusion Dominated Limit

If  $\lambda$  is sufficiently large, the diffusion term  $\lambda \nabla^2 \mathbf{b}$  in eqn. (8.4) is much greater than the induction term  $\nabla \wedge (\mathbf{u} \wedge \mathbf{b} - \langle \mathbf{u} \wedge \mathbf{b} \rangle)$ , and this latter term may be neglected. In dimensionless form, the criterion is evidently

$$R_m = \frac{u_0 l}{\lambda} \ll 1, \quad (8.10)$$

where  $u_0$  is a typical fluid velocity (say the rms velocity). If the only time scale for velocity fluctuations is  $0(l/u_0)$ , the term  $\partial \mathbf{b} / \partial t$  is also negligible, and the equation reduces to

$$\lambda \nabla^2 \mathbf{b} = -\nabla \wedge (\mathbf{u} \wedge \mathbf{B}_0) \approx -(\mathbf{B}_0 \cdot \nabla) \mathbf{u}, \quad (8.11)$$

since  $\mathbf{B}_0$  is slowly varying compared with  $\mathbf{u}$ . (Actually in order to obtain  $A_{ij}$ , we can assume that  $\mathbf{B}_0$  is uniform; if we want to obtain  $C_{ijk}$ , we need to retain terms involving  $\partial B_{0j} / \partial x_k$ .)

Now let

$$\mathbf{u}(\mathbf{x}, t) = \int \mathbf{p}(\mathbf{k}, t) e^{i\mathbf{k} \cdot \mathbf{x}} d^3 \mathbf{k}, \quad \mathbf{b}(\mathbf{x}, t) = \int \mathbf{q}(\mathbf{k}, t) e^{i\mathbf{k} \cdot \mathbf{x}} d^3 \mathbf{k}; \quad (8.12)$$

then from (8.11),

$$\lambda k^2 \mathbf{q} = i(\mathbf{B}_0 \cdot \mathbf{k}) \mathbf{p}, \quad (8.13)$$

and the mean electromotive force is

$$\mathcal{E}_i = \langle \mathbf{u} \wedge \mathbf{b} \rangle_i = \epsilon_{ijk} \iint \langle p_j(\mathbf{k}, t) q_k(k', t) \rangle e^{i(\mathbf{k} + \mathbf{k}') \cdot \mathbf{x}} d^3 \mathbf{k} d^3 \mathbf{k}'. \quad (8.14)$$

Using (8.13), and translating this into spectral terminology, we have

$$\mathcal{E}_i = A_{ij} B_{0j}, \quad A_{ij} = i \epsilon_{ikl} \lambda^{-1} \int k^{-2} k_j \Phi_{kl}(\mathbf{k}) d^3 \mathbf{k}, \quad (8.15)$$

where  $\Phi_{kl}(\mathbf{k})$  is the usual Eulerian spectrum tensor of the turbulence (see Orszag's lectures in this volume). The Hermitian symmetry of  $\Phi_{kl}$  ensures that  $A_{ij}$  is real; the incompressibility conditions  $k_l \Phi_{kl}(\mathbf{k}) = 0$  guarantee moreover that  $A_{ij}$  is symmetric.

For pseudo-isotropic turbulence,

$$\Phi_{ij} = \frac{E(k)}{4\pi k^4} (k^2 \delta_{ij} - k_i k_j) + \frac{iF(k)}{8\pi k^4} \epsilon_{ijk} k_k, \quad (8.16)$$

where  $E(k)$  is the energy spectrum function and  $F(k)$  is the *helicity spectrum function*, satisfying

$$\langle \mathbf{u} \cdot \boldsymbol{\omega} \rangle = \int_0^\infty F(k) dk. \quad (8.17)$$

Substitution of (8.16) in (8.15) leads to  $A_{ij} = \alpha \delta_{ij}$  where

$$\alpha = -\frac{1}{3\lambda} \int_0^\infty k^{-2} F(k) dk. \quad (8.18)$$

Note the (expected) dependence of  $\alpha$  on the helicity spectrum, and the appearance of the minus sign in (8.18) for the reason implied pictorially in figure 8.1. An order of magnitude estimate for  $\alpha$  is evidently

$$\alpha \approx -\frac{1}{3\lambda} l^2 \langle \mathbf{u} \cdot \boldsymbol{\omega} \rangle, \quad (8.19)$$

valid provided  $F(k)$  is sharply peaked in a neighbourhood of the wave-number  $l^{-1}$ .

The parameter  $\beta$  may be obtained by similar methods, but is of limited interest in the diffusion-dominated limit since it is found that  $\beta = 0(R_m^2)\lambda$  so that  $\beta$  is negligible compared with  $\lambda$  in eqn. (8.9) when  $R_m \ll 1$ .

#### 8.4 The Weak Diffusion Limit

If  $R_m \gg 1$ , then it may be legitimate to neglect the diffusion term  $\lambda \nabla^2 \mathbf{b}$  entirely in eqn. (8.4) in a first approximation. This is effectively the procedure followed by Parker (1970); the following treatment has certain points of contact with Parker's treatment, but is somewhat more general.

We return to the exact (Cauchy) solution of the induction equation (with  $\lambda = 0$ ), viz.

$$B_i(\mathbf{x}, t) = B_j(\mathbf{a}, 0) \frac{\partial x_i}{\partial a_j} \quad (8.20)$$

(cf. eqn. (4.5) in the vorticity context). We now construct

$$\begin{aligned} \mathcal{E}_i(\mathbf{x}, t) &= \langle \mathbf{u} \wedge \mathbf{b} \rangle_i = \langle \mathbf{u} \wedge \mathbf{B} \rangle_i \\ &= \epsilon_{ijk} \langle v_j(\mathbf{a}, t) B_i(\mathbf{a}, 0) \frac{\partial x_k}{\partial a_i} \rangle, \end{aligned} \quad (8.21)$$

where  $v_j(\mathbf{a}, t) (= u_j(\mathbf{x}, t))$  is the Lagrangian velocity of the fluid particle  $\mathbf{x} = \mathbf{x}(\mathbf{a}, t)$ , i.e.  $\mathbf{v} = \partial \mathbf{x} / \partial t$ . Note that  $(\mathbf{x}, t)$  are non-random in (8.21); in different realisations of the ensemble, the fluid particle which arrives at  $\mathbf{x}$  at time  $t$  comes from different initial positions  $\mathbf{a}$ ; the function  $\mathbf{a} = \mathbf{a}(\mathbf{x}, t)$  is random and the average in (8.21) takes account of this.

In order to calculate the tensor  $A_{ii}$ , we may now assume (for the moment) that  $\mathbf{B}_0$  is uniform (and therefore constant). Moreover since by assumption the fluctuation field vanishes at time  $t = 0$ , we have in (8.21),  $B_i(\mathbf{a}, 0) = B_{0i}$ , and hence

$$\mathcal{E}_i = A_{ii} B_{0i}, \quad A_{ii} = \epsilon_{ijk} \langle v_j(\mathbf{a}, t) \frac{\partial x_k}{\partial a_i} \rangle. \quad (8.22)$$

Since  $x_k(\mathbf{a}, t) = \int_0^t v_k(\mathbf{a}, \tau) d\tau$ , we have equivalently

$$A_{ii} = \epsilon_{ijk} \int_0^t \langle v_j(\mathbf{a}, t) \frac{\partial}{\partial a_l} v_k(\mathbf{a}, \tau) \rangle d\tau. \quad (8.23)$$

Again, in the pseudo-isotropic situation,  $A_{ii} = \alpha \delta_{ii}$  where

$$\alpha = -\frac{1}{3} \int_0^t \langle \mathbf{v}(\mathbf{a}, t) \cdot \nabla_{\mathbf{a}} \wedge \mathbf{v}(\mathbf{a}, \tau) \rangle d\tau. \quad (8.24)$$

Note again the appearance of a type of helicity correlation, but this time in terms of Lagrangian variables (and no-one has yet succeeded in finding a method of expressing Lagrangian correlations in terms of more measurable Eulerian correlations). The expression (8.24) is reminiscent of the expression obtained by Taylor (1921) for eddy diffusion for a convected scalar in a turbulent flow, *viz.*

$$D = \frac{1}{3} \int_0^t \langle \mathbf{v}(\mathbf{a}, t) \cdot \mathbf{v}(\mathbf{a}, \tau) \rangle d\tau. \quad (8.25)$$

Taylor's expression certainly converges to a limit as  $t \rightarrow \infty$ , and it is at least plausible (though a point where caution is called for) to anticipate that the same is true of the expressions (8.23) and (8.24).

An expression for the eddy diffusivity  $\beta$  may be obtained by expanding  $B_i(\mathbf{a}, 0) = B_{0i}(\mathbf{a}, 0)$  in (8.21) about the point  $(\mathbf{x}, t)$ . In this limit ( $R_m \gg 1$ ), we obtain  $\beta = 0(u_0 l)$  and this is large compared with  $\lambda$ . The precise expression for  $\beta$  in terms of the statistical properties of the turbulence is therefore a matter of some importance. There are certain difficulties however (related to the convergence properties of the integrals that appear) and it would be inappropriate to pursue the matter further here.

## 8.5 Exponential Growth of the Mean Field

With  $\Lambda = \lambda + \beta$ , and dropping the suffix zero, eqn. (8.9) becomes

$$\frac{\partial \mathbf{B}}{\partial t} = \alpha \nabla \wedge \mathbf{B} + \Lambda \nabla^2 \mathbf{B}. \quad (8.26)$$

Let us suppose for the moment that  $\alpha > 0$ . Consider magnetic modes having a spatial structure satisfying

$$\nabla \wedge \mathbf{B} = K \mathbf{B}, \quad (8.27)$$

where  $K$  is a constant (with the dimensions of a wave-number). Such fields are *force-free* in magnetohydrodynamic terminology because the associated Lorentz force vanishes. The simplest example of a force-free field in a fluid of infinite extent is

$$\mathbf{B} = B_0(t) (\sin Kz, \cos Kz, 0). \quad (8.28)$$

Another example, in cylindrical polars  $(r, \theta, z)$  is

$$\mathbf{B} = B_0(t) (0, J_1(Kr), J_0(Kr)). \quad (8.29)$$

Substitution of (8.27) in (8.26) gives

$$\frac{\partial \mathbf{B}}{\partial t} = \alpha K \mathbf{B} - \Lambda K^2 \mathbf{B},$$

so that

$$\mathbf{B}(\mathbf{x}, t) = \mathbf{B}(\mathbf{x}, 0)e^{\omega t}, \quad \omega = \alpha K - \Lambda K^2. \quad (8.30)$$

Hence if  $K < \alpha/\Lambda$ , the field grows exponentially in intensity. The length scale characteristic of the growing field is  $L = K^{-1}$ , so that the condition  $K < \alpha/\Lambda$  is equivalent to  $L > \Lambda/\alpha$  and this is of course consistent with the basic condition  $L \gg l$  required to justify the "mean-field" approach.

The existence of exponentially growing solutions of (8.26) means that in the presence of background helical turbulence (giving rise to the  $\alpha$ -effect) the medium is unstable to the growth of magnetic perturbations; those with largest growth rate ( $\alpha^2/4\Lambda$ ) will presumably ultimately dominate the magnetic structure.

The situation is a little more complicated in a bounded region of conducting fluid which cannot support any force-free modes in the absence of external sources (Roberts, 1967). The steady solutions of (8.26) in a sphere which match to vacuum solutions of dipole and quadrupole type outside the sphere have been obtained by Krause and Steenbeck (1967). These solutions, involving Bessel functions of half-integral order, are not force-free but they have nevertheless a fairly simple structure (figure 8.3). The condition that the field should be steady defines a critical value for the eigenvalue  $\alpha a/\Lambda$  where  $a$  is the radius of the sphere; the eigenvalue for the

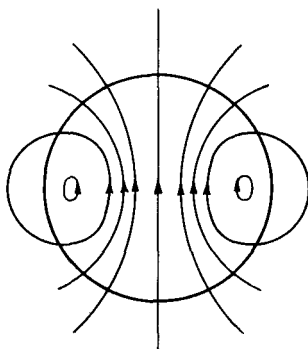


Figure 8.3 Self-excited field of dipole type in a sphere surrounded by insulator (Krause and Steenbeck, 1967)

Simplest solution depicted in figure (8.3) is

$$\frac{\alpha a}{\Lambda} = 4.5. \quad (8.31)$$

If  $\alpha$  is greater than  $4.5 \Lambda/a$ , then the corresponding field structure grows exponentially in time until some other physical mechanism intervenes.

### 8.6 Non-uniform $\alpha$ , Differential Rotation and Meridional Circulation

The above model with uniform  $\alpha$  and zero mean velocity is no more than suggestive and is a poor model for systems such as the Earth and Sun. The presence of mean helicity in these systems is closely associated with the coriolis forces that act because the fluid is rotating; and symmetry considerations suggest that  $\alpha$  should be antisymmetric about the equatorial plane in both cases: converging plumes will rotate clockwise in the northern hemisphere and anticlockwise in the southern. This means that it is more realistic to consider the effects of a mean emf

$$\mathcal{E} = \alpha \mathbf{B} \quad \text{with} \quad \alpha = \alpha_0 \cos \theta, \quad (8.32)$$

where  $\theta$  is the colatitude. We should also include a mean velocity field  $\mathbf{U}(\mathbf{x})$  which in general will include both toroidal and poloidal ingredients. The toroidal ingredient is just the differential rotation whose effects we considered in §7.4; the poloidal ingredient (meridional circulation) may be driven for example by buoyancy forces and (through conservation of angular momentum) will itself have a controlling effect in maintaining the distribution of differential rotation.

Inclusion of these effects leads to the equation

$$\frac{\partial \mathbf{B}}{\partial t} = \nabla \wedge (\mathbf{U} \wedge \mathbf{B}) + \alpha_0 \nabla \wedge (\cos \theta \mathbf{B}) + \Lambda \nabla^2 \mathbf{B}, \quad (8.33)$$

in which (in a kinematic approach)  $\mathbf{U}(\mathbf{x})$  must be assumed known. Unfortunately the equation is just too complicated to admit analytical solution (even if attention is limited to axisymmetric solutions) and recourse must be had to computational methods. The most comprehensive study to date of the solutions of (8.33) for a spherical region surrounded by vacuum (or insulator) is that of Roberts (1972). Among Roberts's most interesting conclusions are the following:

i) If the meridional circulation is negligible, and if the dynamo operates according to the Parker scheme

$$\mathbf{B}_{\text{tor}} \xrightarrow{\alpha\text{-effect}} \mathbf{B}_{\text{pol}} \xrightarrow[\text{rotation } \omega(R)]{\text{differential}} \mathbf{B}_{\text{tor}} \quad (8.35)$$

then the most easily excited dynamo mode is not steady but oscillatory in time; if  $\alpha_0 \omega'(R) < 0$  this mode, has a dipole structure and the periodic evolution consists of amplifying waves (cf. Parker, 1955) propagating from the poles towards the equator. Such oscillatory modes can be used to explain features of the Sun's 22-year sunspot cycle, if it is assumed that sunspots appear by eruption of a toroidal field below the surface when it reaches a certain critical level (see, for example, Steenbeck and Krause, 1969).

ii) If the meridional circulation is sufficiently strong and has an appropriate structure, the most easily excited mode is steady; the (relative) steadiness of the Earth's dipole field suggests that meridional circulation may be important in this context. If the meridional circulation becomes too strong, then the dynamo fails, presumably because the poloidal flux is then excluded from the region of  $\alpha$ - $\omega'$  regeneration by the process described in §7.3.

### 8.7 Self-Regulating Mechanisms

Exponential growth of a magnetic field as suggested by eqn. (8.27) cannot of course continue indefinitely, and is in fact limited by the back reaction of the growing Lorentz force on the fluid motion. This Lorentz force can modify both the turbulence structure (and hence the tensors  $A_{ij}$ ,  $C_{ijk}$ , ---) and also the mean velocity field. Analysis of these effects is really much more difficult than the kinematic analysis presented so far, because it involves consideration of the Navier-Stokes equations (with Lorentz force) coupled with the induction equation (7.9). Nevertheless some progress has been made indicating the sort of effects that may be important.

A model in which the velocity field consists of a random sea of inertial waves in a rotating fluid has been considered by Moffatt (1970b, 1972); in order to have an  $\alpha$ -effect it is necessary that there should be a net flux of energy in these waves parallel to the rotation vector. Under these circumstances, force-free growing magnetic modes of the type (8.28) exist, and attention may be focussed on the mode of maximum growth rate. As this mode intensifies it reacts back upon the constituent inertial waves of the velocity field and gradually modifies their dispersion relation. This leads to a reduction in the value of the parameter  $\alpha$  which ultimately reaches the critical level at which the magnetic field is steady (rather than exponentially growing). If there is no source of energy, then the total energy (magnetic plus kinetic) density decays to zero; if there *is* a source of energy (e.g. *via* a random body force) then a statistically steady state is reached; in the steady state the magnetic energy density may be an order of magnitude greater than the kinetic energy density in the background motion.

An alternative self-regulating mechanism has been suggested by Malkus and Proctor (1975), who take account of the meridional circulation driven

the Lorentz force in the fundamental growing mode in a sphere (Figure 8.3). As the field grows, the meridional circulation becomes more vigorous, and as observed at the end of §8.6 the dynamo process is rendered less efficient, so that again a balance is possible.

## 8.8 Conclusion

It will be evident that in the time available I have had to skate over certain difficult topics with indecent haste. I hope however that I have succeeded in conveying something of the excitement of current research in dynamo theory and something of the general flavour of the subject. Those already acquainted with the subject will know that my account is woefully one-sided in that I have concentrated almost entirely on the turbulent dynamo and have in these lectures ignored the vast literature on laminar dynamo theory. This has been a deliberate choice however, partly because (paradoxically) turbulent dynamo theory is easier than laminar theory (many of the difficulties are ironed out in the averaging process), and partly because I felt it useful to demonstrate that, although turbulence may present an unsolved problem in its dynamic aspects, the use of statistical methods in a context in which turbulence is important can nevertheless lead to simple conclusions.

## Acknowledgement

My approach to problems of high Reynolds number flows as discussed in Lectures 4 and 5 owes much to a stimulating set of lectures on this topic given by Professor Ian Proudman in Cambridge, England, in 1959.

## References and Bibliography

- Ackesberg, R. C. (1965) The viscous incompressible flow inside a cone. *J. Fluid Mech.* **21**, 47–81.
- Allan, D. W. (1958) Reversals of the Earth's magnetic field. *Nature, Lond.* **181**, 469.
- Batchelor, G. K. (1950) On the spontaneous magnetic field in a conducting fluid in turbulent motion. *Proc. Roy. Soc.* **A201**, 405.
- Batchelor, G. K. (1967) *Introduction to Fluid Dynamics*. Cambridge University Press.
- Brown, S. N. and Stewartson K. (1969) Laminar Separation. *Ann. Rev. Fluid Mech.* **1**, 45–72.
- Bullard, E. C. (1968) Reversals of the Earth's magnetic field. *Phil. Trans. Roy. Soc.* **A263**, 481.
- Chandrasekhar, S. (1961) *Hydrodynamic and Hydromagnetic Stability*. Oxford: Clarendon.
- Coles, D. (1965) Transition in circular Couette flow. *J. Fluid Mech.* **21**, 385.
- Cowling, T. G. (1934) The Magnetic field of sunspots. *Mon. Not. R. astr. Soc.* **94**, 39–48.
- Dean, W. R. and Montagnon P. E. (1949) *Proc. Camb. Phil. Soc.* **45**, 389.
- Eagles, P. M. (1974) On the torque of wavy vortices. *J. Fluid Mech.* **62**, 1–9.

- Ferraro V. C. A. and Plumpton C. (1966) *An Introduction to Magneto-Fluid Mechanics* (2nd edition). Oxford University Press.
- Gibson, R. D. (1968) The Herzenberg dynamo, I and II. *Quart. J. Mech. Appl. Math.* **21**, 243–267.
- Goldstein S. (Ed) (1938) *Modern Developments in Fluid Dynamics, I*. Oxford: Clarendon.
- Happel J. and Brenner H. (1965) *Low Reynolds Number Hydrodynamics*. Prentice-Hall.
- Herzenberg, A. (1958) Geomagnetic dynamos. *Phil. Trans. Roy. Soc.* **A250**, 543–585.
- Hide R. and Roberts, P. H. (1961) The origin of the main geomagnetic field. *Phys. and Chem. of the Earth* **4**, 25–98.
- Hunter C. (1960) On the collapse of an empty cavity in water. *J. Fluid Mech.* **8**, 241.
- Jeffery, G. B. (1922) The motion of ellipsoidal particles immersed in viscous fluid. *Proc. Roy. Soc.* **A102**, 161.
- Kaplun S. (1957) Low Reynolds number flow past a circular cylinder. *J. Math. Mech.* **6**, 595–603.
- Kaplun S. and Lagerstrom, D. A. (1957) Asymptotic expansions of Navier–Stokes solutions for small Reynolds numbers. *J. Math. Mech.* **6**, 585–593.
- Kraichnan R. H. and Nagarajan S. (1967) Growth of turbulent magnetic fields. *Phys. Fluids* **10**, 859.
- Krause F. and Steenbeck M. (1967) Untersuchung der Dynamowirkung einer nichtspiegelsymmetrischen Turbulenz an einfachen Modellen. *Z. Naturforsch.* **22**, 671–675.
- Landau, L. D. and Lifshitz E. M. (1959) *Fluid Mechanics*. Pergamon Press.
- Lighthill, M. J. (1973) On the Weis-Fogh mechanism of lift generation. *J. Fluid Mech.* **60**, 1–17.
- Lin C. C. (1955) *Theory of Hydrodynamic Stability*. Cambridge University Press.
- Malkus W. V. R. and Proctor, M. R. E. (1975) The macrodynamics of  $\alpha$ -dynamos in rotating fluids. *J. Fluid Mech.* **67**, 417–443.
- Malkus, W. V. R. and Veronis, G. (1958) Finite amplitude cellular convection. *J. Fluid Mech.* **4**, 225–260.
- Moffatt, H. K. (1964) Viscous and resistive eddies near a sharp corner. *J. Fluid Mech.* **18**, 1–18.
- Moffatt, H. K. (1969) The degree of knottedness of tangled vortex lines. *J. Fluid Mech.* **35**, 117.
- Moffatt, H. K. (1970a) Turbulent dynamo action at low magnetic Reynolds number. *J. Fluid Mech.* **41**, 435–452.
- Moffatt, H. K. (1970b) Dynamo action associated with random inertial waves in a rotating conducting fluid. *J. Fluid Mech.* **44**, 705.
- Moffatt, H. K. (1972) An approach to a dynamic theory of dynamo action in a rotating conducting fluid. *J. Fluid Mech.* **53**, 385.
- Oseen, C. W. (1910) *Ark. Mat. Astr. Fys.* **6** no. 29. Über die Stokessche Formel und über eine verwandte Aufgabe in der Hydrodynamik.
- Parker, E. N. (1955) Hydromagnetic dynamo models. *Astrophys. J.* **122**, 293–314.
- Parker, E. N. (1970) The generation of magnetic fields in astrophysical bodies. I. The dynamo equations. *Astrophys. J.* **162**, 665–673.
- Parker, R. L. (1966) Reconnection of lines of force in rotating spheres and cylinders. *Proc. Roy. Soc.* **A291**, 60–72.
- Phillips, O. M. (1972) The entrainment interface. *J. Fluid Mech.* **51**, 97–118.
- Prandtl, L. (1905) Über Flüssigkeitsbewegung bei sehr kleiner Reibung. *Verh. III int. Math. Kongr., Heidelberg*, 484–491. Teubner, Leipzig.
- Proudman, I. and Pearson, J. R. A. (1957) Expansions at small Reynolds numbers for the flow past a sphere and a circular cylinder. *J. Fluid Mech.* **2**, 237.
- Roberts, P. H. (1971) Dynamo theory, in *Lectures in Applied Mathematics* (ed. W. H. Reid) pp. 129–206. American Mathematical Society, Providence.
- Roberts, P. H. (1967) *An Introduction to Magnetohydrodynamics*. Longman.

- Roberts, P. H. and Stix, M. (1971) The turbulent dynamo; a translation of a series of papers by F. Krause, K.-H. Rädler and M. Steenbeck. Technical note IA-60, Boulder Col.
- Rosenhead, L. (Ed) (1963) *Laminar Boundary Layers*. Oxford: Clarendon.
- Saffman, P. G. (1963) On the fine-scale structure of vector fields convected by a turbulent fluid. *J. Fluid Mechn.* **16**, 545.
- Steenbeck M. and Krause F. (1969) Zur Dynamotheorie stellarer und planetarer Magnetfelder. I. Berechnung sonnenähnlicher Wechselfeldgeneratoren. *Astronom. Nachr.* **291**, 49-84.
- Steenbeck M., Krause F. and Radler K.-H. (1966) Berechnung der mittlerer Lorentz-Feldstärke  $\langle \mathbf{v} \wedge \mathbf{B} \rangle$  für ein elektrisch leitendes. Medium in turbulenter, durch Coriolis-Kräfte beeinflusster Bewegung. *Z. Naturforsch.* **21**, 369-376.
- Stuart, J. T. (1963) *Hydrodynamic Stability*. Chap. IX of Rosenhead 1963 (q.v.).
- Stuart, J. T. (1971) Nonlinear Stability Theory. *Ann. Rev. Fluid Mech.* **3**, 347-370.
- Taylor, G. I. (1921) Diffusion by continuous movements. *Proc. London Math. Soc.* **20**, 196.
- Taylor, G. I. (1923) Stability of a viscous liquid contained between two rotating cylinders. *Phil. Trans. Roy. Soc. A* **223**, 289-343.
- Tillett, J. P. K. (1970) Axial and transverse stokes flow past slender axisymmetric bodies. *J. Fluid Mech.* **44**, 401-417.
- Townsend, A. A. (1966) The mechanism of entrainment in free turbulent flows. *J. Fluid Mech.* **26**, 689-715.
- Venezian, G. (1967) Magnetohydrodynamics of the Earth's magnetic field. Rep. no. 85-37. Div. Eng. and Appl. Sc. Cal Tech. Pasadena, Calif.
- Weiss, N. O. (1966) The expulsion of magnetic flux by eddies. *Proc. Roy. Soc. A* **293**, 310-328.
- Weiss, N. O. (1971) The dynamo problem. *Q. J. R. astr. Soc.* **12**, 432-446.
- Weis-Fogh, T. (1973) Quick estimates of flight fitness in hovering animals, including novel mechanisms of lift production. *J. Exp. Biol.* **59**, 169-230.
- Woltjer, L. (1958) A theorem on force-free magnetic fields. *Proc. Nat. Acad. Sci. U.S.A.* **44**, 489-491.